

**MEASUREMENT AND PREDICTION OF ERRORS FOR A THREE AXIS
MACHINE TOOL THROUGH METROLOGY FEEDBACK**

by

Muhammad Hassan Yaqoob

Submitted to the Graduate School of Engineering and Natural Sciences

in partial fulfillment of the requirements for the degree of

Master of Science

Sabanci University

July 2017

**MEASUREMENT AND PREDICTION OF ERRORS FOR A THREE AXIS
MACHINE TOOL THROUGH METROLOGY FEEDBACK**

Approved by:

Prof. Dr. Erhan Budak (Thesis Supervisor)



Assoc. Prof. Dr. Bahattin Koç



Assoc. Prof. Dr. Umut Karagüzel



Date of approval

28.07.17

© M.H. Yaqoob, 2017

All Rights Reserved

To my Family

MEASUREMENT AND PREDICTION OF ERRORS FOR A THREE AXIS MACHINE TOOL THROUGH METROLOGY FEEDBACK

Muhammad Hassan Yaqoob

Industrial Engineering, MSc. Thesis, 2017

Thesis Supervisor: Prof. Dr. Erhan Budak

Abstract

The evolution of machine tools, driven by ever growing requirement for high precision machining, has warranted the importance of understanding and compensation of errors in machine tools. There are a considerable number of research studies dealing with the modelling, measurement and compensation of errors. Machined workpiece geometry provides an opportunity for determination of errors generated during machining process. However, examination of the current literature reveals that the overall progress, in error determination through workpiece measurements, is limited to reporting of mainly positional errors.

There is need for development of a comprehensive methodology that can help determine not only the mechanical errors but also the errors being generated due to process parameters, geometry of workpiece and changes in thermal state of the machine tool. Such a methodology would not only provide comprehensive error magnitude in real-time scenario but would also provide the decision makers with the ability to decide whether to compensate the errors on workpiece or to carry out corrective measures on a machine tool. The current research seeks to develop such a methodology for error measurement and prediction in a Three Axis machining center. A combination of Machining under different conditions followed by subsequent on-machine probing and measurements on a coordinate measuring machine (CMM) are used to obtain error database with appreciation for process, thermal, control and mechanical errors. The proposed methodology is generic with respect to the shape and size of the workpiece, tool geometry and machine tool of similar configuration. The results include a prediction model that enables the user with the ability of pre-machining assessment of expected errors and final geometrical dimensions of a workpiece. This in turns reduces the quality costs, improves decision making meanwhile the simplicity of experimentation essentially offers a low-cost shop-floor friendly solution.

Keywords: Error identification, workpiece measurement, metrology feedback, thermal error measurement, dynamic error measurement.

METROLOJİ GERİ BİLDİRİMİ TEMELLİ 3 EKSENLİ TAKIM TEZGAHLARINDA HATA ÖLÇÜLMESİ VE TAHMİNİ

Muhammad Hassan Yaqoob

Endüstri Mühendisliği, Yüksek Lisans Tezi, 2017

Tez Danismanı: Prof. Dr. Erhan Budak

Özet

Takım tezgahlarının gelişimi ve yüksek hassasiyetli işleme gereksiniminin giderek artması, takım tezgahlarındaki hataların anlaşılmasının ve önlenmesinin gerekliliğini önemli ölçüde arttırmıştır. Hataların modellenmesi, ölçülmesi ve telafisi ile ilgili çok sayıda araştırma çalışması bulunmaktadır. İşlenmiş parça geometrisi, işleme sürecinde ortaya çıkan hataların belirlenmesi için bir fırsat sağlamaktadır. Bununla birlikte, mevcut literatürün incelenmesi, iş parçasının üzerinde yapılan ölçümler yoluyla hata tespitinde genel eğilimin, çoğunlukla pozisyonel hataların raporlanmasıyla sınırlı olduğunu ortaya koymaktadır.

Mekanik hataların yanı sıra aynı zamanda süreç değişkenleri, iş parçasının geometrisi ve takım tezgahının termal durumu dolayısıyla oluşan hataların tahmin edilmesine yardımcı olan kapsamlı bir metodolojinin sunulmasına ihtiyaç vardır. Böyle bir metodoloji yalnızca gerçek-zaman senaryosunda kapsamlı hata tahmini sağlamaz, aynı zamanda sorumlu üreticiler iş parçasındaki hataları telafi edip etmeyeceğine veya bir makine üzerinde düzeltici tedbirler alıp almayacağına karar verebilir. Bu araştırma, üç eksenli bir takım tezgahında hata ölçümü ve tahmini için böyle bir metodoloji geliştirmeyi amaçlamaktadır. Süreç, termal, kontrol ve mekanik hatalar için hata veritabanı elde etmek amacıyla farklı koşullardaki parça işlenir, ardından bir koordinat ölçme makinesi (CMM) üzerinde ölçümler yapılır ve daha sonra makine üzerinde ölçüm işlemi uygulanmaktadır. Önerilen metodoloji, iş parçasının şekli ve boyutu, takım geometrisi ve benzer konfigürasyonda takım tezgahı göz önünde bulundurulduğunda genelleştirilebilir. Sonuçlar, bir iş parçasının beklenen hataları ve son geometrik boyutları için ön işleme değerlendirmesi yapma olanağı veren bir tahmin modeli içermektedir. Bu, dönüşümlü olarak kalite maliyetlerini düşürür ve planlamayı geliştirir. Sade bir iş parçası üzerinde yapılan deneyler ile düşük maliyetli bir işyeri dostu çözüm sunulmaktadır.

Anahtar Kelimeler: Hata tanımlama, iş parçası ölçümü, metroloji geri bildirim, termal hata ölçümü, dinamik hata ölçümü.

Acknowledgement

Thanks to ALLAH ALMIGHTY for making it all possible.

I would like to express my deepest gratitude towards my supervisor, Prof. Dr. Erhan Budak for his guidance, support and valuable time. His continuous guidance has been a driving factor behind the right direction of the current research. My sincere thanks to Dr. Emre Özlü for his valuable feedback and suggestions during the research.

I would also like to extend my appreciation to my committee members Assoc. Prof. Dr. Bahattin Koç and Dr. Umut Karagüzel for their valuable time and efforts.

I would like to recognize the support and efforts of personal working at MRL. My Special thanks to Esmâ Baytok for her continued support in setting up experiments. The logistic and technical support of Süleyman Tutkun, Ertuğrul Sadıkoğlu and Mr. Veli Naksiler is also an important part of this research journey.

A warm gratitude is also extended towards my friends at Sabanci University and especially Yaser Mohammadi, Mert Gurtan, Esra Yuksel, Başak Tavşanoğlu, Milad Azvar, Faran, Waqar, Sohaib and Babar for the great times spent together. Mert Koçefe, Yiğit and Faruk added memorable moments to my lab life. Special thanks to Faraz and Zahra for their excellent organizational skills during lab gatherings and deep regards for Kaveh, Arash, Mehmet, Batuhan, and Hamid for the friendly environment in MRL.

I would like to extend my deepest gratitude to Ami Jan, Atia and Ahmad for their courage, resilience, endless love and support that made it possible for me to Study at Sabanci University. I am thankful for the prayers and relentless efforts of Ami Jan, the love and friendship of Atia and the motivation of Ahmad. I also want to acknowledge Mr. and Mrs. Alam for their efforts and support throughout this time. Special thanks to my Sisters for their love and kindness and all my family for their continuous support and encouragement.

Table of Contents

Abstract.....	ii
Acknowledgement	iii
Table of Contents	v
List of Figures	viii
List of Tables	xi
List of Symbols	xii
Chapter 1. Introduction	1
1.1 State of the Art	3
1.1.1 Review of Error Measurement	5
1.2 Opportunity Analysis:	10
1.3 Motivation and Objectives:	11
1.4 Scope.....	12
Chapter 2. Theory	13
2.1 Machine tool errors:	13
2.1.1 Fixturing Errors:	13
2.1.2 Thermal Errors:	14
2.1.3 Geometric Errors:	17
2.1.4 Process Errors:.....	21
2.1.5 Motion errors due to Control:.....	23
2.2 Error Separation:	23
2.3 Error Measurements through metrology feedback:.....	24
2.3.1 Challenges in Error measurement:	24
2.4 Conclusion:	25
Chapter 3. Methodology	27
3.1 Workpiece and Fixture Design:	27
3.2 Workpiece machining requirements	32
3.3 Experiment design for position error profiling	34
3.4 On machine probing of workpiece:.....	35
3.4.1 Separation of Spindle and table tilt angles:	36
3.5 Determination of thermal Errors:	38
3.5.1 Changing the thermal state:	41
3.6 Feed based process and control Errors:.....	44
3.6.1 Process Errors due to feed	44
3.6.2 Control Error Separation:	45
3.7 Software based Process errors calculation:	49

3.8	Regression model Error analysis:.....	50
3.9	Development of prediction Model:.....	50
3.10	Conclusion:.....	50
Chapter 4.	EXPERIMENTAL DESIGN.....	52
4.1	Machining Setup:.....	52
4.2	Probing Setup:.....	56
4.3	CMM setup:.....	57
4.4	Conclusion:.....	57
Chapter 5.	Results and Analysis.....	59
5.1	Results:.....	59
5.2	Position Errors Results:.....	59
5.2.1	Position Error Analysis:.....	66
5.3	Thermal Error Measurement Results and Analysis:.....	67
5.3.1	Change in Spindle length:.....	67
5.3.2	Error in Position due to change in Temperature state:.....	68
5.3.3	Spindle deflection along X axis.....	70
5.3.4	Change in table tilt due to Temperature change:.....	71
5.3.5	Thermal Stage 2:.....	72
5.3.6	Thermal Stage 3:.....	74
5.4	Thermal Error Prediction Model:.....	76
5.4.1	Thermal Prediction Equation for <i>e_{pty}</i> :.....	76
5.4.2	Prediction Model for <i>e_{ptx}</i>	78
5.4.3	Prediction Model for <i>e_{spl_z}</i> :.....	79
5.4.4	Prediction Model for Spindle Deflection and table tilt.....	81
5.4.5	Prediction Model for Table tilt:.....	83
5.5	Process Error Results and Analysis:.....	84
5.5.1	Conversion to Force Based Process Error:.....	88
5.6	Control errors Results and analysis:.....	89
5.6.1	Distance and Feed Based Control Errors:.....	90
5.6.2	Conversion to Force based Control Errors:.....	91
5.7	Prediction Model Variation analysis:.....	93
5.8	Conclusion.....	95
Chapter 6.	IMPLEMENTATION.....	96
6.1	Case 1: MRR Maximization.....	96
6.2	Case 2: Change in Shape.....	99
6.3	Conclusion:.....	104
Chapter 7.	Summary and Conclusion.....	106

7.1	Summary	106
7.2	Conclusion:	107
7.2.1	Applications:	109
7.2.2	Original Contribution:	109
7.2.3	Future Work:	110
	References.....	111

List of Figures

Figure 1.1 Errors in a three-axis machining center	1
Figure 1.2 R-Test setup Figure 1.3 Laser Interferometer Setup	7
Figure 2.1 Actual and desired position due to orientation Error	14
Figure 2.2 Machine deformation under thermal Influence	15
Figure 2.3 Test setup for thermal deformation of spindle	16
Figure 2.4 Geometric errors on a three axis machine tool	17
Figure 2.5 Squareness Errors between X, Y and Z axis	18
Figure 2.6 Artifact for on-machine probing	20
Figure 2.7 Part for process error verification	22
Figure 3.1 3D model of workpiece	28
Figure 3.2 Workpiece detailed design	28
Figure 3.3 Deflection of workpiece under simulated residual stress (90N)	30
Figure 3.4 Deflection of workpiece under simulated residual stress (1000N)	30
Figure 3.5 Deflection after fixture addition under 90N force	31
Figure 3.6 Deflection after fixture addition under 1000N force	32
Figure 3.7 Difference in Repeat measurement using Touch Probe	35
Figure 3.8 Measurement points on the surface of workpiece	36
Figure 3.9 Spindle tilt demonstration	37
Figure 3.10 effect of spindle tilt on the final workpiece geometry	38
Figure 3.11 Workpiece geometry under Thermal error influence	39
Figure 3.12 Thermal error influence -Table tilt	40
Figure 3.13 Process flow for thermal error Extraction	43
Figure 3.14 Tool path for Feed based process errors	44
Figure 3.15 Tentative Post-machining surface for W8	45
Figure 3.16 Actual cut for Control Error Separation	46
Figure 3.17 Feed and Process Error Separation	48
Figure 4.1 Workpiece and Fixture placement	53
Figure 4.2 Runout Radius Effect Figure 4.3 runout determination setup	53
Figure 4.4 Machining setup	54
Figure 4.5 Probing setup for Mechanical position errors	56

Figure 5.1 Position errors in x, y and z axis.....	64
Figure 5.2 Orientation error along X and Y axis.....	64
Figure 5.3 Orientation Error around Z axis.....	65
Figure 5.4 Step wise mechanical Spindle tilt angle	65
Figure 5.5 Step wise mechanical position error in Y-axis	66
Figure 5.6 Temperature state wise change in spindle length	67
Figure 5.7 Temperature state wise difference in backward prediction	68
Figure 5.8 Temperature state wise change in position error in X-Axis	69
Figure 5.9 Temperature state wise change in position error in X-Axis	69
Figure 5.10 Temperature state wise change in position error (Y-Intercept)	70
Figure 5.11 Spindle deflection X-Axis Figure 5.12 Spindle deflection Y-Axis.....	71
Figure 5.13 Thermal Table tilt X-Axis Figure 5.14 Thermal Table Tilt Y-Axis	71
Figure 5.15 Temperature state wise <i>ept2x</i> Figure 5.16 Temperature state wise <i>ept2y</i>	72
Figure 5.17 Temperature state wise <i>espd2x</i> Figure 5.18 Temperature state wise <i>espd2y</i> ...	73
Figure 5.19 Temperature state wise <i>ett2y</i> Figure 5.20 Temperature state wise <i>ett2x</i>	73
Figure 5.21 Temperature state wise position error (Stage 3)	75
Figure 5.22 Temperature State and Stage Wise Position Error in Y-Axis.....	78
Figure 5.23 Temperature State and Stage Wise Position Error in X-Axis.....	79
Figure 5.24 Temperature State and Stage Wise error in Z-Axis.....	80
Figure 5.25 Feed wise change in Position error in Y-Axis	85
Figure 5.26 Feed wise change in Table tilt along Y-Axis.....	85
Figure 5.27 Feed wise changes in Process error along Z-Axis	86
Figure 5.28 Feed wise change in spindle deflection along Y-Axis.....	86
Figure 5.29 Feed wise change in Table tilt along Y-axis.....	86
Figure 5.30 Feed wise program generated process errors	88
Figure 5.31 Program generated wise change in actual process errors.....	89
Figure 5.32 Distance wise control error due to Feed change	90
Figure 5.33 Feed based control error along Y-Axis.....	92
Figure 5.34 Software Generated process error wise Change in control errors.....	93
Figure 5.35 Temperature state wise backward prediction difference <i>esplz</i>	94
Figure 5.36 Temperature state wise backward prediction difference (<i>eptx</i>)	94
Figure 6.1 Stepwise percentage reduction in errors along X, Y and Z axis	97

Figure 6.2 compensated vs uncompensated error magnitude in X and Y axis.	98
Figure 6.3 Point wise observed and predicted errors along Z-Axis	101
Figure 6.4 Point wise Total and various error components along X-Axis	103
Figure 6.5 Point wise Total and various error components along Y-Axis	103
Figure 6.6 Point wise error in X and Y Axis.....	104

List of Tables

Table 3.1 Cutting conditions and expected error behavior	33
Table 4.1 Machining conditions for various workpieces	55
Table 5.1 Dimensional probing results for W8.....	60
Table 5.2 CMM Measurement results.....	61
Table 5.3 Step wise CMM and Probed Dimensions	62
Table 5.4 CMM data based Orientation Errors	63
Table 5.5 Probing Data based orientation Errors:	63
Table 5.6 Reported X and Y dimensions for W2, W5 and W8.....	91
Table 5.7 Errors calculated using prediction model for W2 and W5.....	92
Table 5.8 Backward Prediction Error analysis.....	94
Table 6.1 Step wise Compensations used:	96
Table 6.2 Measured coordinate data for X and Y axis.....	99
Table 6.3 Actual and measured Z dimensions and error components.....	100
Table 6.4 Model based error components	100
Table 6.5 Model based error components	101
Table 6.6 Calculated Errors in X and Y axis- Part 1	102
Table 6.7 Calculated Errors in X and Y axis- Part 2.....	102

List of Symbols

e_{pos_x}	:	Error in position due to mechanical issues along X-Axis
e_{pos_y}	:	Error in position due to mechanical issues along Y-Axis
e_{pos_z}	:	Error in position due to mechanical issues along Z-Axis
α	:	Initial Mechanical table tilt angle
θ	:	Initial Mechanical Spindle tilt angle
e_{pt_x}	:	Error in position at thermal state ‘t’ along X-Axis
e_{pt_y}	:	Error in position at thermal state ‘t’ along Y-Axis
e_{spl_z}	:	Error in spindle length along Z axis.
$e_{pt_{2x}}$:	Error in position at thermal state ‘t’ stage 2 along X Axis
$e_{pt_{2y}}$:	Error in position at thermal state ‘t’ stage 2 along Y Axis
$e_{spl_{2z}}$:	Error in position at thermal state ‘t’ stage 2 along Z Axis
$e_{pt_{3x}}$:	Error in position at thermal state ‘t’ stage 3 along X Axis
$e_{pt_{3y}}$:	Error in position at thermal state ‘t’ stage 3 along Y Axis
$e_{spl_{3z}}$:	Error in position at thermal state ‘t’ stage 3 along Z Axis
e_{tt_x}	:	Table tilt along X Axis at thermal state ‘t’
e_{tt_y}	:	Table tilt along Y Axis at thermal state ‘t’
e_{spd_x}	:	Spindle tilt along X axis at temperature state ‘t’
e_{spd_y}	:	Spindle tilt along Y axis at temperature state ‘t’
$e_{tt_{2x}}$:	Table tilt along X Axis at thermal state ‘t’ Stage 2
$e_{tt_{2y}}$:	Table tilt along Y Axis at thermal state ‘t’ Stage 2
$e_{tt_{3x}}$:	Table tilt along X Axis at thermal state ‘t’ Stage 3
$e_{tt_{3y}}$:	Table tilt along Y Axis at thermal state ‘t’ Stage 3
$e_{spd_{2x}}$:	Spindle tilt along X axis at temperature state ‘t’ Stage 2
$e_{spd_{2y}}$:	Spindle tilt along Y axis at temperature state ‘t’ Stage 2
$e_{spd_{3x}}$:	Spindle tilt along X axis at temperature state ‘t’ Stage 3

$e_{spd_{3y}}$:	Spindle tilt along Y axis at temperature state 't' Stage 3
$e_{pt_{xpred}}$:	Predicted thermal position error in X- Axis
$e_{pt_{ypred}}$:	Predicted thermal position error in Y- Axis
$e_{splz_{pred}}$:	Predicted thermal error in Z- Axis
$e_{spd_{ypred}}$:	Predicted Thermal spindle tilt along Y-Axis
$e_{spd_{xpred}}$:	Predicted Thermal spindle tilt along X-Axis
$e_{tt_{xpred}}$:	Predicted Thermal table tilt along X- Axis
$e_{tt_{ypred}}$:	Predicted Thermal Table tilt along Y-Axis
e_{pfx}	:	Process Error due to feed along X-Axis
e_{pfy}	:	Process Error due to feed along Y-Axis
e_{splfz}	:	Process Error along Z-axis due to Feed
e_{ftx}	:	Table tilt along X-axis due to Feed
e_{fty}	:	Table tilt along Y-axis due to Feed
e_{spdfx}	:	Spindle tilt along X-axis due to Feed
e_{spdfy}	:	Spindle tilt along Y-axis due to Feed
e_{prog}	:	Program generated process errors
e_{psfx}	:	Predicted process errors along X-axis based on e_prog
e_{psfy}	:	Predicted process errors along Y-axis based on e_prog
e_{splsfz}	:	Predicted process errors along Z-axis based on e_prog
dy_{w2}	:	Measured stepwise dimension of W2 along Y-Axis
dx_{w2}	:	Measured stepwise dimension of W2 along X-Axis
dy_{w5}	:	Measured stepwise dimension of W5 along Y-Axis
dx_{w5}	:	Measured stepwise dimension of W5 along X-Axis
$e_{pfy_{w2}}$:	Predicted error due to feed in workpiece 2 along Y-Axis
$e_{pfy_{w5}}$:	Predicted error due to feed in workpiece 5 along Y-Axis
$e_{pfy_{w8}}$:	Predicted error due to feed in workpiece 8 along Y-Axis
$e_{pfx_{w2}}$:	Predicted error due to feed in workpiece 2 along X-Axis

$e_{pf_{xw5}}$:	Predicted error due to feed in workpiece 5 along X-Axis
$e_{pf_{xw8}}$:	Predicted error due to feed in workpiece 8 along X-Axis
$e_{pt_{yw2}}$:	Predicted thermal error in workpiece 2 along Y-Axis
$e_{pt_{yw5}}$:	Predicted thermal error in workpiece 5 along Y-Axis
$e_{pt_{yw8}}$:	Predicted thermal error in workpiece 2 along Y-Axis
$e_{pt_{xw2}}$:	Predicted thermal error in workpiece 2 along X-Axis
$e_{pt_{xw5}}$:	Predicted thermal error in workpiece 5 along X-Axis
$e_{pt_{xw8}}$:	Predicted thermal error in workpiece 8 along X-Axis
$e_{pos_{yw2}}$:	Predicted error in position in workpiece 2 along Y-Axis
$e_{pos_{yw5}}$:	Predicted error in position in workpiece 5 along Y-Axis
$e_{pos_{yw8}}$:	Predicted error in position in workpiece 8 along Y-Axis
$e_{pos_{xw2}}$:	Predicted error in position in workpiece 2 along X-Axis
$e_{pos_{xw5}}$:	Predicted error in position in workpiece 5 along X-Axis
$e_{pos_{xw8}}$:	Predicted error in position in workpiece 8 along X-Axis
$e_{ctrl_{y(2400-100)}}$:	Error in control due to feed transition between 2400 and 100mm/min
$e_{ctrl_{x(2400-100)}}$:	Error in control due to feed transition between 2400 and 100mm/min
e_{cpr_y}	:	Error in control due to process forces along Y-Axis
e_{cpr_x}	:	Error in control due to process forces along X-Axis
e_{ctrl_y}	:	Error in control due to displacement and Feed along Y-Axis
e_{ctrl_x}	:	Error in control due to displacement and Feed along X-Axis
$e_{cpr_{yprog}}$:	Error in control based on program generated process errors
$e_{cpr_{xprog}}$:	Error in control based on program generated process errors

Chapter 1. Introduction

The advent of high precision products has necessitated the accuracy improvement in machining more than ever. Throughout the industry ranging from aerospace to automobile manufacturing, the overall requirement for accuracy have become challenging overtime. This need for accuracy has driven research focus of the relevant scientific community towards accuracy improvements in machining. The current research intends to take the existing science a step further in an ongoing accuracy improvement drive.

It is important to establish the concept of accuracy. Accuracy has historically been defined with different references. The basic definition of accuracy in machine tools is the proximity of measured result to the true value. There are also other definitions appearing in the existing literature that define the geometric accuracy of a machine tool with reference to the precision in shape and the local of several parts and the precision in their mutual moments. Although there are several definitions of accuracy yet the deviation in each case is known as errors. The overall errors observed in a Three axis machining center can be observed at Figure 1.1.

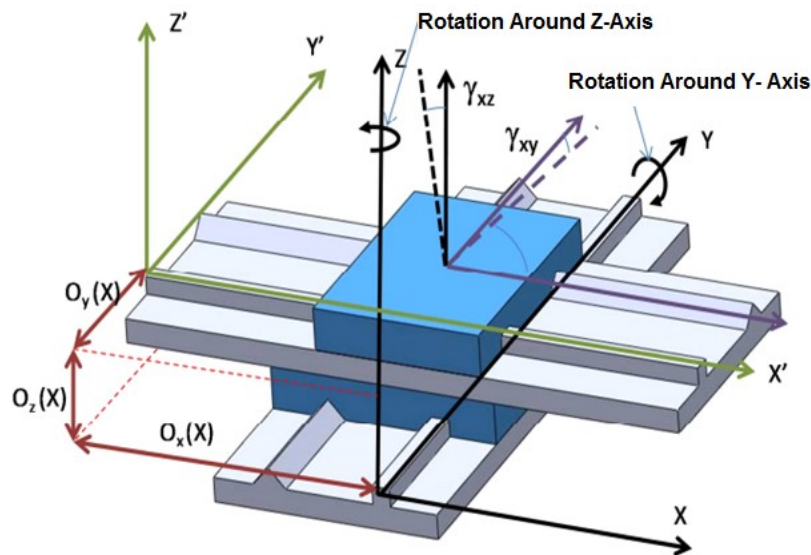


FIGURE 1.1 ERRORS IN A THREE-AXIS MACHINING CENTER

Here the Symbol $O_z(X)$ presents the orientation error in X-Axis with respect to Z-Axis, $O_x(X)$ and $O_y(X)$ represent the orientation errors due to X and Y axis respectively. The symbol γ_{xz} and γ_{xy} presents the rotations in X with reference to Z and Y axis respectively. It is pertinent to mention here that the errors represented in Figure 1.1 may be generated through one source or a combination of multiple error generating sources, the latter being true for all machining operations. These combinations may include mechanical, thermal, process and control errors. Alongside errors in machine tool due to inherent manufacturing inaccuracies, the errors observed on machined workpiece results from the interaction between the workpiece and the tool. In a machining center, the cutting tool being part of machine tool spindle and workpiece being attached to the table, necessitates that any changes in spindle and table dynamics influences the final geometry of the workpiece. Therefore, any changes in temperature, cutting forces or even the speed with which the tool changes its position influences the overall errors observed.

The optimum performance for a machine tool may be achievable through design, highly accurate manufacturing, a high stiffness to weight ratio, a rigid control mechanism, vibration damping and resistance to temperature based physical changes. The list requirements as a prelude to a highly accurate machine includes many other factor and extends as far as the installation of machine on the shop floor and the subsequent operational environment. However, achieving such an ideal machine tool is difficult due to constraints that include capability, capacity and cost. Therefore, along with the research on new materials, manufacturing methods and improved mechatronics, a significant body of research has been focused towards determination and elimination of errors in a machine tool. Consequently, many methodologies have been developed. Such methodologies include determination, modelling, measurement and compensation of errors through use of various techniques ranging from neural network, use of FEM softwares to measurements of artifacts and machined workpieces. However, very few of the developed methodologies have been utilized at an industrial scale. This gap can be attributed to the complexity, cost and restricted general applicability of the methodologies.

To address these gaps there is a need for error determination methodology which can carry the ability of reporting a combination of errors and consequently links them with their respective error generating parameters so that the errors can not only be reported by a forward prediction tool can also be generated. Meanwhile the technique also needs to be cost effective in terms of both capital and experimental costs.

1.1 State of the Art

It is also of primary importance here to review the work that has already been done regarding the error measurement and prediction models for various types of errors. It is however also interesting to observe the various classification of errors as found in existing literature

Being the most relevant to the current research H. Schwenke et. al. [1] has provided an error classification based on the error sources. The authors divided geometrical errors into Kinematic, Thermo-mechanical, load based, force based and control based errors. This is an interesting classification for the current research as the proposed model also seeks to identify different errors based on their sources. Meanwhile, S Mekid et. al [2] classified errors in machine tools, based on their types as being either systematic or random while the authors also provided a severity level for each individual error. R. Ramesh et al. [3] have classified errors based on the source of generation. The authors have divided the errors into three different categories namely geometric and kinematic errors, errors due to cutting forces and thermally induced errors. Similarly, A.C. Okafor et al. [4] have also emphasized on error classification based on these three categories. It is however, important to understand that categorization of errors is significant as it points towards the methods for error modelling, measurement, compensation and error prediction. While the error source identification provides an important aspect for modelling of errors, the measurement of errors requires the understanding of the random or systematic nature of errors.

As noted earlier error modelling in machine tools have mostly been carried out with appreciation of the error sources. Therefore, in the current literature the models for each type of error have been presented separately. Beginning with geometric errors Shaowei Zhu et al. [5] have presented an error model for five axis machining center that identifies the geometric error parameters while also proposing an error model utilizing the parameters to provide the overall geometrical errors. This has been followed through with a G-code based compensation. Wang JingDong et. al. [6] provided a mathematical model for volumetric error measurement and compensation in 3 Axis machine tools. The authors have considered multibody approach for the modelling process and the modelling process is therefore centered on the relative motion between the two bodies i.e. the cutter and workpiece.

Seng Khim et. al. [7] have provided a similar error model in their study. Meanwhile, A.K. Srivastave et. al. [8] have provided a mathematical model for geometric error modelling in five axis machine tools. The approach is similar in terms of multi body system but differs in the respect that it considers the errors due to various individual components as well. The individual error components and relevant transformation matrices are then used to provide the final error matrices for individual components. The model is then used towards error measurement followed by compensation. Wenji Tian et. al. [9] have presented a study where the error modeling has been done considering the geometric errors in five axis machine tools as well as the errors due to cutting tool kinematic chains. This is then used to generate mathematical models for various error types. It is important to mention here that the author have also studied the separation of individual errors to minimize the superposition effects.

Similarly, a significant number of articles have been found dealing with the thermal error modelling through various approaches. Thermal errors are mainly non-linear with due to the nonlinear temperature changes in machine tools. Wu Hao et. al. [10] presented an optimization model for thermal errors that uses artificial neural networks to provide the required optimization in error models. S. Yang et al. [11] also presented a neural network based thermal error model that utilizes the data collected for machine tool temperature and links the same with the overall error generated to provide a learning set for the neural network. The network is further utilized to provide the required compensation against temperature and time. It is important to mention here that much research on thermal error modelling has been focused on utilization of artificial neural networks in conjunction with the measurements obtained on the machine for error magnitude and corresponding temperatures. Meanwhile examples exist where Finite element methods (FEM) have been used for modelling of thermal errors. Kim et. al. [12] utilizes such a method to analyze the temperature distribution in ball screw in machining center. Various other approaches have also been used for mathematical modelling of thermal errors through heat budget information.

Meanwhile, the current review found that process errors in the machine tools are the least modelled errors mainly due to the complexity involved and their random nature.

As the current research focuses mainly on Error modelling and measurement followed by prediction therefore it is important to analyze the work carried out in the field of error measurement.

1.1.1 Review of Error Measurement

Error measurement in machine tool have always been a laborious task where the measurement itself have been subdivided into direct and indirect measurements. Direct measurement allows the measurement of single error motion for a single machine component at a time, without any contribution from other axes or components. This can be further subdivided into online and offline measurements where online measurements refer to the measurements taken and used during the actual machining process while the offline measurement involves the interruption of process.

J.M. Fines et. al [13] presented an approach for positioning error compensation through measurement using a laser Interferometer. The authors record the difference in obtained and commanded positions as the position errors. The difference however, may constitute the error in motion due to control dynamics which has not been considered. S. Aguado et al. [14] presents a similar methodology where laser interferometer has been used for error measurement and subsequent compensation is carried out based on obtained measurement results. Bryan Jb. et. al. [15] used an angular interferometer that combined a laser beam and an angular mirror for measurement of angular errors. This however have the limitation that the rotation around axis cannot be measured using this method. Use of electronic levels provides a solution to this limitation. However, the existing studies have used them individually. It would however be interesting to observe the results obtained through combination of both techniques into one single technique. Another technique has been presented by Lin et al. [16] where the authors have evaluated the volumetric errors based on the joint configuration of the machine tools.

Existing literature also provides examples of direct measurements where standards such as ISO 230 series have been used to obtain the desired measurements. These are mainly used by machine tool manufacturers.

Indirect measurements have the ability of considering motion of and between multiple axis. This type of measurement can detect superposed errors associated with simultaneous motion of two or more machine axes. These methods may involve the manufacturing of a test artifact which links part errors to the machine errors enabling the assessment of the machine tool accuracy. Wang Jin Dong et. al. [17] presented a volumetric error compensation technique in which the measurements have been taken using Tracking interferometer. The experimental procedure involved the

collection of a large number of data points in space which are then used towards a measurement algorithm defined for each axis and their combinations. This therefore yields the error against each measured point.

Several indirect measurement approaches have also been used in the existing literature with focus on control based errors. These includes tracking Interferometer (TI) based measurement followed by generation of compensation values. These values are than used in form of look up tables in the controllers. Eung Suk Lee et al. [18] have made use of such a method for error measurement and compensation in a three-axis machine tool. The method utilizes measurements from Tracking Interferometer and volumetric error model to obtain the true position in each axis. In another control based error measurement and compensation technique M.A. Donmez et. al. [19] provided a mathematical model for error compensation that is based on comparison between true and measured position therefore providing the required compensation. Jie Gu et. al. [20] presented a global offset method for compensation of errors in machine tool. The method utilizes the difference between the intended and obtained dimensions of a part to provide the compensation data.

Meanwhile indirect techniques for thermal error measurement and compensation or prediction techniques have also been reported in the existing literature. One such study provided by Martin Mares et al. [21] focuses on measurement and subsequent control of thermal errors through control of participating sources. The method involves the measurement of temperature of different components of machine tool that is further used in a transfer function model to provide the necessary compensation. The measurement in the experiment involved the use of RTD (resistance thermometers) while the TCP deflection have been carried out through neural networks. Use of small number of thermocouples in the experiment (only 4 used where 70 were planned) calls for a reliability assessment of the obtained data. In contrast to this C.H. Lo. et. al. [22] have identified the need for using 80 thermocouples for temperature measurement to accurately predict the heat sources and the deflections caused thereby. K.C. Fan et al. [23] have also provided a method of measurement and compensation of thermal error through use of thermocouples for temperature measurement at critical points. The data is further combined with a displacement measurement to provide the time and position based error profiles. Chen et al. [24] have also provided an error measurement and compensation method that deals with the measurement of positional and thermal errors followed by compensation through an Artificial Neural Network (ANN).

Soichi Ibaraki [25] presented an R-Test setup for measurement of error motions on five axis machine tools. Similar R-test based kinematic error measurement has been presented by Bringmann et al. [26] which utilizes displacement sensors for measuring the relative position, in three dimensions, of a spindle mounted sphere. The experimental setup for the same is given as Fig 1.2 below. It is important to mention here that significant research have been done by this group for error measurement in rotary axis using R-Tests. Figure 1.3 shows an experimental setup for tracking interferometer. This is most commonly used measurement technique for evaluation and compensation of volumetric errors in machine tools.

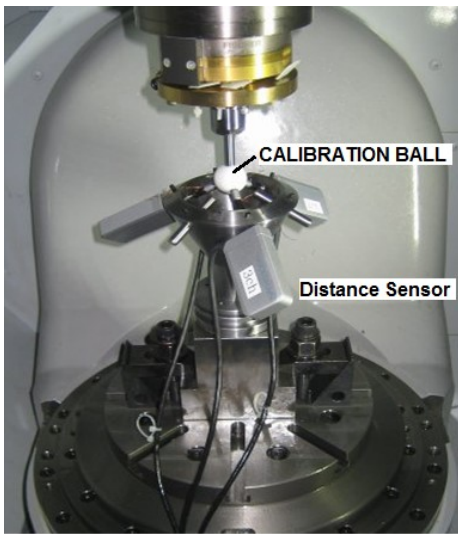


FIGURE 1.2 R-TEST SETUP

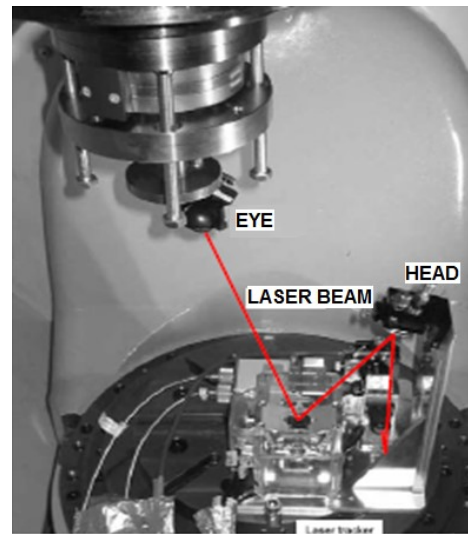


FIGURE 1.3 LASER INTERFEROMETER SETUP

Having reviewed some of the direct and indirect error measurement and compensation techniques, it may be of interest to establish at this point that there are some techniques which can neither be characterized as direct nor as indirect techniques. These techniques may only be described as an amalgam of both procedures. Among these non-conventional methods for error measurements Kentaro Ota et. al. [27] have presented an error measurement technique through on machine measurement of workpiece where measurements are than used for error analysis in the sensors.

JE Muelaner et. al. [28] presented a method for geometric error measurement through introduction of a complete solution path that utilizes a combination of techniques for step by step error compensation. The author has combined the use of artifact probing with probing of a machined workpiece. The errors at each step are evaluated and compensated. At first an artifact is probed for establishing a baseline which is further used to compare with the results obtained during

verification of the machine tool. It is important to notice here that such a practice can generate error compensation data but the effect of random errors may not be verifiable during such practice. This being since the random errors are prone to changes with changes in time domain and hence a one fit for all solution cannot be obtained through the current probing method.

Ji-HunJung et. al. [29] presented an approach which includes the use of touch trigger probe to perform complex dimensional measurements. These are then used towards generating compensation data. The compensation is directly applied on the same part to analyze the improvement and an improved post machining part geometry is reported. It is important to notice that this research performed a comprehensive on-machine part measurement and while the author appreciated the presence of position errors yet the errors are not separated by directly compensated. Soichi Ibaraki et. al. [30] also presented an approach for measurement of errors on a five-axis machine tool through a touch trigger probe.

While many methods use a touch-trigger based probe to evaluate errors there are methods that incorporates the use of touch trigger probes in conjunction with the workpiece measurement.

J. Mou et al. [31] provides an error evaluation method that utilizes different shapes for separation and identification of different error magnitudes. The evaluation is than followed by statistical analysis resulting in generation of characteristic error models. The technique however, focuses on geometry of the workpiece therefore falling short of providing an appreciation for thermal and process based errors.

Yoshitaka Morimoto et. al. [32] have presented a method in their study dealing with accuracy evaluation of a 5 Axis machining center. The authors have detailed a complete methodology for designing of a setup to eliminate the thermal elongation and other errors in the spindle. A setup with a stationary tool held in the spindle has been proposed where a rotary table rotates to perform the boring operation. The design of the workpiece has also been discussed in detail. The design takes into consideration the final requirement to evaluate the errors in each individual axis. It is however important to notice that a time-based error profiling is also missing in the current study. The study therefore can only evaluate the linear inaccuracies in the axis while the measured errors also includes the controller based errors, thermal elongations and tool deformations as well as

errors due to axis inertia. The final workpiece is measured using a CMM and the overall errors have been reported.

Sousa A.R. et. al. [33] have presented a technique for geometric test of machining center in which a probe is used against an artifact to measure the errors in positioning, straightness and squareness. The overall approach has then been developed into a software indicated as QUALIMAQ. The major advantage of this process is related to cost saving when comparing with the classical techniques. There have been numerous other approaches reported in the existing literature that utilizes a similar approach to the ones discussed above.

Soichi Ibaraki et. al. [34] have presented their work that includes the error identification through machining test and subsequently measuring the workpiece. The authors first modelled the kinematic errors of a five-axis machining center followed by a machining procedure definition to include all the required errors. The machining has been performed at different conditions defined by positions of rotary tilting table and linear axis. It is important to notice that several machining patterns have been identified in the study to help examine each kinematic error separately. The workpiece has then been measured to provide the actual error magnitude and the results have been reported. It is also vital to observe here that the error profiling have been carried out based on the position of axis and the corresponding effects on the error magnitude. The errors in time domain, thermal errors, errors due to controller and other feed and force related errors have not been examined in the study.

In another article Soichi Ibaraki et. al. [35] have furthered their study towards proposing a calibration method for rotary axis error motion of five axis machine tools. This study also discusses the method that can be used for thermal deformation tests. At first the modelling of errors has been done similar to the approach carried out in [30] followed by performing of finishing cuts at different heights and different axial positions on the workpiece faces. It is important to notice here that to reach a thermal equilibrium the author have indicated the initial run of spindle to obtain the thermal expansion therefore phasing out the effect of thermal errors as far as possible. The geometrical errors of the finished test piece are than measured and reported. A similar study by Soichi Ibaraki et. al. [36] also deals with the same subject matter. The results and the experiments performed are also identical.

A survey of the existing research being carried out in different industries have also been performed. While most of the industries are inclined towards use and improvement of laser interferometer based methods, no significant research has been found regarding the use of techniques for error measurement through machining a workpiece.

Meanwhile it has also been observed that most of the work being carried out in the field of error measurement through machined part dimensional analysis has been demographically distributed in east Asia including the Japanese and Chinese region.

1.2 Opportunity Analysis:

Throughout the survey of existing literature, the one error found to be either neglected or eliminated through use of alternative technique is the error due to thermal elongation of the spindle itself. Other similar errors, mostly changing in the time domain, related to the temperature changes have also been found as being less studied. The error due to machining process itself have also not been detailed in the existing literature. Therefore, a future research may also include the evaluation of errors being generated due to the machining process. These errors have been suppressed through use of techniques such as stationary tools. However, actual machining process always contains these errors therefore a combination technique based on error analysis with stationary tool followed by an actual rotating end mill may be able to quantify these errors. The study may then be moved further towards the quantification of actual increase in magnitude of error with the increase in magnitude of various elements causing such errors. Such a quantification can then be used towards a controller based compensation through use of a comprehensive data linking different parameters to the errors magnitude they may result in.

The position based errors have been studied in the existing literature. However, the number of articles providing the positioning based errors through measurement of workpiece are still limited and there is a need to improve the current methods through inclusion of error terms that have otherwise been neglected or over simplified.

There is a strong need to provide a comprehensive error profiling for the machine tool with changes in machine temperature. It is however important to notice that such profiling would generate a complete database where the error magnitude may be different at different temperatures and hence

for the compensation an adaptive compensation may need to be proposed. Such a compensation may include the error compensation based on temperature feedback of the machine. The resulting compensation however can be predicted as being very accurate in terms of removing the thermal and control errors.

1.3 Motivation and Objectives:

Although simple error reporting can be done through probing of machine using tracking laser interferometer or similar measurement equipment, yet it has been observed that the errors reported do not include the Thermal, process and control errors. The general approach is towards development of separate models for each error where the other errors are either neglected or eliminated. There is always a risk of overlapping and misreporting of error magnitudes in such cases. The cost of equipment used in such cases also adds to the limited applicability in general machining environment.

The current research focuses on development of an error determination and prediction methodology using the dimensions of a machined part measured through equipment generally available to a machine shop. The main motivation is to obtain the errors a prediction model that can predict the errors in different parts to be machined while using a different tool diameter, and machining parameters. The error model resulting from the application of such a methodology will have appreciation for mechanical errors, thermal errors, process errors and control errors.

The model can hence predict the errors for any workpiece prior to machining and also have the ability to provide the simulation for errors under different machining scenarios so as to obtain maximum material removal rate while keeping the manufactured parts within the desired tolerance limits. This would reduce quality costs and in turn reduces the cost of manufacturing operation.

The objective of current research is the development of a comprehensive technique for profiling, analysis and subsequent prediction of Mechanical, Thermal, Process and Control errors for a 3-Axis machining center that can be independent of part shape and size and generic with respect to the 3-Axis machine tool of application. To further Elaborate the statement, the current research focuses on achieving the following goals.

- Development of a technique with an end goal of prediction of , thermal, process and control errors with independence from part shape and size.
- Focused error generation based on the conditions proposed by the model through machining of workpieces.
- On-machine and off-machine measurement of errors, Regression analysis of errors and error separation.
- Development of error database for all errors with respect to input machining parameters.
- Prediction and validation of predicted errors for various machining conditions and part shapes and sizes.

1.4 Scope

The scope of current research includes error profiling for a three-axis machining center using workpiece machining followed by on machine and CMM based measurements. The study also seeks to provide a comprehensive error database for each of thermal, mechanical, control and process based errors. This database would therefore enable the appreciation of each category of error separately. Following will be the structure of the current research.

Chapter 1 presents Introduction of the problem and motivation while also laying down goals for the current research.

Chapter 2 details the Theory and Literature review related to error measurement and prediction.

Chapter 3 provides a detailed methodology proposed in the current research.

Chapter 4 presents the experimental Experiment Design and various machining parameters used for the current research.

Chapter 5 details the Results and a further Analysis of the reported results is performed and a final prediction model based on analysis is also presented in this chapter

Chapter 6 deals with Implementation of the developed model on two different scenarios.

Chapter 7 presents the summary of the current research along with a conclusion and identification of applications for the current research. Future research has also been made part of this chapter.

References are presented at the end of research.

Chapter 2. Theory

The errors observed on a machined workpiece surface are the accumulated form of all errors that can occur on a machining center during machining. These errors include process errors, control errors, thermal errors, errors due to fixturing inaccuracies and mechanical errors. The surface of a machined workpiece therefore provides a good opportunity for identification of errors. However, it is important to observe at this point that the errors apart from being in accumulated form their occurrence also overlaps. Similar machining parameters may be responsible for generation of multiple errors on a workpiece surface. Meanwhile the magnitude of such errors may be interdependent on each other. The interdependence of such errors therefore adds to the difficulty in their separation. Meanwhile without clear distinction between such errors, quantifying the relative effect of a set of machining parameters on the final errors can be cumbersome and unreliable.

2.1 Machine tool errors:

The determination of errors from machined workpiece requires the understanding and separation of all related errors. The first step towards developing such an understanding is establishment of all relevant contributors of errors in the overall error magnitude. The following section seeks to identify the effects and contributors behind each of the error categories under consideration.

2.1.1 Fixturing Errors:

In machining process, fixture is used to keep the position and orientation of a workpiece with respect to machine tool frame [37]. The first step towards the determination or measurement of errors on a machine tool is the determination of fixturing inaccuracies and their removal or incorporation in the overall results. The fixturing errors mainly occur in a machine tool during the setup due to various reasons. There are several contributors for the fixturing errors such as

clamping force, cutting force and inaccuracies in location. The most common of fixturing errors can occur due to the orientation or placement inaccuracies of a workpiece. An example orientation of a workpiece can have been presented here as Fig 2.1

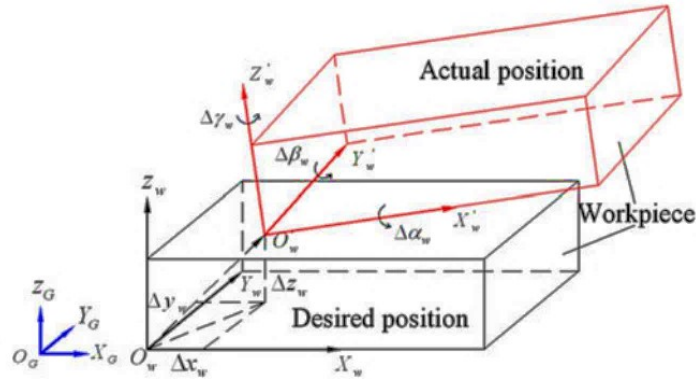


FIGURE 2.1 ACTUAL AND DESIRED POSITION DUE TO ORIENTATION ERROR

It can be observed from Fig 2.1 that due to the difference between desired and actual position of the workpiece there will be inaccuracies that can transform into final error on workpiece surface. Such fixturing errors may therefore also influence the overall process related errors mainly due to differences in radial and axial depths of cut. The differences may also cause a difference in the amount of heat generated during cutting hence disrupting any thermal error prediction while due to the overall location differences the mechanical errors would also be different from expectations. Any fixture developed for a machine therefore has the primary goals of fixing the workpiece at a desired position as well as keeping the workpiece rigid at the intended location with minimal effect of clamping force on the overall fixturing. However, dealing with such fixturing error is easier as they can be handled with the use of a customized positioning fixture as well as force tools.

There may however be fixturing errors due to location of the workpiece and fixture on a machine tool table. Such fixturing errors are mainly location sensitive with respect to the machine table and they may further result in differences in any measured mechanical, process or thermal errors on a machine tool. Therefore, any error evaluation that is based on error comparison with due to changing parameter requires the appreciation for the location of workpiece.

2.1.2 Thermal Errors:

Thermally induced errors account for 70% of the total errors [38]. Thermally induced errors can be most simply defined as the errors arising due to changes in temperature of machine tool

components and the subsequent thermal expansions. There have been several classifications in the existing literature for thermally induced errors. The simplest and most basic classification is based on the heat sources that generate such errors. This classification divides errors into two types that includes errors due to internal sources and those due to external sources. The internal heat sources may be spindle, lead screw, friction between various parts exhibiting relative motion and motors. The study of various articles revealed that the current literature dealing with thermal errors is overwhelmed with the studies on spindles of machine tools as these are core components and the largest single sources of heat generation in machine tools. The external sources however include heating bodies in close proximity and the environment. There have been several studies dealing with measurement and control of errors due to ambient temperature and other external sources.

Thermal error occurs due to the overall changes that various machine components undergo during a change in their temperature. The primary source of thermal errors is the changes in size and orientation of the spindle under the influence of heat generated within the spindle due to several factors including bearing friction and high speed of rotation. Meanwhile it is also important to understand that there is a cooling system applied in general that constitutes a part of spindle yet, due to high rotational speeds and the capacity and design constraints of cooling systems, the overall heat generated overwhelms the cooling system and hence the heat is further transferred to various components in the spindle assembly. An exaggerated heat source based machine deformation schematic is presented below as Figure 2.2.

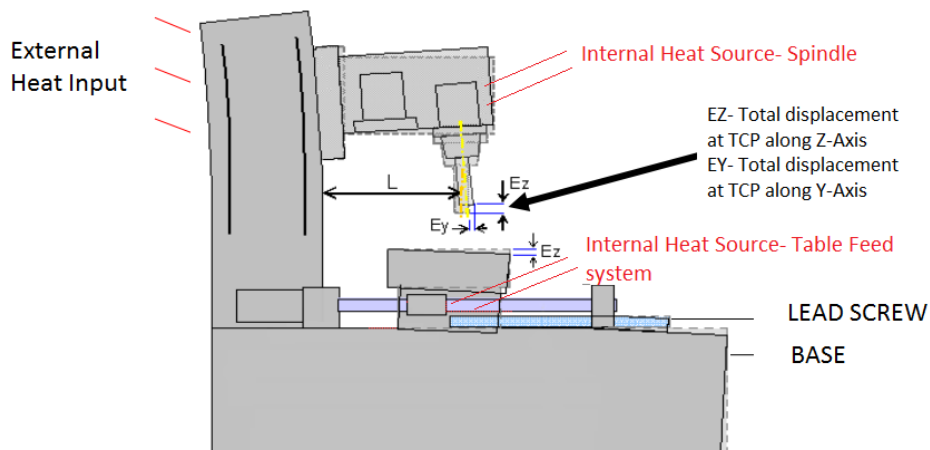


FIGURE 2.2 MACHINE DEFORMATION UNDER THERMAL INFLUENCE

Several approaches have been used for dealing with thermal errors in the spindle. These includes analytical approaches, Neural networks, Displacement measurements against temperature and

Numerical methods. Most analytical approaches utilize the total energy principle. However due to the transient nature of heat generation the equations must be converted into a time-based phenomenon, hence adding to the complexity of the problem. This in author's view is the major reason for the limited use of these models at industrial scale.

There are several methods for displacement measurement against temperature. ISO 230-3 [39] provides a complete test setup that includes the measurement of overall spindle distortions against the effect of both internal and environmental heat generating factors. The same has been presented here as Fig 2.3.

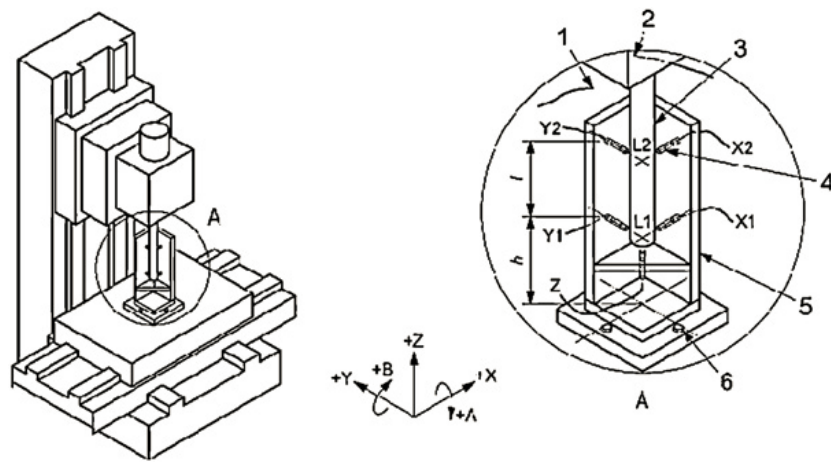


FIGURE 2.3 TEST SETUP FOR THERMAL DEFORMATION OF SPINDLE

Here the spindle is run for a specific period during which the displacement sensors, mentioned here as X1, X2, Y1, Y2 and Z, measure the change in position of the test bar Indicated as 3. This therefore provides the overall distortions and deformations of spindle in all three directions.

It is important to notice here that due to relatively lesser spindle speeds and slower motions involved in the feed drive systems, the overall heat generated is much less than that generated due to spindle. However, the same has also been studied in the existing literature.

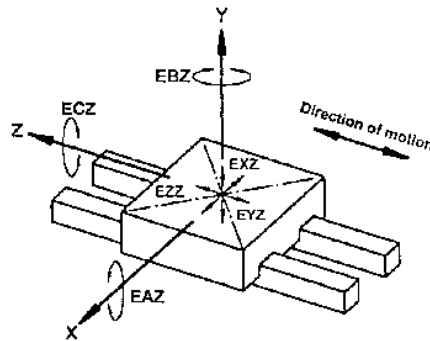
One of the different methods for thermal error measurement has been presented by Soichi Ibaraki et al. [35]. As discussed in the previous chapter the authors have proposed a test method for measurement of thermal error in a rotary table of a five-axis machining center. The method presented is one of its kind however, the use is limited to one spindle speed only and in the absence of a uniform heating maneuver the method may render results with high variations in accuracy depending upon the geometry of workpiece.

The current research however focuses on presenting a different model that takes into effect the requirement for a generic model that can not only measure but also predict the thermal errors for a range of spindle speeds. A uniform heating maneuver for both table and spindle ensures that the method provides the errors regardless of the shape of workpiece.

2.1.3 Geometric Errors:

Geometric errors constitute the largest part of errors after thermally induced errors. Geometric errors are mainly induced in the machine tools during either manufacturing due to manufacturing inaccuracies or due to assembly issues. These errors are therefore mostly systematic in nature and are easier to deal with in terms of measurement and compensation. The details for geometric errors will also be discussed in the later sections. All these errors contribute towards reduction in accuracy of machine tools and are therefore important to be compensated or controlled at source or before manufacturing. It is important to establish here that significant research have also been done for reduction of errors through control of errors at source rather than utilizing error measurement and compensation techniques. However, as discussed earlier in chapter 1 the control of these errors at sources poses a significant increase in the cost of manufacturing process which therefore calls for their post manufacturing determination and control.

Fig 2.4 show the six error components observed on a three-axis machining centre mainly due to reasons mentioned above. Notations corresponding to ISO230-3 have been used in all three figures.



- EXZ: horizontal straightness error motion of Z (straightness error motion of Z in X direction)*
- EYZ: vertical straightness error motion of Z (straightness error motion of Z in Y direction)*
- EZZ: positioning error*
- EAZ: pitch error motion of Z (tilt error motion around X)*
- EBZ: yaw error motion of Z (tilt error motion around Y)*
- ECZ: roll error motion*

FIGURE 2.4 GEOMETRIC ERRORS ON A THREE AXIS MACHINE TOOL

From the figure above it can be noticed that the respective errors in three linear axes and the three rotational errors can be defined by the equation 2.1 to 2.2.

$$\begin{aligned}
 e_{x(x,y,z)} &= E_{XX} + E_{XY} + E_{XZ} + [E_{BX} + E_{BY}] \cdot z - E_{CX} \cdot y \\
 e_{y(x,y,z)} &= E_{YX} + E_{YY} + E_{YZ} - [E_{AX} + E_{AY}] \cdot z \\
 e_{z(x,y,z)} &= E_{ZX} + E_{ZY} + E_{ZZ} + E_{AZ} \cdot y
 \end{aligned}
 \tag{Eq. 2.1}$$

$$\begin{aligned}
 e_{a(x,y,z)} &= E_{AX} + E_{AY} + E_{AZ} \\
 e_{b(x,y,z)} &= E_{BX} + E_{BY} + E_{BZ} \\
 e_{c(x,y,z)} &= E_{CX} + E_{CY} + E_{CZ}
 \end{aligned}
 \tag{Eq. 2.2}$$

There are however, a total of 21 error components in a three-axis machining center with vertical spindle orientation. These consist of three positional errors, six straightness errors, nine different orientation errors and three different squareness errors. Figure 2.5 represents the squareness errors between the three axes.

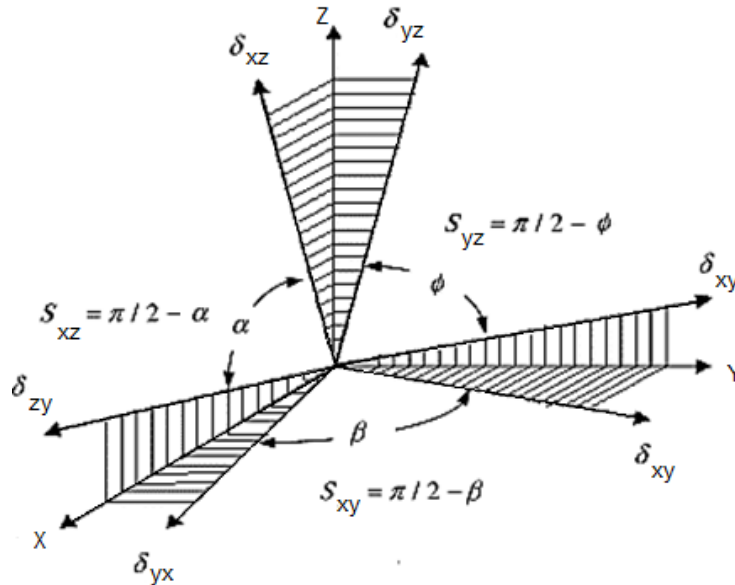


FIGURE 2.5 SQUARENESS ERRORS BETWEEN X, Y AND Z AXIS

The most common method for determination of such errors employees the use of Tracking Laser interferometer. Chana Raksiri et al. [40] have presented such an error model where the geometric errors have been modelled through use of an artificial neural network while the learning data for the network is fed by measurements taken through laser Interferometer. The author has than presented the total error in X and Y axis as following:

$$\begin{aligned}
P_x = & \delta_{xx} + \delta_{xy} + \delta_{xz} - \varepsilon_{zx} + \varepsilon_{yxz} + \varepsilon_{yyz} + S_{xy}y - S_{xz}z - \delta_{yy}\varepsilon_{zx} - \delta_{yz}\varepsilon_{zx} \\
& - \delta_{yz}\varepsilon_{zy} + \delta_{zy}\varepsilon_{yx} + \delta_{zz}\varepsilon_{yx} + \delta_{zz}\varepsilon_{yy} + \varepsilon_{zx}\varepsilon_{xy}z + \varepsilon_{zx}\varepsilon_{yy}z \\
& + \varepsilon_{zy}S_{yz}z
\end{aligned} \tag{Eq. 2.3}$$

$$\begin{aligned}
P_y = & \delta_{yx} + \delta_{yy} + \delta_{zy}\varepsilon_{xx} - \delta_{yz}\varepsilon_{zx} - \delta_{yz}\varepsilon_{zy} + \delta_{zy}\varepsilon_{yx} + \delta_{zz}\varepsilon_{yx} + \delta_{zz}\varepsilon_{yy} \\
& + \varepsilon_{zx}S_{xy}y + \varepsilon_{zx}\varepsilon_{yy}y + \varepsilon_{zy}S_{yz}z
\end{aligned} \tag{Eq. 2.4}$$

It should be noticed here that the Squareness error in each axis with respect to other axis is presented here with a symbol ‘S’. Meanwhile the overall orientation errors are presented with symbol ‘ ε ’.

Many similar research articles also form part of existing literature that utilizes a laser Interferometer for determination of position based errors. The use of Laser Interferometer is popular with the manufacturers also, due to reason that the same is accurate and less time consuming. The results are also generated in form of a step motion based error which can then be used towards building look up tables. Such tables therefore provide the machines with the ability to correct its position based on a predetermined error magnitude against a specific stroke length or position. The limitation of tracking laser Interferometer includes its limited ability to measure the rotation around axis due to the structural constraints of the equipment. Meanwhile it should be noted that the capital cost due to costly equipment reduces the possibilities of extensive use in machine shops across the globe.

There have been examples for use of machine touch probe in combination with CMM for measurement of position and orientation errors. Examples also exist in the current literature where artifact probing is used for measurement of position errors. Although these methods are shop floor friendly due to the nature of utilized equipment, yet, the number of articles dealing with errors in

such a manner are quite limited. An example artifact from [28] has been presented here as Figure 2.6.



FIGURE 2.6 ARTIFACT FOR ON-MACHINE PROBING

Meanwhile, it has also been noticed that the current studies consider the errors based on dimensions of workpiece only while the actual distance travelled by the machine tool for probing the surface is often different based on the probe diameter in case of an artifact probing or also the cutter diameter in case of using a machined workpiece as the errors profile available on the surface is due to the total distance moved by the machine that includes the cutter compensations. This in turn may generate error in the error identification.

The current research aims to utilize the machined dimension of a workpiece to obtain the overall errors of a machine tool with appreciation for various types of errors. Therefore, to serve the purpose position error are also obtained from the machined workpiece surface. It is important to note that the methodology proposed later in chapter 3 has the ability to provide the squareness errors, orientation errors and positioning error for each axis. The current research however also adds the consideration for the overall distance moved for error determination while also proposing a repeatability analysis for the touch probe in order evaluate the errors within the measured points. The same will be presented in the next chapter.

2.1.4 Process Errors:

Cutting forces are an important parameter of machining. As the whole workpiece and tool holding system along with the tool and workpieces are flexible to some extent therefore they are prone to bending and deflections under the cutting forces. This in turn generates errors on the surface of a machined part. Adding to the error is the fact that during a machining process, the cutting forces can change due to several factors. The changes in deflection hence causes changes in the errors observed on the machined workpiece. However due to the nature of the overall forces and the machining system the errors can be of a constant magnitude for a specific set of machining parameters. Further elaborating the statement, it can be safely assumed that the machining forces would be same for a specific material against a specific tool with a specific set of machining conditions such as Feed, Spindle Speed and radial and axial depths of cut. However, the forces may undergo changes in case any of the parameter is changed. This therefore necessitates that any study dealing with process based error takes into consideration the effect of all relevant machining parameters.

Several approaches have been adopted towards the determination of such errors, these include mostly analytical approaches while they also include some numerical approaches. R.E. Devor et al. [41] presented a cutting force model based process error prediction where the overall error is calculated based on the deflections calculated under the influence of cutting forces. The equation for cutter deflection is presented here as equation 4:

$$\delta = \frac{F}{6EI} [(z_F - z)^3 - (L - z)^3 + 3(L - z)^2(L - z_F)] \quad Eq. 2.6$$

Here the cutting force is represented as ‘F’ meanwhile ‘E’ represents the Young’s modulus, moment of inertial is represented by ‘I’, while ‘L’ is the total length of cutter outside the holder and the position of cutting force application is represented by ‘ z_F ’ followed by the position at which the deflection is being analyzed represented as ‘z’. The error is then compared with a measured error magnitude and the predicted results have been found as being 85-90% accurate.

C. Raksir et al. [42] have also presented a model that utilizes the mathematical model of [41] for calculation of cutting tool deflection as a part of an analytical model to predict the overall process

errors on the surface of a machined part. The author has further developed the deflection model into:

$$\sigma_t = \sigma_s + \sigma_f + \phi_s(L_f - z) \quad Eq. 2.7$$

$$\sigma_t = \frac{F}{6EI} [E(L - L_f)^3 + 3(L - L_f)^2(L - Z_f)] + \frac{F}{6EI_f} [(Z_f - z)^3 - (L_f - z)^3 + 3(L_f - Z)^2(L_f - Z_f)] + \frac{F}{2EI} [-(L - L_f)^2 + 2(L - L_f)(L - Z_f)](L_f - Z) \quad Eq. 2.8$$

Here δ_s represents the shank deflection while the flute deflection is represented by δ_f meanwhile ϕ_s is the angle due to deflection observed at the cutter shank.

The model is then used in an ANN for further predictions and the results are compared with process errors observed on the surface of a workpiece through machining of a hole and a slot. Figure 2.7 presents the schematic for the part used for verification.

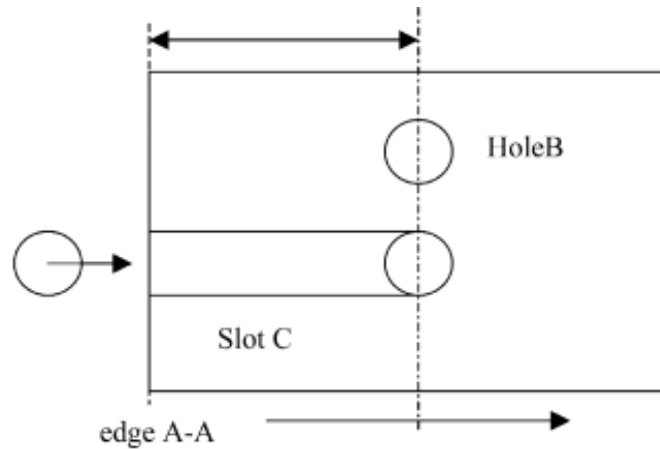


FIGURE 2.7 PART FOR PROCESS ERROR VERIFICATION

However, it should be noticed that the errors observed on the walls may also include the thermal errors as the spindle deflection towards one of the axis would generate a slot size larger than expected to be generated by process errors only. Meanwhile any inherent alignment errors may also take part in generating inaccuracies in the results.

Although the studies have dealt with the calculation of tool deflection only and the deflections due to workpiece and machine components have not been taken into consideration, yet it can be observed, and further mapped onto the whole case, that the deflection in all cases is proportional to the cutting force. The behavior of cutting force against machining parameters therefore needs

to be determined for analyzation of the effects of these parameters on the process errors. There are also similar approaches reported in the existing literature for the prediction of process errors.

The current research however, utilizes a radically different approach for the determination of process errors. A machined workpiece based methodology is proposed that determines the process errors based on the comparison of changes in error magnitude under the influence of changing machining parameters. The methodology has the capability to provide a database for process errors through use of a combination of machined data and model based software simulation. The detailed methodology will be laid out in the next chapter.

2.1.5 Motion errors due to Control:

When the CNC is given a command for execution of a certain motion, there is a possibility that the command is not executed in its entirety. Rather several issues pertaining to feed drive systems can cause the machine tool to either execute the distance command with an overshoot or undershoot. Such errors can be referred to as being errors due to control.

The control errors change due to displacement and feed. However, the magnitude of total control errors may vary due to the effect of cutting forces during motion. The avoidance of this portion of control errors requires fast and rigid response on the part of feed drive system. The absence of required level of response therefore results in motion control errors.

With the introduction to different errors and their sources it is also important to introduce the concept of error separation which constitutes an important part of the methodology proposed in the current research.

2.2 Error Separation:

Error separation has always been a topic of interest for many researchers that work towards determinations of several errors in a single model. Meanwhile the elimination of a particular error through source isolation has been the strategic focus for the researchers working towards determination and/or prediction of single type of error.

Generally, researchers focusing on determination of positional errors often tend to use methods that do not involve the generation of process or thermal errors. This is possible through use of

equipment such as Interferometer. Researchers working with metrology feedback, especially that employees the probing of artifacts also focus on positional error due to mechanical issues only and therefore the thermal and process errors are not considered. This may however be an oversimplification since the control errors may be present during the probing of artifacts or even during the motion tracked by Laser Interferometer therefore, there seems to be a requirement for an iterative process that can predict and compensate the actual thermal and control errors present during such processes. Examples of process error elimination through use of a stationary tool have also been found in the existing literature. However, they pose the potential issue of having a larger heat generation during the cut and excessive bending of tool or workpiece that in case of actual cutting may not be present. This hence limits their applicability.

The current research views the inclusion or isolation of all errors as mandatory for any error separation strategy to work. Therefore, the technique presented not only provides error isolation and separation but also focuses on the inclusion residual error magnitudes of all respective errors so that an improved magnitude of individual errors can be obtained.

2.3 Error Measurements through metrology feedback:

Error measurement for all type of errors through metrology feedback presents a unique opportunity to identify several errors in a single mode. The separation as discussed earlier is based on source freezing, error isolation and change determination. Metrology feedback techniques are user friendly however there are certain issues that have to be taken into consideration before reporting the actual measurements. These challenges have been highlighted in the following sub section.

2.3.1 Challenges in Error measurement:

With the error measurement in discussion, it is important to highlight the various challenges in error measurement. These challenges include the selection of correct measurement system, the design of proper experimentation that exactly depicts the true nature of measurements required. The measurement of all relevant error parameters is also important in the wake of errors being mostly superposed. In this regard taking care of all related errors and their effects is also of key importance here. A few literature articles were identified during this study that either neglects the effects of errors or fail to identify the superposed errors.

Repeatability and accuracy of measurement equipment is another challenge that is often seen neglected in the research. Only as few as 2 articles studied for the current research mentioned the accuracy and/or repeatability of measurement equipment in some form while the rest of the articles only mentioned the type of experimentation and the equipment used therein. The same trend was seen in review articles considered. A partial or in some cases total absence of measurement equipment, their properties and the possible usage areas was observed. It is however of extreme importance that the accuracy and repeatability of equipment be mentioned when dealing with the errors in machine tools. The number of experimental runs therefore to be performed should also be designed considering these aspects.

Alongside these challenges the selection of time domain gets important when dealing with errors that are dynamic in nature. In case of volumetric errors, it is also important to define the temperature states with respect to time of measurement as any variations in temperature would cause the errors to super pose and therefore there would be time dependant changes in magnitude of errors that may be reported towards volumetric errors only.

Once the issues in measurements have been taken into consideration and the incorporated into proposed methodology it would be important to calculate the actual position of any point on the surface of the workpiece under the influence of measured errors. A general relation used in [] has been reported in the next section for determination of actual position based on error magnitudes and desired position.

2.4 Conclusion:

The main purpose of presenting a theory is to lay down the several errors and their corresponding influence factors. It is therefore necessary to list the various factors to be considered in the proposed methodology:

- The mechanical position errors are to be related to the changes in position.
- The thermal errors due to spindle speed are changing in time domain however, the effect of spindle speed also has to be considered.
- The process errors must be linked with a cutting force base system as this would enable the prediction of errors under different machining parameters and cutting tool geometries.

- The control errors are prone to changes under the influence of cutting force. Such changes also need to be considered and the measured errors needs to be linked with cutting forces for prediction model.
- The effect of both displacement and feed needs to be considered when developing prediction models for Control errors.

Chapter 3. Methodology

The current research seeks to develop a comprehensive methodology for not only measurement of errors but also the development of an error database that can subsequently be used for error prediction prior to actual machining. Such a database can predict errors under the changing machining conditions and is therefore particularly helpful in determination of not only systematic errors but also random errors that are prone to changes under the changing machining conditions and time instance for machining.

Pertaining to the goals set in the previous paragraph and in the first chapter the current chapter details the proposed methodology for error measurement through use of machine workpiece. The proposed methodology treats thermal errors in a time-based scenario, process errors in a machining parameter based scenario, control errors in a feed and motion based scenario and the mechanical errors in a position based scenario. Once these laid out goals for each individual error are implemented through the methodology the overall model obtained carries the ability to provide error magnitude irrespective of the shape, size and machining time of a workpiece. It is also important to notice at this point that since the methodology is intended to serve both production as well as job shop scenarios, hence a slight variation in how the process errors are treated is also made a part of current research.

As the current research focuses on error determination through workpiece machining and measurement therefore the first step calls for a workpiece definition that can serve the purpose of supplying with different combinations of motions, feeds, speeds and surfaces. The workpiece defined in the following section has therefore been designed to deal with the different requirements for the current research.

3.1 Workpiece and Fixture Design:

The workpiece presented here as Figure 3.1 has been proposed for the current research.

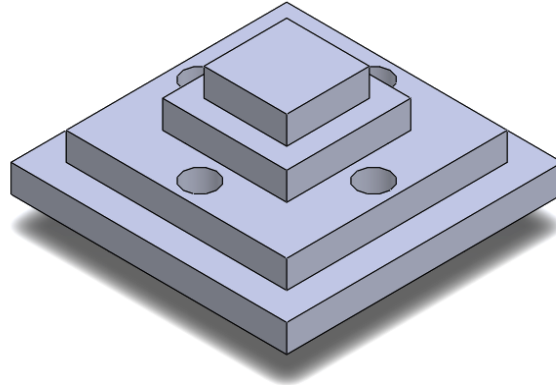


FIGURE 3.1 3D MODEL OF WORKPIECE

Aluminum 7071 is used as workpiece material. The workpiece has four steps progressively increasing in dimensions along both horizontal axis. Each step is designed to observe the effect of changing single or a set of machining parameters. The steps are also used to identify different thermal stages. Therefore, the workpiece has a total number of 20 faces that would be used to relate the changes in machining parameters to the obtained geometry. Figure 3.2 represents the detailed geometry of the workpiece.

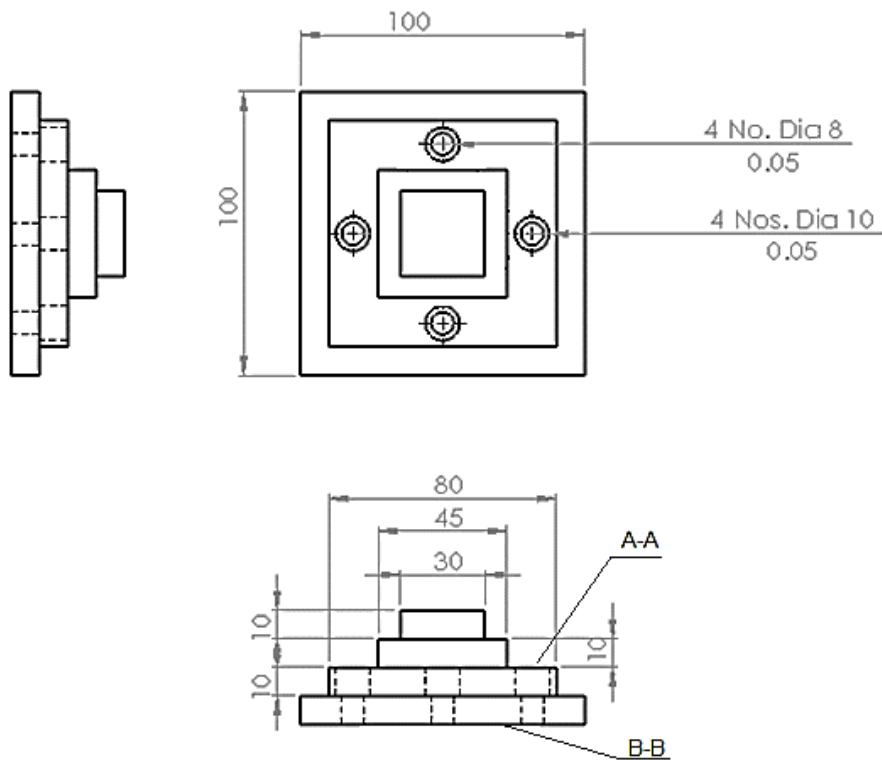


FIGURE 3.2 WORKPIECE DETAILED DESIGN

(ALL DIMENSIONS ARE IN MM)

As the current research is based on the separation of errors through use of a machined workpiece therefore for providing the actual magnitude of changes in various types of errors under the influence of changing machining parameters it is important to minimize geometrical anomalies during the workpiece preparation process. To attain this goal, the workpiece is to be prepared through a two-stage process to facilitate the decrease of fixturing error possibility in the later stages. The steps are detailed as following:

- Machining from top down with a finishing margin left as of 0.5mm on all faces except for drilling holes, which are drilled to their full diameter.
- The bottom face of the workpiece indicated in Figure 3.2 as B-B is to be machined with Face A-A set on parallel blocks. The contact with parallel blocks is ensured before the start of machining through light test and manually moving the blocks.

Step 2 is particularly important as any variation in parallelism would result in changes in process error. However, this in no way implies that a perfect parallelism is achieved following these steps but only the possibility of having a large process error variation is decreased.

Once the workpiece design is finalized the same is subjected to a total displacement analysis to assess whether the same can be used as a standalone component and to determine the bending expected in the workpiece due to machining based residual stresses.

For the process of analyzing the overall post machine bending in the workpiece it is assumed that due to deformations the workpiece experiences a change in shape with the outermost edge being deflected towards positive Z direction. To analyze the maximum effect of residual stress fixed constraints are used in places of screws and a force of 90 N applied on the outermost edges of workpiece. The resulting analysis indicates that the workpiece experiences a deflection of about 0.7 micrometres at the maximum deflection points while there is a persistent presence of deflection throughout the workpiece geometry with gradual decrease in magnitude of the same from bottom up. The result of analysis is presented here as Figure 3.3.

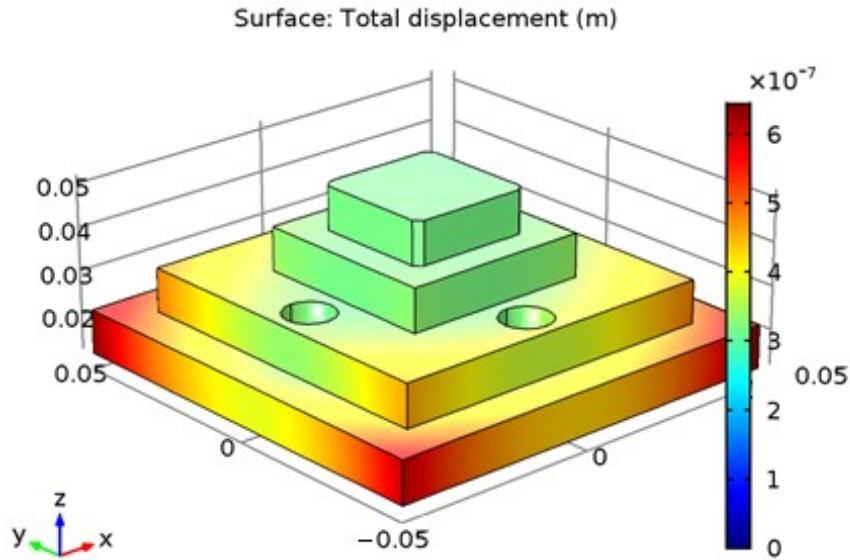


FIGURE 3.3 DEFLECTION OF WORKPIECE UNDER SIMULATED RESIDUAL STRESS (90N)

The force is further gradually increased to 1000 N to observe the changes in workpiece geometry under the influence of residual stresses. The results indicate a total deflection of approximately $7\mu\text{m}$ observed at the maximum deflection point. The same is presented here as Figure 3.4

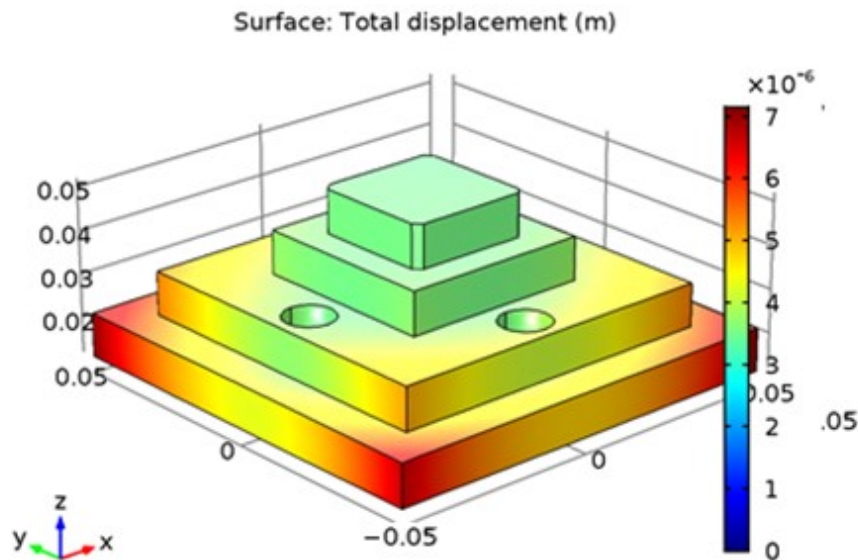


FIGURE 3.4 DEFLECTION OF WORKPIECE UNDER SIMULATED RESIDUAL STRESS (1000N)

The analysis indicates that the workpiece is prone to deflections as soon as the clamping forces are removed. Once taken to CMM the difference in clamping forces may play a vital role in causing

major differences in actual and observed errors. Apart from bending issues one other major issue is regarding the correct flushing of the workpiece surface B-B with the CMM table surface.

There is a need to resolve these issues before the procession of actual experiment. To remove such issues a fixture design is proposed. The fixture made of stainless steel with a circular geometry with threaded holes for workpiece clamping is proposed. Meanwhile it should also be noted that the fixture is to be machined on a Lathe machine with both faces prepared as per geometrical requirements presented in Figure 3.5. It should be noted at this point that any issues in parallelism between the two fixture surfaces in contact with table and workpiece simultaneously will not affect the final measurement due to their consistency in terms of presence on both machine table and CMM table.

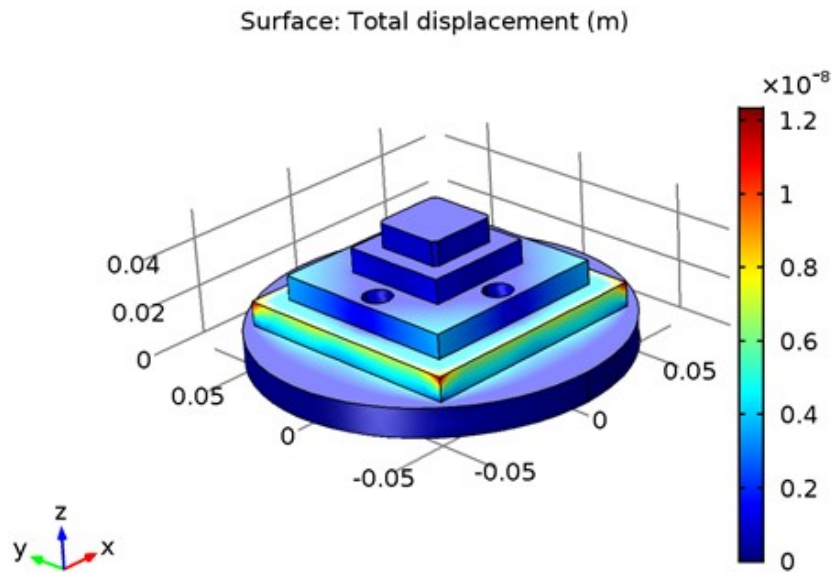


FIGURE 3.5 DEFLECTION AFTER FIXTURE ADDITION UNDER 90N FORCE

The fixture is further subjected to analysis on similar conditions and it can be notice that a force of 90 N when applied on the workpiece as bending force in presence of fixture brings about a deflection of approximately 0.012microns with the maximum amplitude only occurring at the edges. Meanwhile by increasing the force up to 1000 N the overall deflection observed at workpiece corners towards positive Z direction the increases to 0.12microns. This observation is important as it suggests two important perspectives. The first one is the direct change observed in the bending of workpiece which presents improved results with the use of fixture in form of lesser bending observed. Meanwhile it has also been observed that the fixture itself does not exhibit any

considerable bending due to the residual forces applied on the workpiece. The results of both analysis have been presented here as Figure 3.6.

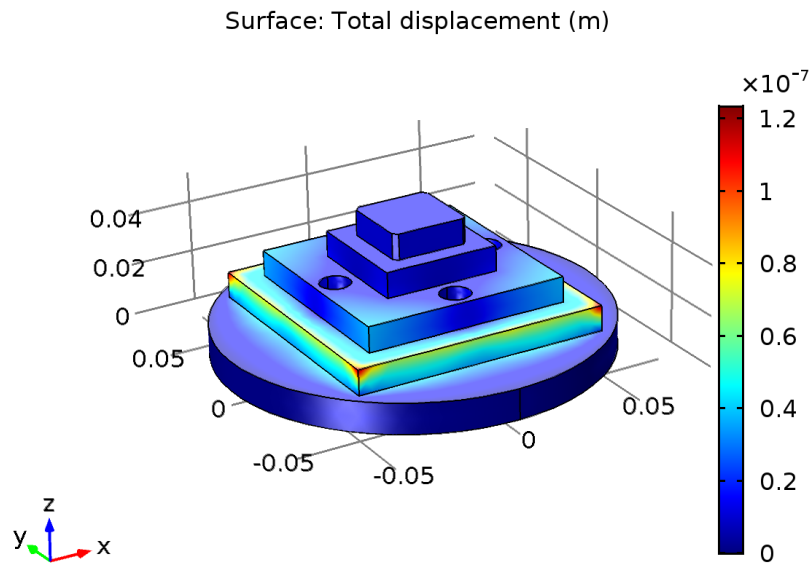


FIGURE 3.6 DEFLECTION AFTER FIXTURE ADDITION UNDER 1000N FORCE

It can therefore be safely assumed that the use of Stainless steel fixture will provide a better result where the aim is to minimize and hence neglect the deflection in workpiece due to residual stresses generated during machining. The next step therefore is to proceed with the machining of workpiece.

3.2 Workpiece machining requirements

The machining is carried out on Mazak three axis machining center. The machining is to be carried out under various, predetermined conditions. These conditions include several variations of feed speed and the overall distance to be machined with a specific feed and speed. The combinations will then be used to determine different error magnitudes while also enabling us to perform statistical analysis of the data as required.

The first the workpiece is machined with each step machined at a different temperature state. The first step and top surface are machined immediately after the machine start and the temperature state is taken as 'To'. For the subsequent steps the temperate state for both the spindle and the axis is changed. The temperature state for the spindle is changed through idle running at a specific speed for a specific time interval. The temperature state for the table is changed through a

specifically designed maneuver for the axis. The maneuver resembles the actual machining of the workpiece with no cutting. Same feed and spindle speeds are used for all steps for the first workpiece. Hence it can be safely assumed that the errors due to feed and spindle speed are similar in magnitude. Table 3.1 provides a detail for the machining condition for all workpieces and the errors expected therein.

TABLE 3.1 CUTTING CONDITIONS AND EXPECTED ERROR BEHAVIOR

Workpiece	Machining Conditions	Expected Error changes	Comparison Workpiece/s
W1	Cutting Feed 100 Transition Feed 100 Spindle Speed 3500 rpm	<ul style="list-style-type: none"> • Changing Position Errors • Changing Thermal Errors • Constant Process Errors • Constant Control Errors 	W6, W7
W2	Step wise Cutting Feed Change Transition Feed 1200mm/min Spindle Speed 3500 rpm	<ul style="list-style-type: none"> • Changing Position Errors • Changing Thermal Errors • Changing Process Errors • Changing Control Errors (Due to Position only) 	W5, W8
W3	Step wise Spindle Speed Change Transition Feed 100 mm/min Cutting Feed Multiple (Verification experiment)	<ul style="list-style-type: none"> • Changing Position Errors • Changing Thermal Errors • Changing Process Errors • Changing Control Errors 	Verification workpiece for errors
W4	Repetition of W1 for statistical Significance	<ul style="list-style-type: none"> • Changing Position Errors • Changing Thermal Errors • Constant Process Errors • Constant Control Errors 	W6, W7
W5	Step wise Cutting Feed Change Continuous Tool path Spindle Speed 3500 rpm	<ul style="list-style-type: none"> • Changing Position Errors • Changing Thermal Errors • Changing Process Errors • Changing Control Errors (Due to Force and position) 	W8, W2
W6	Cutting Feed 100 Transition Feed 100 Spindle Speed 1000 rpm	<ul style="list-style-type: none"> • Changing Position Errors • Changing Thermal Errors • Constant Process Errors • Constant Control Errors 	W1, W7
W7	Cutting Feed 100 Transition Feed 100 Spindle Speed 5500 rpm	<ul style="list-style-type: none"> • Changing Position Errors • Changing Thermal Errors • Constant Process Errors • Constant Control Errors 	W1, W6
W8	Step wise Cutting Feed Change Transition Feed 100 Spindle Speed 3500 rpm	<ul style="list-style-type: none"> • Changing Position Errors • Changing Thermal Errors • Changing Process Errors • Constant Control Errors 	W5, W2

Once the workpieces have been machined the next step is the measurement of respective errors through a sequence of steps. The first step is measurement of separation of errors through on machine probing.

3.3 Experiment design for position error profiling

The measurement of position error through metrology feedback has been done through various approaches where the most common approach is through probing of artifacts or in case of use of machined part, the probing of machined part is done followed by part measurement. Such probing is either done through a touch probe or a simple dial gauge.

In case of measurement on a machined workpiece the procedure includes the machining of workpiece followed by a substantial cooling period. Once the machine has cooled down a dial gauge or touch probe is used to provide the overall dimension of the workpiece measured through a reading on the machine control panel at the dial gauge and/or probe's zero positions on the surface of the workpiece. This is followed by a measurement of the workpiece outside the machine. It is important to notice here that being 'blind' of its own positional errors the machine will only be able to provide a measurement that includes the actual dimension of the part in combination with the process, control and thermal errors. Therefore, a difference in dimensions obtained on and off the machine would provide the actual magnitude of position errors.

This procedure has been used for measurement of positional error for the current research and an extensive study over the use of touch probe was conducted. During the initial measurement tests through the touch probe it has been observed that the accuracy of measurements, to be obtained on machine, is limited by the sensitivity of the touch probe which in most cases falls within a few micrometers. However, as the methodology relies on the difference of error magnitudes obtained due to changes in machining parameters therefore the repeatability of touch probe needed to be analyzed. The same was done by making random measurement repetitions during the experiment and comparison of final results. The observation made for step 3 of workpiece 8 has been presented here as Figure 3.7.

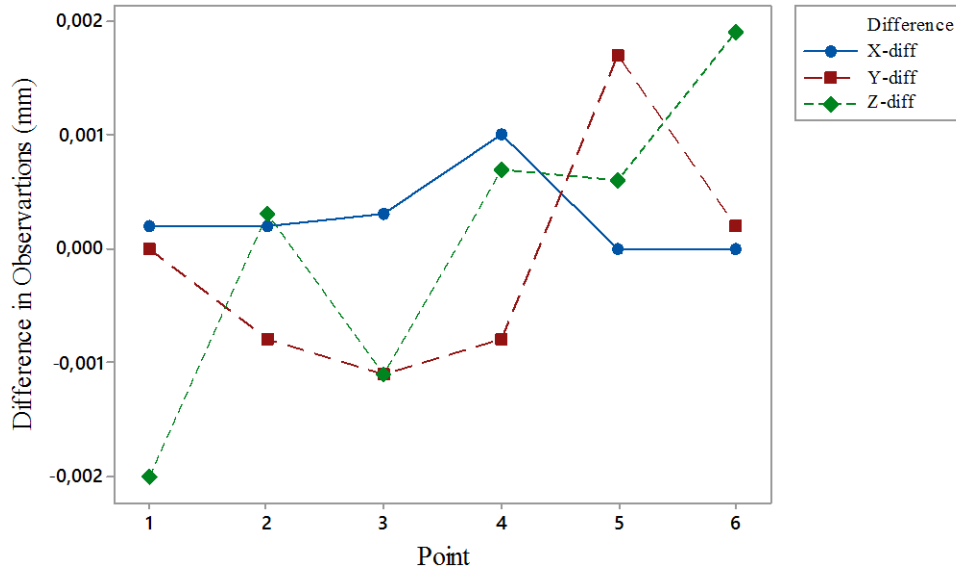


FIGURE 3.7 DIFFERENCE IN REPEAT MEASUREMENT USING TOUCH PROBE

Once it has been established that the repeatability has a maximum value of $\pm 2\mu\text{m}$ the touch probe is deemed feasible for use. However, the use of touch probe also presents a further challenge. As touch probe measure the part location with respect to the spindle center therefore the actual moment or the tool path is not considered. This results in minor adjustments made in the measurements regarding the actual movement and movement during measurement. Hence position error due to unreported movement is also associated with the overall position error for a reported movement of axis.

To avoid the above-mentioned issue the offset distance for the same amount as the tool is incorporated in the overall distance reported against measured position errors.

It is important to notice that the simplicity and robustness of touch probe with respect to setup and measurement ability warranties the favoring of touch probe over other instruments.

3.4 On machine probing of workpiece:

During the on machine probing 09 different points are measured on each face. The selection of these points takes into consideration the overall bending observed in the analysis of workpiece. The points are than used to provide a complete error profile for the workpiece. Figure 3.8 presents a view of such points selected on the workpiece surface.

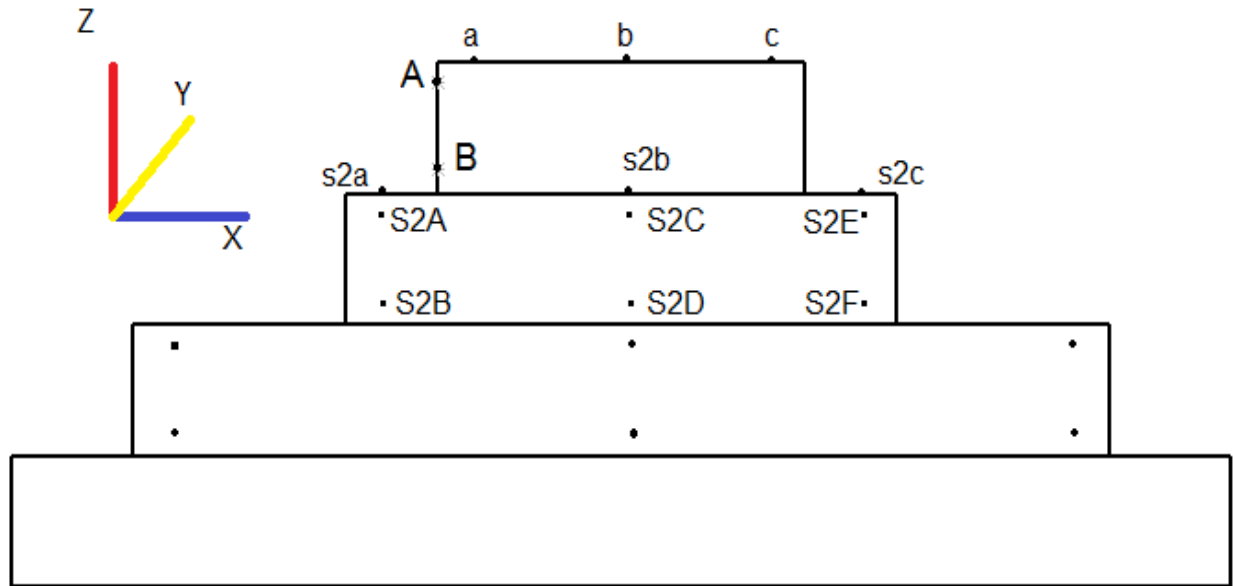


FIGURE 3.8 MEASUREMENT POINTS ON THE SURFACE OF WORKPIECE

It can be observed from figure 3.8 that the X-coordinates of point A and B should ideally be the same however, on measurement after machining they may change. This may happen primarily due to table alignment error and possible spindle deflections due to changes in spindle orientation under influence of increase in spindle temperature. The difference in X coordinate of both points and the distance between them in Z-direction will therefore provide us the overall inclination angle observed due to combined effect of spindle deflection and table tilt under the influence of thermal and process errors only. The reason for the non-inclusion of mechanical errors in the observation is that the machine is itself ‘blind’ towards its own mechanical errors and therefore the errors reported will not include the errors due to mechanical orientation misalignments. Meanwhile it is also important to understand what type of misalignments will contribute to which errors on a surface. The following subsection intends to establish that understanding particularly regarding separation of errors due to table and spindle tilt.

3.4.1 Separation of Spindle and table tilt angles:

Once the magnitude of tilt angles on various surfaces under the influence of process and thermal errors has been obtained it is necessary to separately identify the table and spindle tilt angles. For such an identification, it is mandatory to explain the actual cutting process and the effect that each tilt angle may have on the different faces. Figure 3.9 is presented here for such demonstration.

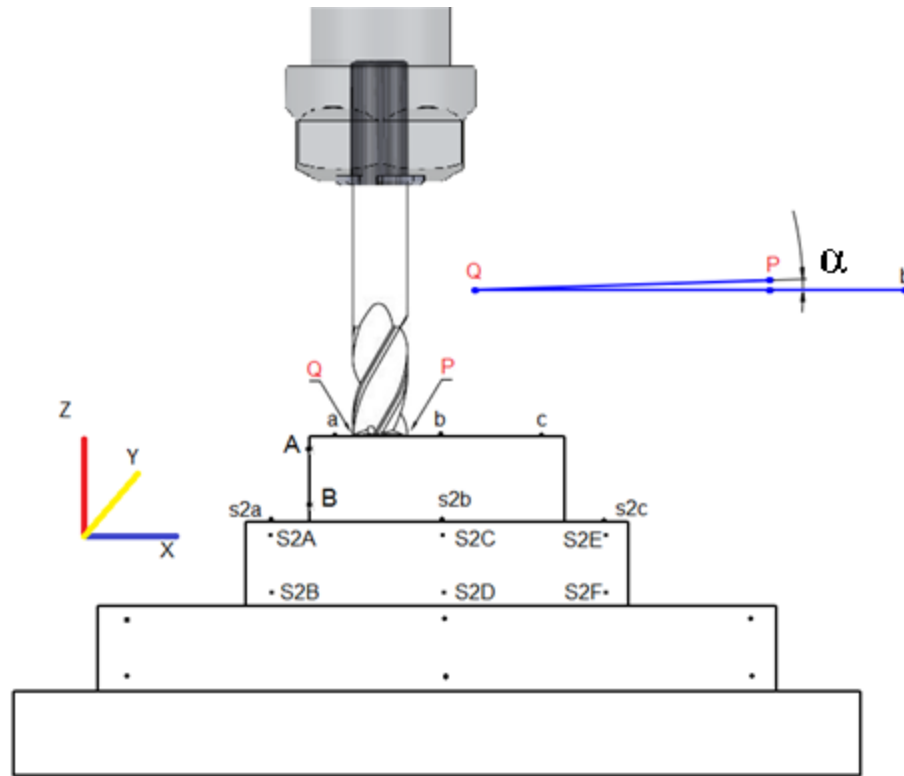


FIGURE 3.9 SPINDLE TILT DEMONSTRATION

It needs to be observed from the above figure that an anticlockwise spindle tilt will cause the two points 'P' and 'Q' differ in distance from a horizontal surface. If a straight line is drawn between the two points the overall angle between the line represented by PQ and the horizontal will be represented by 'alpha'. This however will not create any effect on the generation of final surface of workpiece. If there is in fact a tilt angle observed due to difference in Z-height of point 'a' and 'b' during the probing of workpiece on the machine itself, that tilt angle is due to table tilt under the influence of thermal and process errors only. Therefore, the angle observed will be reported as table tilt angle. The mathematical formulation will be presented in the later part of this chapter.

Meanwhile it is also important to understand the effect of spindle tilt on the final workpiece geometry. The same is represented here as Figure 3.10.

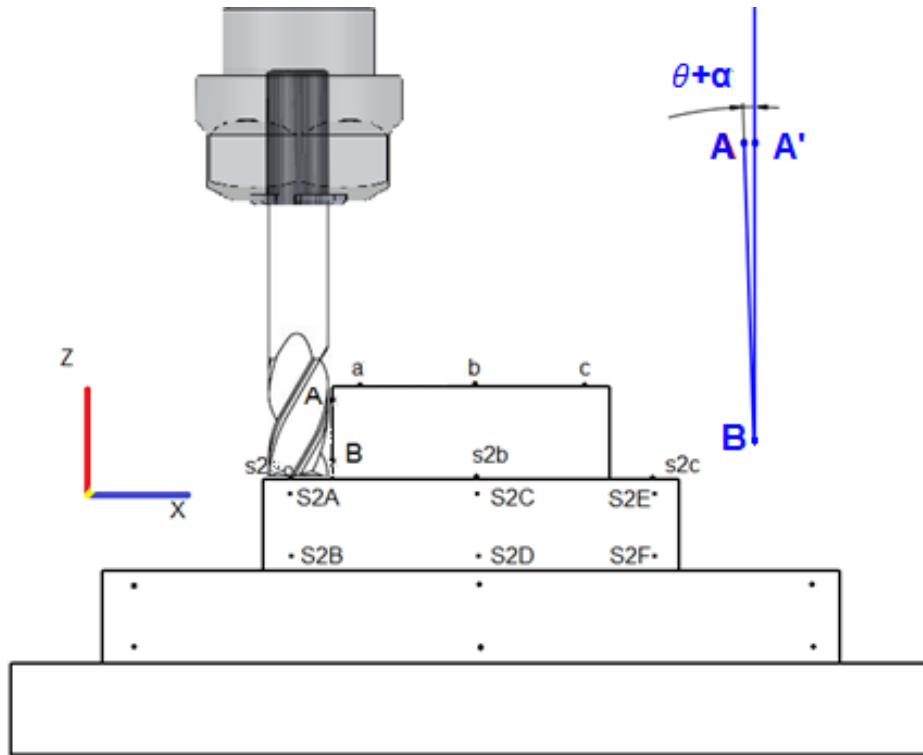


FIGURE 3.10 EFFECT OF SPINDLE TILT ON THE FINAL WORKPIECE GEOMETRY

It can be observed that the points represented by capital letters 'A' and 'B' may have a difference in their respective X-Axis coordinates. This difference therefore means that the actual geometry will be at an angle with the Z-Axis. It should be notice here that the point obtained after machining represented by 'A' and the actual point represented by 'A'' may have a difference in Z height but due to the small angle the arc connecting A-A' can be considered as a straight line. The resulting geometry therefore would provide the angle obtained due to combination of table and spindle tilt angles. The same has been represented in Fig 3.13 as ' $\theta + \alpha$ '. A simple subtraction operation provides the spindle tilt angle under the influence of Thermal and process errors.

3.5 Determination of thermal Errors:

From the obtained probing data, the stepwise change in errors in X, Y and Z axis can be obtained through comparison of probed dimensions with the actual dimension.

It Is also important to establish at this point that the overall error magnitude of process errors remains constant while the control errors due to feed and speed are also of constant magnitude

because of no changes in the machining parameters. The thermal errors however change in each step and therefore any increase or decrease in the magnitude of overall errors would be due to the changes in thermal errors. Figure 3.11 represents the condition of workpiece at various steps.

It is important to mention here that in Figure 3.11 K and L represents the surfaces made while starting the machine at time 't=0'. Therefore, it can be safely assumed that the error due to thermal expansion of the spindle is minimal. Once the spindle has been heated up the cut represented by height h_7 and surface 'M' is made. As the other parameters are constant therefore it can be concluded that the difference in dimension between 'h3' and 'h7' provides the magnitude of spindle expansion in Z direction. The same can be mathematically represented as:

$$e_{splz} = h_7 - h_3$$

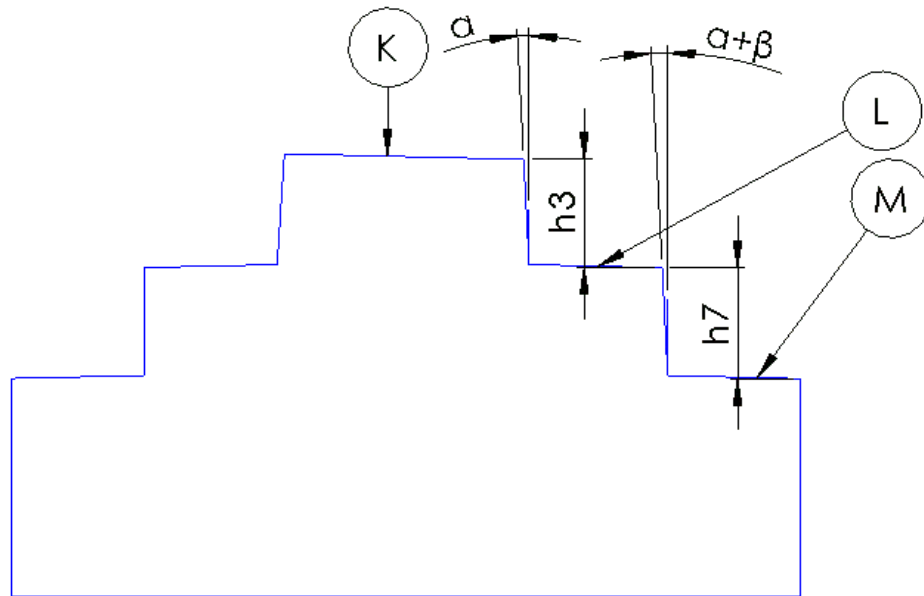


FIGURE 3.11 WORKPIECE GEOMETRY UNDER THERMAL ERROR INFLUENCE

However, only the expansion in Z direction may not be enough to define the overall behavior of spindle undergoing changes due to increase in temperature. For a complete error profile, the tilting of the spindle along both X and Y direction also needs to be investigated. Since from the last section the magnitude of angle represented by ' α ' is known along both X and Y directions therefore the new spindle tilt due to temperature changes can also be evaluated. As represented in Fig 3.12 it is apparent that due to the new tilt in spindle; the angle formed would be greater or lesser than that previously obtained. Therefore, a difference in new and previous angle will provide us with

the actual value of spindle tilt due to thermal deflection only. The same can be mathematically represented as:

$$e_{spdx} = \alpha_x - (\alpha + \beta)_x \quad Eq. 3.1$$

$$e_{spdy} = \alpha_y - (\alpha + \beta)_y \quad Eq. 3.2$$

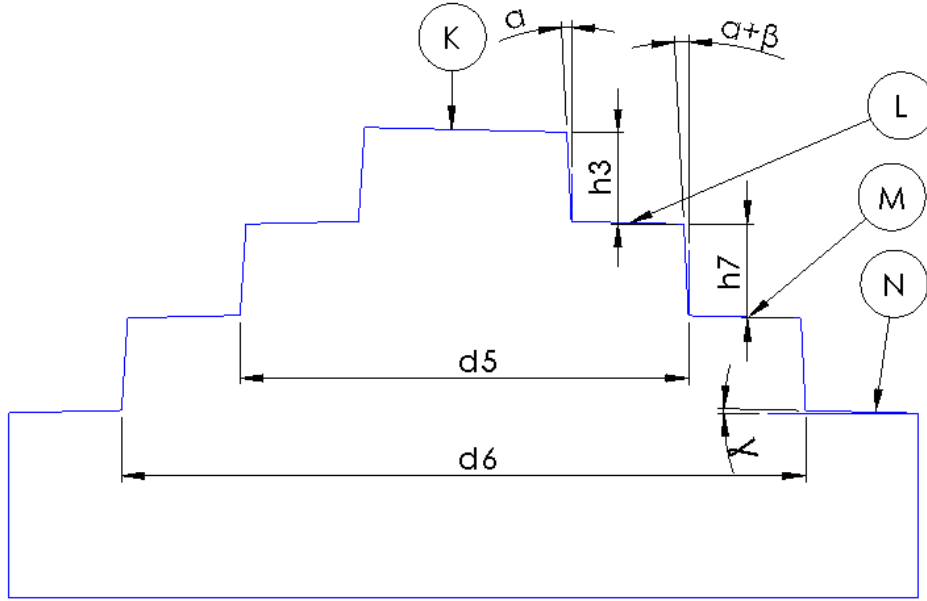


FIGURE 3.12 THERMAL ERROR INFLUENCE -TABLE TILT

It can be observed from Fig 3.12 that the new table tilt angle can be measured through measurement of angle denoted by 'Y'. The change in tilt angle due to thermal deflection of table components can therefore be denoted as:

$$e_{ttx} = \theta_x - \gamma_x \quad Eq. 3.3$$

$$e_{tty} = \theta_y - \gamma_y \quad Eq. 3.4$$

It is important to notice that not only the change in tilt angle but also the overall change in dimension due to change in temperature can also be evaluated through a comparison of difference of the dimensions denoted as 'd5' and 'd6' against their respective dimensions mentioned in equation below as d_{5xa} and d_{6xa} respectively. Here e_{ptx} represents the stepwise thermal error.

$$e_{ptx} = (d_{6x} - d_{6xa}) - (d_{5x} - d_{5xa}) - (e_{pos_x}) \quad Eq. 3.5$$

$$e_{pty} = (d_{6x} - d_{6xa}) - (d_{5x} - d_{5xa}) - (e_{pos_y}) \quad Eq. 3.6$$

It is important to notice here that the terms e_{ptx} and e_{pty} are initially taken as zero as the thermal state of machine is near to zero. Yet their actual magnitude will be reported and compensated in final thermal error calculations and the corresponding regression for thermal error.

The increase in error in each step is taken as being due to thermal error only and the trend for various elements of thermal error is used for regression analysis. The regression analysis is performed with an open value for Y-intercept. The value obtained for Y- Intercept hence represents the constant magnitude of errors other than thermal errors at actual thermal zero stage. ' T_o ' is however evaluated through use of actual time.

3.5.1 Changing the thermal state:

Once the thermal error at two different points in time, with respect to different temperatures, have been evaluated the next step is repetition of the same experiment under two more thermal conditions with the same spindle speed and feed parameters. Once completed, the thermal error is known for at least three different temperature states. This is then plotted on a time scale to provide the change in error magnitude through time based on different spindle speeds.

There is however a change in the cutting forces when the spindle speed is changed and therefore the process and control errors change in different thermal stages. However, as the error determination process is based on the increase in error magnitude only and since the process errors are constant, therefore the comparison of dimensions at several steps after subtraction of position errors will provide the thermal errors for each temperature stage. The inter-stage error prediction is further obtained through the following equations:

For prediction between State 1 and 3 (3500 rpm and 5500 rpm respectively):

$$e_{pt_{xpred}} = ((Spindle\ speed - 3500)/2000) \times (e_{pt_{1x}}) + ((5500 - Spindle\ speed)/2000) \times (e_{pt_{3x}}) \quad Eq. 3.7$$

For prediction between Stage 1 and 2 (3500 and 1000 rpm respectively):

$$e_{pt_{xpred}} = ((Spindle\ speed - 1000)/2500) \times (e_{pt_{2x}}) + ((3500 - Spindle\ speed)/2500) \times (e_{pt_{1x}}) \quad Eq. 3.8$$

For Prediction Below Stage 1 (Below Spindle Speed 1000 rpm):

$$e_{pt_{xpred}} = (Spindle\ speed/1000) \times (e_{pt_{1x}}) \quad Eq. 3.9$$

For Prediction above Spindle speed of 5500 rpm the following formulae is proposed.

$$e_{pt_{xpred}} = (Spindle\ speed/5500) \times (e_{pt_{3x}}) \quad Eq. 3.10$$

Similar equations are developed for all errors in each respective axis. A completed form of all equations is presented in chapter 5 under results and analysis. Once the thermal error profiling is completed the model provides the magnitude of thermal errors for the actual temperature states. Hence the overall magnitude of control and process based errors can be obtained through subtracting the position error due to mechanical issues and the thermal error at the machining time instance.

The complete process is depicted in form of flow chart presented here as figure 3.13.

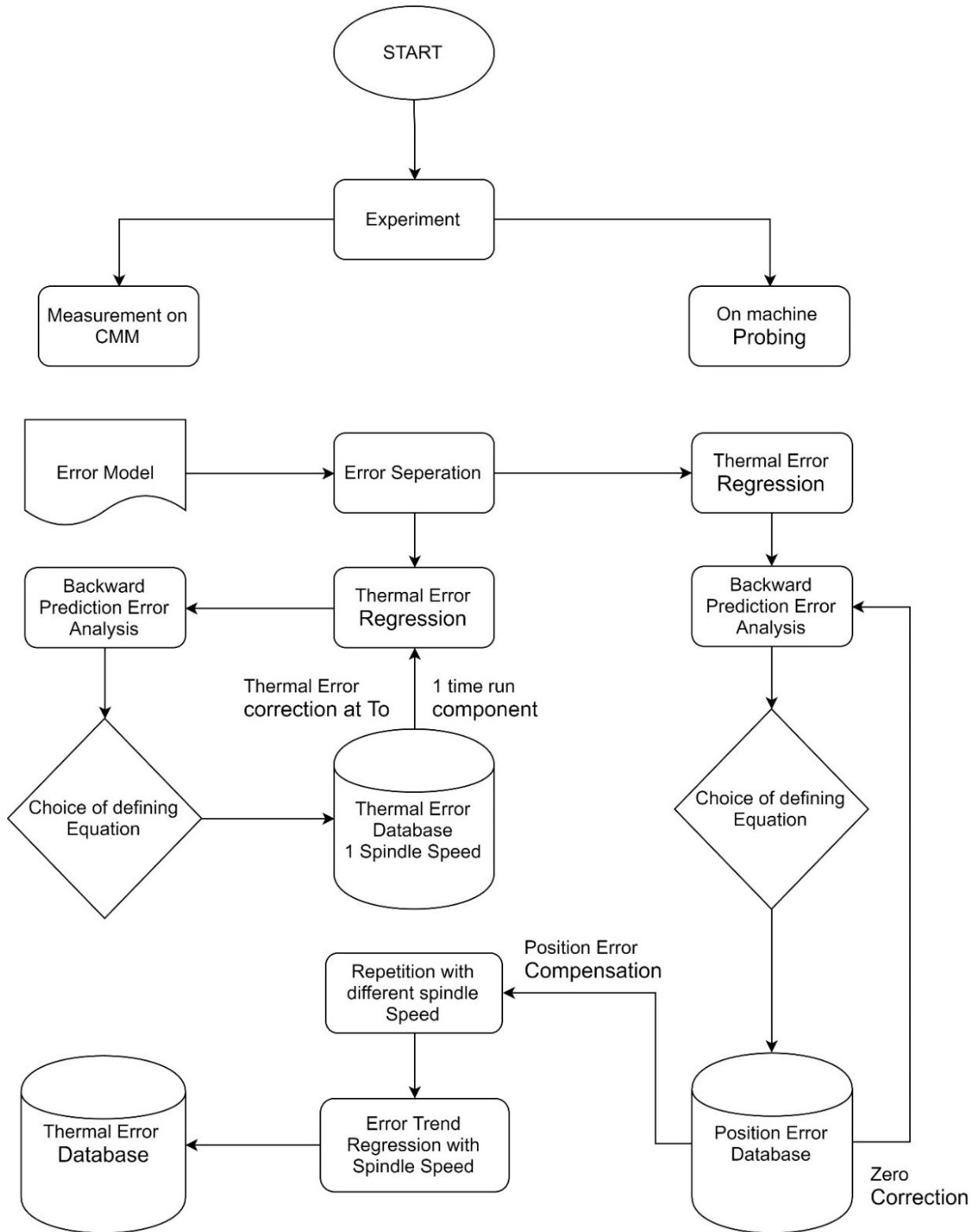


FIGURE 3.13 PROCESS FLOW FOR THERMAL ERROR EXTRACTION

3.6 Feed based process and control Errors:

The process and control errors due to feed are known to be interdependent. This can be further elaborated by the fact that once the cutting feed is changed the cutting force undergoes changes. The resulting changes in cutting forces effects the process errors while the forces also cause errors in motion due to changes in loading conditions on the servo drive and other elements. Meanwhile as asserted earlier, a complete shape and size independence can only be achieved for an error prediction model when the process and control errors are separately identified. It is therefore mandatory to devise a strategy for separation of control errors from the process errors. The following methodology is therefore proposed as part of current research for such error separation.

3.6.1 Process Errors due to feed

At first different feed is used while cutting each step of workpiece 8. Meanwhile the transition between two different surfaces on the same step is made through a non-cutting path with minimal feed. This ensures that the difference in errors on the workpiece surface is due to changes in cutting feed only. The tool path is presented here as figure 3.14

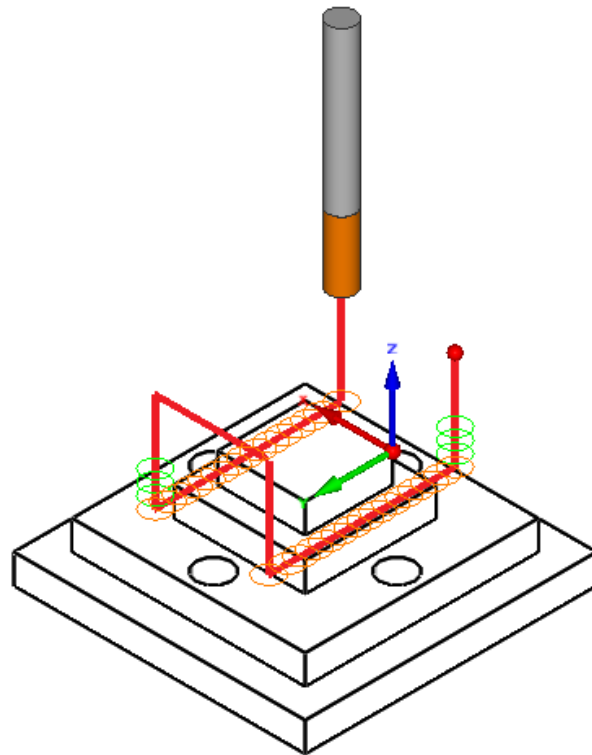


FIGURE 3.14 TOOL PATH FOR FEED BASED PROCESS ERRORS

Meanwhile Figure 3.15 represents a tentative workpiece surface to be obtained after machining.

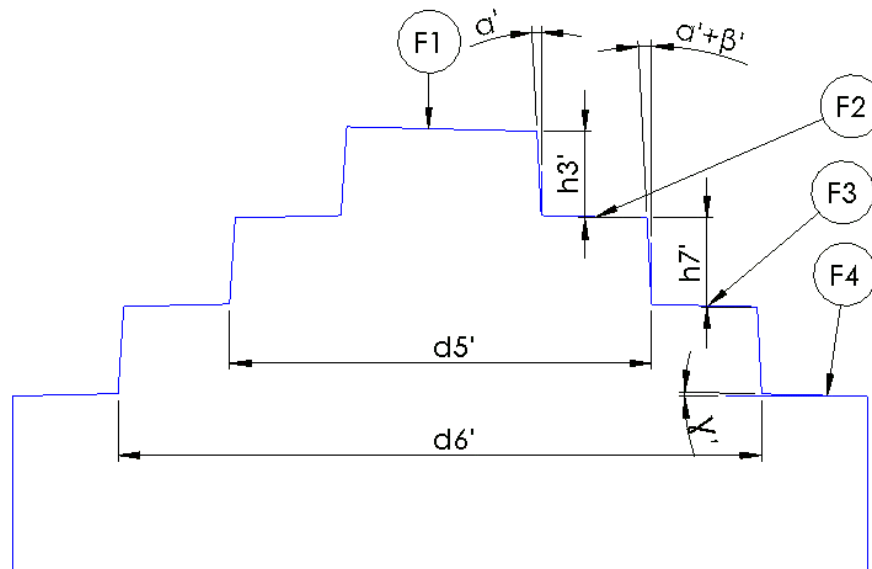


FIGURE 3.15 TENTATIVE POST-MACHINING SURFACE FOR W8

It can be noticed from figure 3.15 that the feed is different on every face while the speed is constant and is the same as used in the experiment for thermal errors. The different feeds at the surfaces, represented in figure 3.15 as F1, F2, F3 and F4, are expected to generate different results for the errors on each respective surface. It is also pertinent to mention here that the position errors and thermal errors are also considered along with the process errors due to spindle speed used for this experiment. For calculation of thermal errors in real time the time and position stamps are important. The time stamp against each position will be calculated through the G code and verified during experimentation. The same time stamp would then be used in the equations established earlier to calculate the thermal errors for a specific position.

3.6.2 Control Error Separation:

The cutting experiment is followed through with another experiment for feed based cutting where a continuous cut is performed with a constant feed on each step. Meanwhile the feed is changed at each step while the temperature state arrangement is kept the same as in previous experiments. The actual cut is represented by figure 3.16.

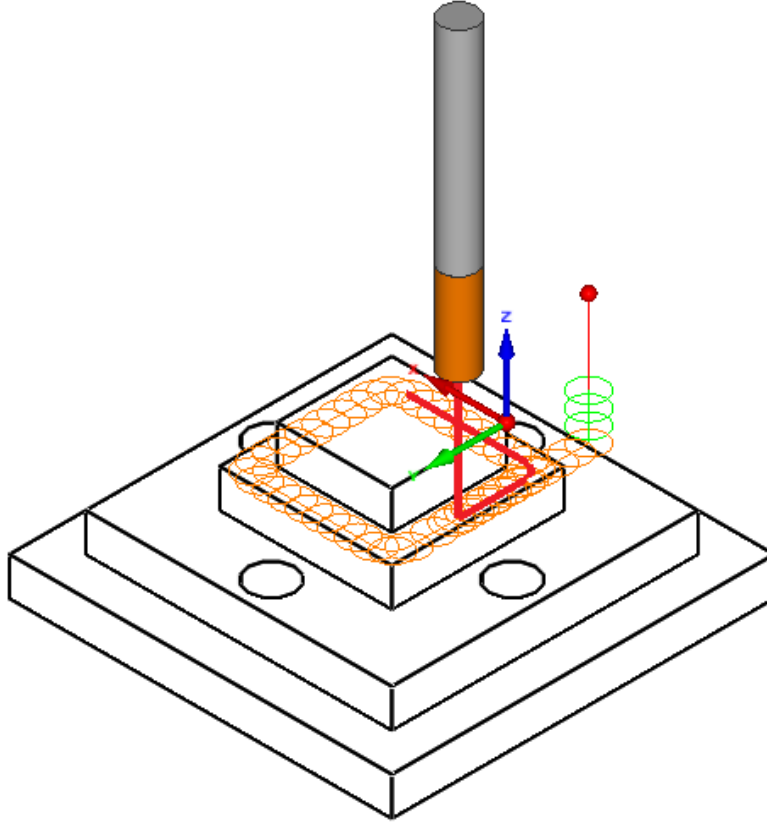


FIGURE 3.16 ACTUAL CUT FOR CONTROL ERROR SEPARATION

Once the workpiece is machined the same is inspected on CMM and the overall errors are reported. After taking out the thermal errors, mechanical issues based position and orientation errors and the process errors due to speed and Feed from the overall error magnitude at each step, the resulting changes in error magnitude at each step are due to changes in feed. The mathematical model for the same is given as equation 2525-2526

$$e_{ctrl_y(2400-100)} = (dy_{W2} - dy_{W8}) - (e_{pfy_{W2}} - e_{pfy_{W8}}) - (e_{pty_{W2}} - e_{pty_{W8}}) - (e_{posy_{W2}} - e_{posy_{W8}}) \quad Eq. 3.11$$

$$e_{ctrl_x(2400-100)} = (dx_{W2} - dx_{W8}) - (e_{pfx_{W2}} - e_{pfx_{W8}}) - (e_{ptx_{W2}} - e_{ptx_{W8}}) - (e_{posx_{W2}} - e_{posx_{W8}}) \quad Eq. 3.12$$

Here the $e_{ctrl_x(2400-100)}$ denotes the control error observed as a change of feed from 100 to 2400. Meanwhile dy_{W2} represents the distance moved along Y-axis for workpiece 2, $e_{pf_{y_{w2}}}$ denotes the process errors along y axis observed due to a particular feed in the respective workpieces, $e_{pt_{y_{w2}}}$ represents the position error observed on surface of workpiece 2 at a particular temperature state while $e_{pos_{x_{w2}}}$ denotes the mechanical position errors due to distance moved. The above equations provide the control errors due to change in distance for a feed change from 100-2400 therefore in order to generalize the model for prediction of control errors at different feeds there is a need for incorporating the feed in the distance based equations given above. A simple bisection method is used for identification of such variation. The following equations are therefore presented for control errors with feed and distance appreciation.

$$e_{ctrl_y} = ((Feed - 100)/(2400 - 100)) \times ((dy_{W2} - dy_{W8}) - (e_{pf_{y_{w2}}} - e_{pf_{y_{w8}}}) - (e_{pt_{y_{w2}}} - e_{pt_{y_{w8}}}) - (e_{pos_{y_{w2}}} - e_{pos_{y_{w8}}})) \quad Eq. 3.13$$

$$e_{ctrl_x} = ((Feed - 100)/(2400 - 100)) \times ((dx_{W2} - dx_{W8}) - (e_{pf_{x_{w2}}} - e_{pf_{x_{w8}}}) - (e_{pt_{x_{w2}}} - e_{pt_{x_{w8}}}) - (e_{pos_{x_{w2}}} - e_{pos_{x_{w8}}})) \quad Eq. 3.14$$

As the control errors are also prone to changes due to change in process forces therefore there is a need for separately identifying the control errors based on feed changes only. The same is done through comparison of dimensions between W2 and W5. The equations for control errors due to changes in Feed are given here as equation 3.15.

$$e_{cpr_y} = (dy_{W2} - dy_{W5}) - (e_{pf_{y_{w2}}} - e_{pf_{y_{w5}}}) - (e_{pt_{y_{w2}}} - e_{pt_{y_{w5}}}) - (e_{pos_{y_{w2}}} - e_{pos_{y_{w5}}}) - e_{ctrl_y(2400-100)} \quad Eq. 3.15$$

A regression analysis is further performed on the obtained results and the resulting equations provide the Feed based control errors. The Process flow for the separation is presented here as Figure 3.17

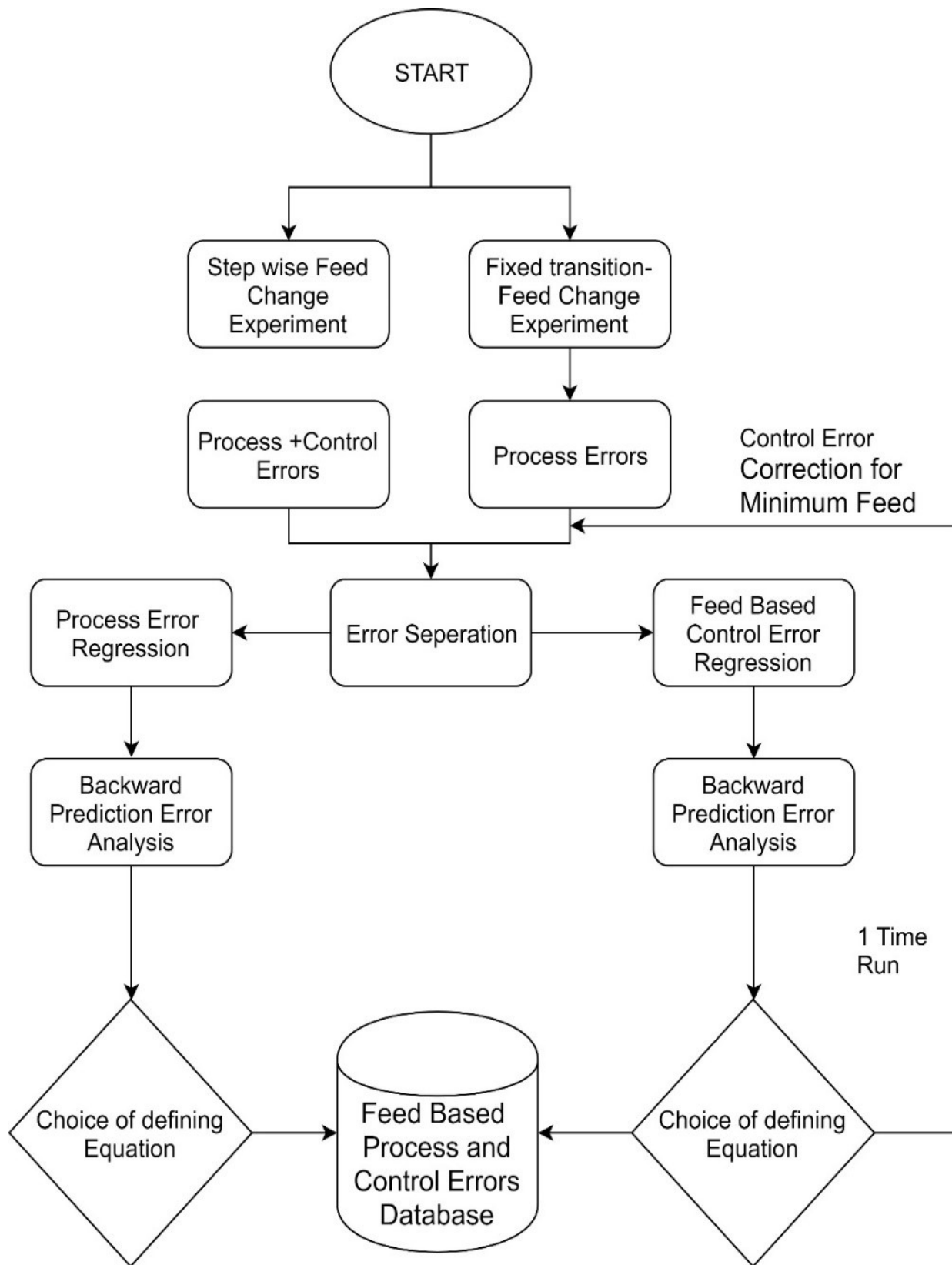


FIGURE 3.17 FEED AND PROCESS ERROR SEPARATION

It is important to notice here that the process errors obtained in the current scenario are usable only for the current tool and material. However, if the material or tool is changed the process errors may be effected. The model until this point is proposed for a production scenario where same tool and workpiece are used. The equations obtained through model can be used for an optimization with the goal of increase in Material removal rate with minimized errors. The details will be discussed in the chapter for Implementation.

3.7 Software based Process errors calculation:

With mechanical issues based position and orientation errors, thermal errors and control errors separately reported the need for obtaining a shape and material independent error prediction is fulfilled using a separate software based process error simulation. The equations presented by E. Budak [43] for milling force calculation and form errors are being used for the process error modeling. It is also important to notice that the current model compares the process errors with software generated errors due to cutting tool and machining parameters only and any change in material may change the process errors. The defining equation for tool bending induced error is given as equation 3.16:

$$y_{max} = \frac{FL_1^3}{3EI} + \frac{1}{6}FL_1 \frac{(L_2 - L_1)(L_2 + L_1)}{EI_1^2} + \frac{1}{6}FL_2 \frac{(L_2 - L_1)(2L_2 + L_1)}{EI_2^2} \quad Eq. 3.16$$

Here the force is represented by ' F ' while ' L_2 ' represents the overall length of the tool while ' L_1 ' represents the flute length, while I_1 and I_2 represents the moment of inertial for the fluted and non-fluted part. For simplicity of calculation in the current scenario the moment of inertia is taken as I only. Meanwhile E denotes the Young's modulus. It is also pertinent to mention here that the force is also calculated using the model presented in [44]. A detailed Matlab program is developed and the cutting forces and errors due to tool deflection are calculated through the program. The error data available through measurements is then compared with the errors and a regression is performed linking the machine generated errors to the program generated errors. This acts as a calibration for the program and hence the change in errors due to spindle speed, feed, depth of cut or tool can be evaluated through use of regression model.

3.8 Regression model Error analysis:

The regression model is intended to provide not only interpolation but also the extrapolation of errors for all error components. Hence it is mandatory to perform an analysis of error in prediction through backward prediction. The difference is reported as prediction error. The error analysis is performed through MiniTab and several regression models and their individual parameters are compared to obtain a suitable regression model with minimum error magnitude for backward prediction. This is repeated for each error model for selection of appropriate prediction model. The results have been reported in Chapter 5.

3.9 Development of prediction Model:

A prediction model is Further developed through use of individual regression for all error equations. The model utilizes the appreciation for feed, Speed process Forces, thermal state as and position based errors. This ability hence enables the user to provide the post-machining error magnitudes expected in a workplace. The prediction model also has the indicative ability towards machine's behavior hence enabling machine designers to view the performance of the machine with respect to error generation and with respect to thermal and process stability.

The prediction model is implemented in Simulink for simulation of errors while the first run is carried out for analysis of backward prediction errors. The developed model is also implemented through machining of workpiece with different conditions including different cutting parameters and geometry. The results will be further discussed in chapter 6.

Once the methodology is completed it is important to provide the details of experimental setup. The same will be discussed in the following chapter.

3.10 Conclusion:

The proposed methodology is quite comprehensive in terms of the number of error parameters considered in the methodology and the number of measurements to be taken for determination of each error. It is important to notice that the proposed methodology synthesizes errors from experimental data and analytical equations have only been used for relating process errors obtained

through use of analytical equations to the actual measured process errors. Meanwhile the methodology has the ability to measure all errors and provide a forward prediction database that predicts the errors based on their respective machining parameters. The methodology provides a generic solution for three axis machining centers in terms of machine, shape and size within a given envelope of workpiece, machining parameters and cutting tools to be used in machining.

Chapter 4. Experimental Design

The experimental design for the current research is driven by the requirements set in the methodology in previous chapter. The experiment therefore required the machining of at least six different workpieces and subsequent measurements to provide the complete error profile required for defining the components of each category of error.

The overall experimentation can be divided in three major phases. The first phase is the machining setup that includes the steps adopted during preparation of workpiece up to actual machining. The second phase consists of on machine probing of workpiece which is carried out for two experiments for averaging out the inaccuracies in position errors. The third phase consists of setting and measurement of workpiece on CMM. The following section therefore details each of the phase with respect to the procedure adopted in the respective phases.

4.1 Machining Setup:

Prior to the start of machining the workpiece is roughed out on the same machine with the bottom surface prepared through face milling operation to provide a near flat surface. The workpiece is then fixed onto the fixture prepared turning. The workpiece and fixture assembly is then planted on the machine table. The machine tool zero is then adjusted for all three axes with the origin carrying faces of the workpiece parallel to X and Y axis within a variation of 5 micrometers. This has been ensured to minimize any variations in the depth of cut and hence the cutting forces on the workpiece during machining. The fixation of workpiece on the machine tool table is presented here as figure 4.1.

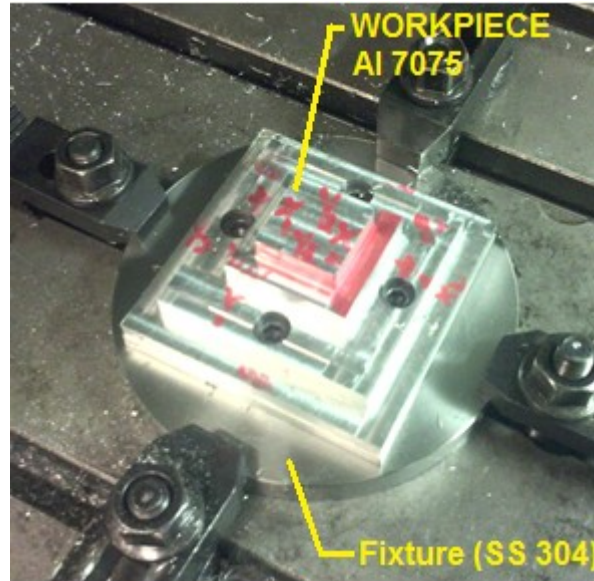


FIGURE 4.1 WORKPIECE AND FIXTURE PLACEMENT

The next step in the setup is the determination of tool runout. The tool runout is used for generation of runout-compensated tool paths through CAM software. Solid CAM is used for the generation of G codes for each experiment as per the conditions described in the previous chapter. Fig 4.2 represents the effect of such runout while Figure 4.3 represents the experimental setup for determination of tool runout through use of dial indicator.

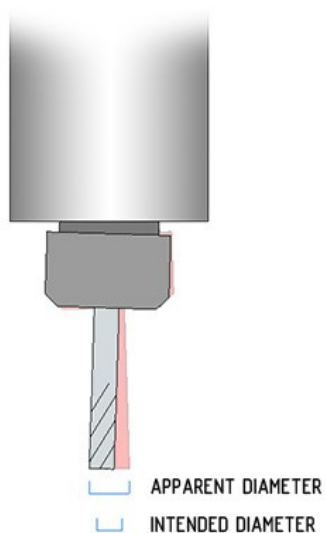


FIGURE 4.2 RUNOUT RADIUS EFFECT

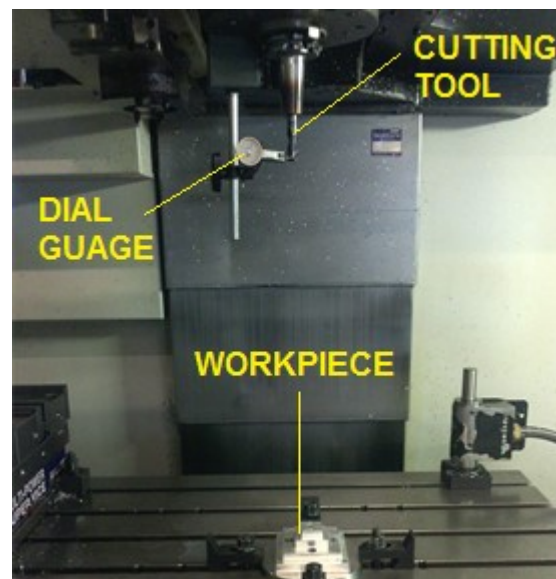


FIGURE 4.3 RUNOUT DETERMINATION SETUP

Once the runout measurement and compensation is finalized the next step involves the machining of workpiece under conditions laid down in the previous chapter. The setup for machining is presented here as Fig 4.4.

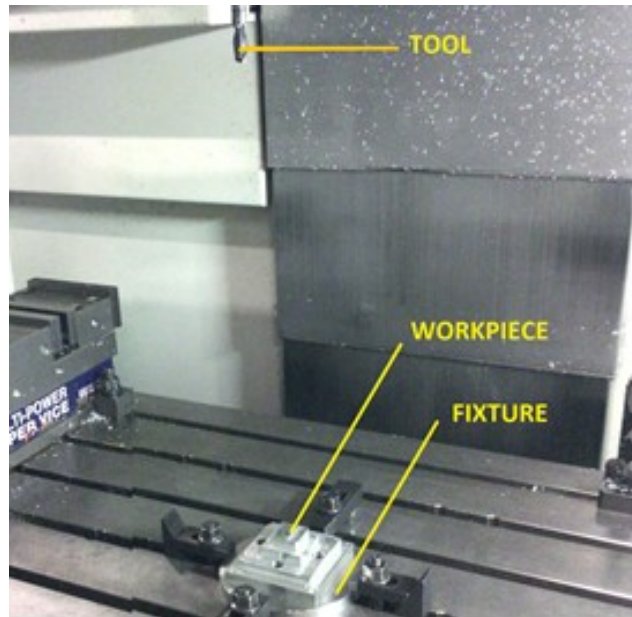


FIGURE 4.4 MACHINING SETUP

It is important to notice that for machining of each workpiece the following common procedure is adopted.

1. Workpiece origin and orientation are set with walls parallel to the axis within a tolerance of 5 micrometers.
2. Machine is turned off for 3 hours.
3. Workpiece origin and orientation is checked again and required adjustments are made.
4. Tool runout is checked and incorporated in CAM program.
5. Machining of first Step is carried out immediately at machine start.
6. Idle running of spindle for 30 minutes with warm up program.
7. Machining of each step followed by 30 minutes of warmup program.

It is also important at this stage to define the actual machining conditions laid down for each workpiece. Table 4.1 further defines the machining conditions along with tool runout observation made during experimentation.

TABLE 4.1 MACHINING CONDITIONS FOR VARIOUS WORKPIECES

Workpiece	Step	Feed XY	Feed Z	Spindle Speed	Tool runout
1	1	100	100	3500	0,004
	2	100	100	3500	
	3	100	100	3500	
	4	100	100	3500	
2	1	200	200	3500	0,004
	2	400	400	3500	
	3	800	600	3500	
	4	1600	800	3500	
3	1	200	200	3500	0,004
	2	100	100	5500	
	3	100	100	1000	
	4	800	800	3500	
4	1	100	100	3500	0,004
	2	100	100	3500	
	3	100	100	3500	
	4	100	100	3500	
5	1	100	100	3500	0,004
	2	200	200	3500	
	3	400	400	3500	
	4	800	800	3500	
6	1	100	100	1000	0,004
	2	100	100	1000	
	3	100	100	1000	
	4	100	100	1000	
7	1	100	100	5500	0,004
	2	100	100	5500	
	3	100	100	5500	
	4	100	100	5500	
8	1	100	100	3500	0,005
	2	200	200	3500	
	3	400	400	3500	
	4	800	800	3500	

Once the experimentation has been completed the next step is to proceed with actual measurement of the workpieces. The first step is determination of position errors through workpiece probing.

4.2 Probing Setup:

Once the machining has been completed the machine is powered off for ‘cooling down’ for three hours. This is followed by on machine probing for two cases. It is important to notice here that the on-machine probing is not taken for each workpiece but rather for only two workpieces for checking the repeatability of measurement system. Figure 4.5 represents the probing setup using a mechanical touch probe.

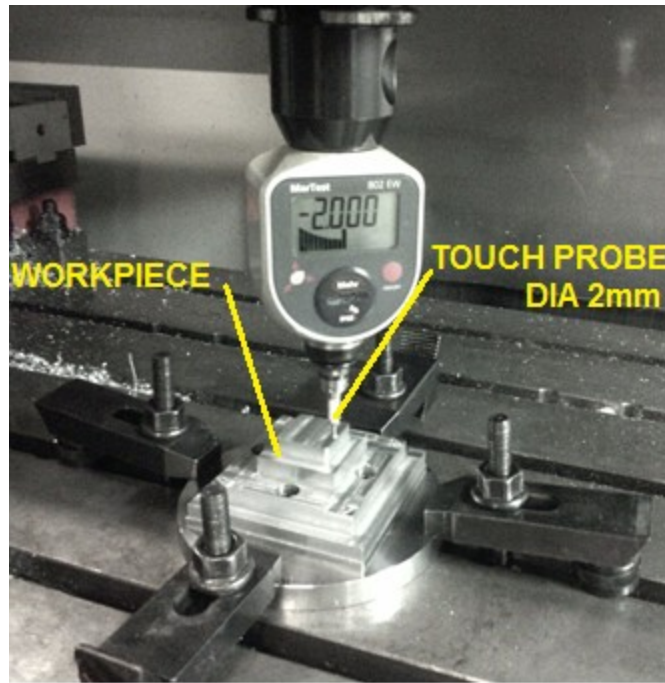


FIGURE 4.5 PROBING SETUP FOR MECHANICAL POSITION ERRORS

One of the key issues in the mechanical touch probe fixturing may be the change in apparent length of the probe due to difference in holder fixturing within the spindle. This however will not change the overall results as the difference in height, and not the pre-process and post process machine reading, is the parameter under consideration.

4.3 CMM setup:

Each workpiece is subjected to CMM measurement once the machining has been completed. It is important to indicate that the origin taken on the surface of workpiece is kept the same in CMM as selected earlier for machining.

At least 06 points have been measured on each vertical face of the machined part with each set of points pertaining to a specific Z height for measurement of linear dimensions as well as orientation of machined faces. Meanwhile a total of 09 number of points have been selected on horizontal faces of the workpiece for measurement of height of various steps as well as the orientation of face for provision of tilt angles along X and Y axis. It is also important to mention here that repeat measurements for random points have been taken for analyzing the repeatability of the setup. The CMM results have been presented in the next chapter. The experimental setup for CMM has been presented here as Figure 4.6.

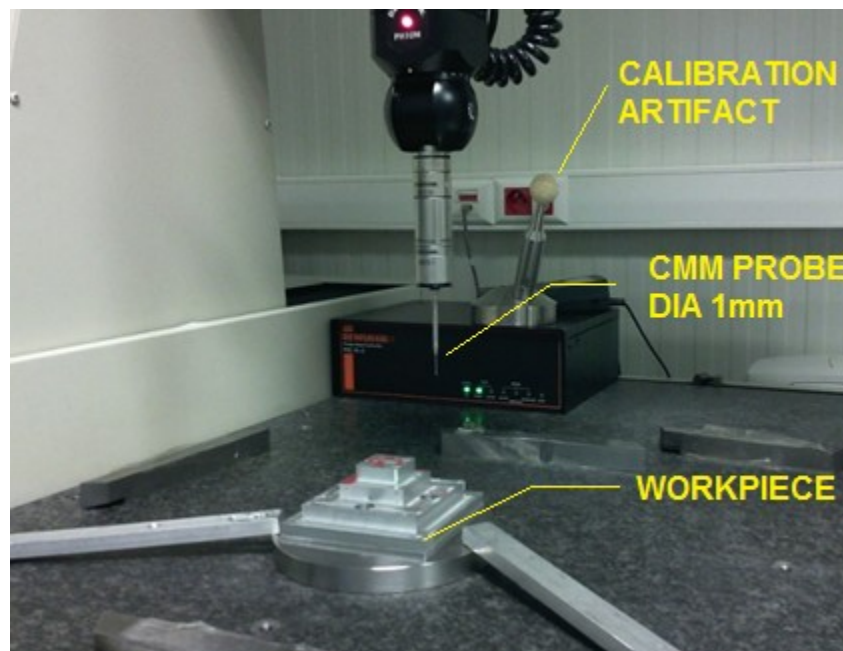


FIGURE 4.6 MEASUREMENT SETUP AT CMM

4.4 Conclusion:

One of the key issues identified during the measurements included the setting and calibration of probe for measurement. The overall probe length is subject to change with changes in tightening

forces for probe component assembly. Meanwhile the fixing of probe can also cause changes in probe length. As the experiment has been done in various setups with CMM being used for other measurements during each measurement setup therefore the calibration of probe was repeated at the start of each setup. This also indicates that the calibration data for each workpiece may differ. However, the general errors variation is in submicron level and hence can be neglected for the current experimentation.

The experimental setup is extensive in terms of number of workpieces required. However, the same workpiece is used for at least three different experiments and their corresponding lengths are considered for further calculation. The overall proposed experimental setup can be easily implemented on shop floor. Meanwhile the experiment provides the user with comprehensive data for further analysis as presented in the following chapter.

Chapter 5. Results and Analysis

This chapter deals with the results from measurement. The analysis of results for various errors and the resulting defining equations based on various machining parameters for different errors are also detailed in this chapter. Meanwhile, the forward prediction models and the analysis of errors within the prediction models have also been made a part of this chapter.

5.1 Results:

As discussed earlier a total of eight workpieces are machined for the current research with different machining parameters and more than 1000 points are measured to evaluate the effect of changing machining parameters on the obtained dimensions. Each dimension is hence measured on both CMM and machine probing at three different locations. This not only provides a deeper insight into the actual post machining geometry of the workpiece, but also improves the reliability of the results.

The results of measurement are used for analysis of behavior of each error separately with appreciation of the causes generating such errors. Some of the errors are simple in calculation while some require multiple factors to be considered for a comprehensive profiling. The first step therefore is to report and analyze the most common repeatable errors. These are errors in position and orientation of a machine tool due to mechanical issues including manufacturing and assembly issues.

5.2 Position Errors Results:

The first step as presented in the methodology is the calculation of mechanical position errors. Workpiece 8 has been utilized for the measurement of positional errors and therefore the on-

machine probing followed by CMM measurement is performed on workpiece 8. Table 5.1 presents the probing results for workpiece 8 corresponding to the side faces.

TABLE 5.1 DIMENSIONAL PROBING RESULTS FOR W8

Y11-1	Y11-2	Y12-1	Y12-2	X11-1	X11-2	X12-1	X12-2	Zx11-1	Zx11-2	Zy11-1	Zy11-2
0,053	0,043	30,086	30,096	-0,026	-0,035	30,013	30,025	55,001	48,001	55,001	48,003
0,192	0,184	30,226	30,239	-0,167	-0,179	29,873	29,886	55,001	48,001	55,000	48,000
0,333	0,328	30,369	30,382	-0,308	-0,32	29,731	29,741	55,002	48,001	55,000	48,001
Y21-1	Y21-2	Y22-1	Y22-2	X21-1	X21-2	X22-1	X22-2	Zx21-1	Zx22-2	Zx21-1	Zx22-2
-7,524	-7,527	37,517	37,528	-7,462	-7,469	37,588	37,598	29,002	22,000	29,000	22,003
-7,311	-7,321	37,729	37,74	-7,674	-7,684	37,382	37,39	29,000	22,003	29,001	22,003
-7,101	-7,107	37,942	37,951	-7,886	-7,892	37,17	37,181	29,003	22,003	29,000	22,003
Y31-1	Y31-2	Y32-1	Y32-2	X31-1	X31-2	X32-1	X32-2	Zx31-1	Zx32-2	Zy31-1	Zy31-2
-25,14	-25,149	54,911	54,924	-24,849	-24,86	55,216	55,228	19,001	12,003	19,001	12,003
-24,989	-24,998	55,066	55,074	-25,006	-25,013	55,062	55,076	19,000	12,002	19,002	12,002
-24,641	-24,647	55,413	55,425	-25,358	-25,366	54,706	54,717	19,000	12,000	19,001	12,003
Y41-1	Y41-2	Y42-1	Y42-2	X41-1	X41-2	X42-1	X42-2	Zx41-1	Zx41-2	Zx42-1	Zx42-2
-34,821	-34,839	64,243	64,266	-34,176	-34,197	64,891	64,915	26,000	22,500	26,000	22,502
-34,492	-34,512	64,571	64,593	-34,508	-34,526	64,561	64,587	26,002	22,502	26,002	22,500
-34,141	-34,159	64,919	64,943	-34,86	-34,879	64,209	64,23	26,002	22,502	26,000	22,500

The probing is followed by CMM measurements. To reduce the measurement uncertainties the same points are measured by on machine probing and CMM however small differences may occur due to difference in workpiece orientation setting on both machines. The difference however will not change the overall reported magnitude for dimensions and angles. The results for CMM measurements are presented here as Table 5.2.

TABLE 5.2 CMM MEASUREMENT RESULTS

Y11-1	Y11-2	Y12-1	Y12-2	X11-1	X11-2	X12-1	X12-2	Zx11-1	Zx11-2	Zy11-1	Zy11-2
0,053	0,043	30,086	30,096	-0,026	-0,035	30,013	30,025	55,001	48,001	55,001	48,003
0,192	0,184	30,226	30,239	-0,167	-0,179	29,873	29,886	55,001	48,001	55,000	48,000
0,333	0,328	30,369	30,382	-0,308	-0,32	29,731	29,741	55,002	48,001	55,000	48,001
Y21-1	Y21-2	Y22-1	Y22-2	X21-1	X21-2	X22-1	X22-2	Zx21-1	Zx22-2	Zx21-1	Zx22-2
-7,524	-7,527	37,517	37,528	-7,462	-7,469	37,588	37,598	29,002	22,000	29,000	22,003
-7,311	-7,321	37,729	37,74	-7,674	-7,684	37,382	37,39	29,000	22,003	29,001	22,003
-7,101	-7,107	37,942	37,951	-7,886	-7,892	37,17	37,181	29,003	22,003	29,000	22,003
Y31-1	Y31-2	Y32-1	Y32-2	X31-1	X31-2	X32-1	X32-2	Zx31-1	Zx32-2	Zy31-1	Zy31-2
-25,14	-25,149	54,911	54,924	-24,849	-24,86	55,216	55,228	19,001	12,003	19,001	12,003
-24,989	-24,998	55,066	55,074	-25,006	-25,013	55,062	55,076	19,000	12,002	19,002	12,002
-24,641	-24,647	55,413	55,425	-25,358	-25,366	54,706	54,717	19,000	12,000	19,001	12,003
Y41-1	Y41-2	Y42-1	Y42-2	X41-1	X41-2	X42-1	X42-2	Zx41-1	Zx41-2	Zx42-1	Zx42-2
-34,821	-34,839	64,243	64,266	-34,176	-34,197	64,891	64,915	26,000	22,500	26,000	22,502
-34,492	-34,512	64,571	64,593	-34,508	-34,526	64,561	64,587	26,002	22,502	26,002	22,500
-34,141	-34,159	64,919	64,943	-34,86	-34,879	64,209	64,23	26,002	22,502	26,000	22,500

Similar measurements are taken for every workpiece with 6 different points taken on every face. The measurement corresponding to Z values represents the Z level corresponding to each measurement and is further used for the calculations for spindle tilt angles at each face. The next step is comparison of measurement obtained through CMM and probing to obtain the position

errors on the machine as discussed in the methodology. The final step wise dimensional results for both CMM and on machine probing are presented here as Table 5.3. It is important to notice here that the Z-error is taken through measurement of height at each step of the workpiece at 9 different points.

TABLE 5.3 STEP WISE CMM AND PROBED DIMENSIONS

Step	CMM measurement					Probing measurement					
	Obs.	Y1	Y2	X1	X2	Z1	Y1	Y2	X1	X2	Z1
1	1	30,048	30,06	30,035	30,052	9,003	30,0408	30,0473	30,039	30,0417	9,004134722
	2	30,052	30,065	30,034	30,055		30,0431	30,0494	30,0392	30,0416	
	3	30,051	30,061	30,036	30,054		30,0469	30,0462	30,0385	30,0415	
2	1	45,05	45,067	45,041	45,055	19,003	45,0435	45,0559	45,0331	45,0441	19,00430556
	2	45,056	45,074	45,04	45,061		45,042	45,0555	45,0309	45,0452	
	3	45,056	45,073	45,043	45,058		45,0414	45,055	45,0309	45,0446	
3	1	80,076	80,088	80,051	80,073	29,003	80,0538	80,0695	80,0423	80,0583	29,00335972
	2	80,075	80,089	80,055	80,072		80,0527	80,0672	80,0424	80,0578	
	3	80,072	80,083	80,054	80,072		80,0483	80,0672	80,0374	80,0569	
4	1	99,084	99,112	99,064	99,105	37,003	99,0725	99,1036	99,075	99,097	37,0029
	2	99,079	99,113	99,063	99,105		99,0705	99,1033	99,0732	99,0965	
	3	99,082	99,109	99,06	99,102		99,0685	99,1063	99,0731	99,0952	

The step wise data for Z position measurement and the data from side face measurements is further used to obtain the various orientation errors in the three Axis. These include the spindle and table tilt angles and the orientation errors along Z axis. The results are presented here as Table 5.4 and Table 5.4

TABLE 5.4 CMM DATA BASED ORIENTATION ERRORS

Step	Orientation Errors CMM				
	Spindle tilt-X	Table Tilt-X	Spindle Tilt-Y	Table Tilt-Y	Oz
1	0,001446346	5,55554E-05	0,000872965	5,55555E-05	0,00865
2	0,001039839	9,52369E-05	0,001170798	-2,77778E-05	0,00865
3	0,001143116	8,88869E-05	0,001154966	-1,19048E-05	0,00865
4	0,005434866	8,04723E-05	0,005329579	3,7037E-06	0,00865

TABLE 5.5 PROBING DATA BASED ORIENTATION ERRORS:

Step	Probing Orientation Error				
	Spindle tilt-X	Table Tilt-X	Spindle Tilt-Y	Table Tilt-Y	Oz
1	0,000226195	-3,125E-05	0,000269431	-1,92497E-06	0
2	0,000874129	-2,14285E-05	0,000823471	-8,66069E-05	0
3	0,001035899	-5,55556E-06	0,001001088	-3,29629E-05	0
4	0,006157857	-6,86E-06	0,003318665	-4,92592E-05	0

The difference in probing and CMM results and the distance travelled by the tool for the dimensions are further utilized for calculating the mechanical position and orientation errors in the machine tool. This is an important factor as the distance wise position and orientation errors are than used for elimination of position errors from calculations of other errors. The results for distance wise mechanical position and orientation errors are presented here as Figure 5.1:

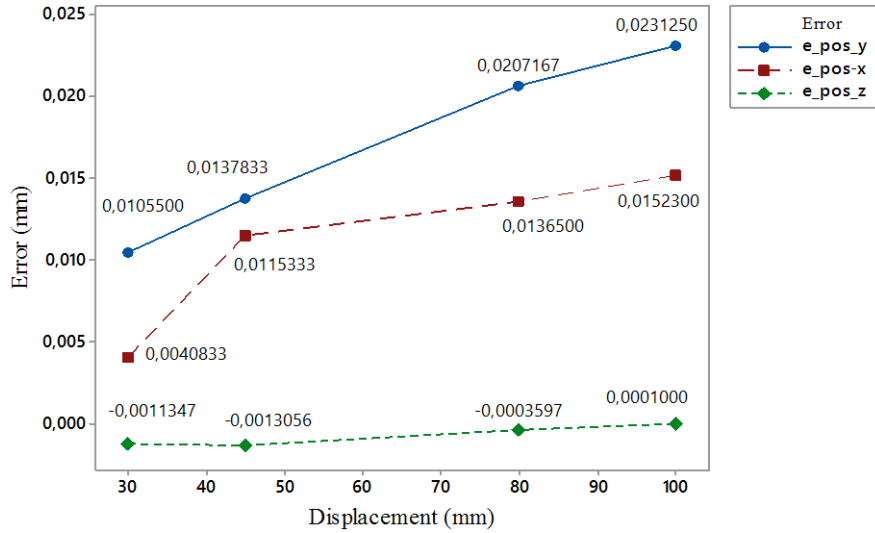


FIGURE 5.1 POSITION ERRORS IN X, Y AND Z AXIS

It can be observed that the position error in both X and Z axis changes almost linearly while for X axis the first value of position error poses a difference. The first point can be considered as an outlier since it deviates much more than the other three points. However, the same will be incorporated in the final regression analysis. Hence the position errors in all three axes can be satisfactorily predicted through use of a linear prediction model or more accurately through use of a quadratic model. The table orientation errors are further calculated and presented here as Fig 5.2 and Fig 5.3.

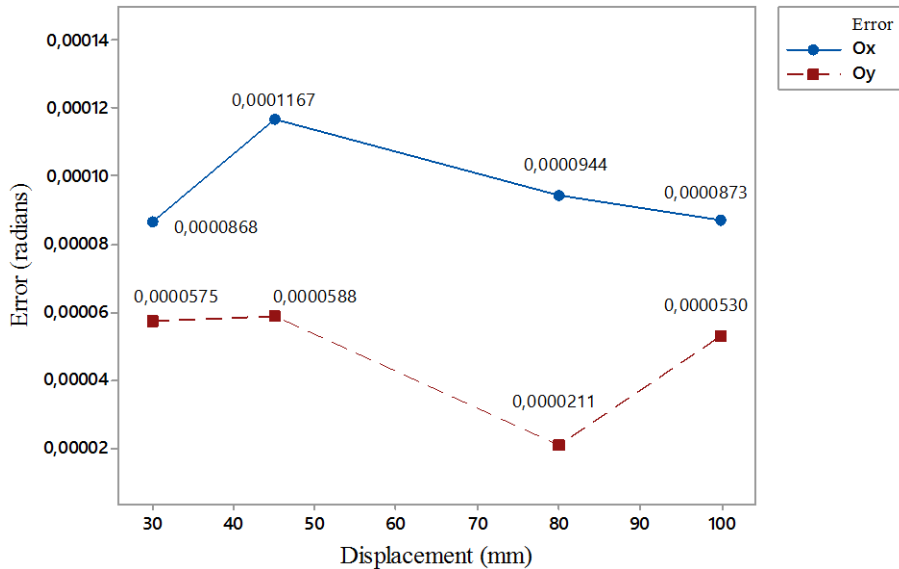


FIGURE 5.2 ORIENTATION ERROR ALONG X AND Y AXIS

The table tilt in both X and Y axis is observed as being very small and the variations is small in all cases. Moreover, the important observation in this case is that the table tilt is observed to be in the

same direction for all steps. The changes in table tilt angle are also small enough to be neglected. The table orientation error around Z axis also indicating the squareness error between X and Y axis is presented in Fig 5.3.

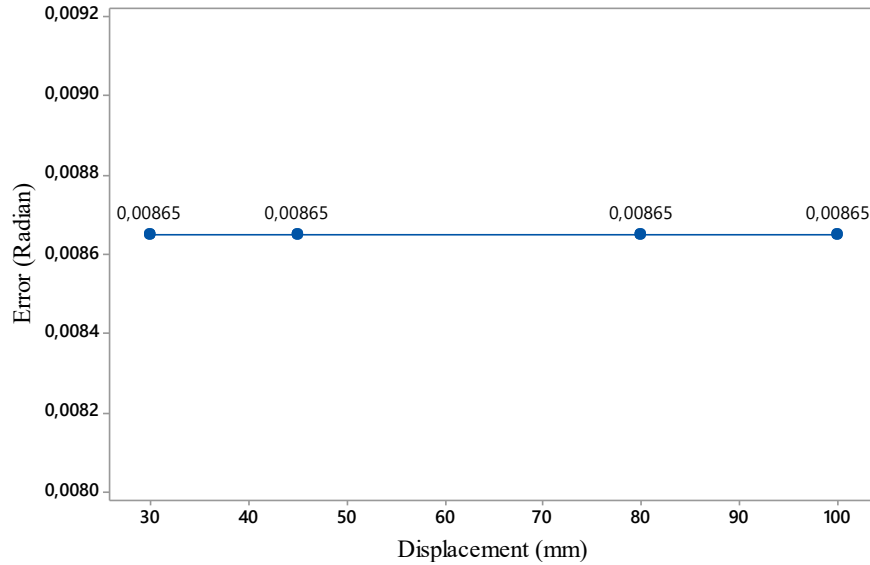


FIGURE 5.3 ORIENTATION ERROR AROUND Z AXIS

The error is measured through the angle between the faces corresponding to X and Y axis and no error is observed in case of probing data while the CMM results indicate an angle of 90.01 degrees between the two surfaces. The error therein is hence reported as the orientation errors along Z axis. The table tilt and the side face tilt is further used for calculation of spindle Tilt angle observed at each step due to mechanical error. The same is presented here as Fig 5.4:

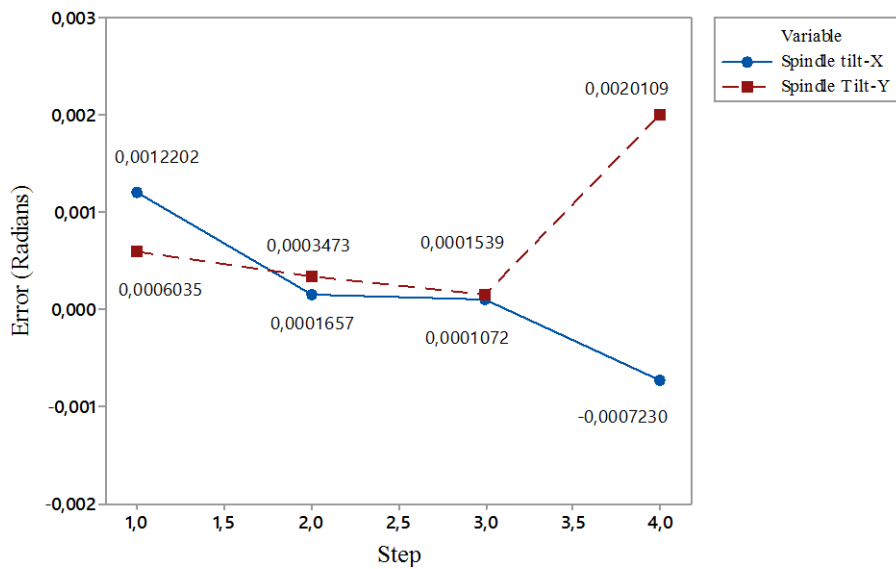


FIGURE 5.4 STEP WISE MECHANICAL SPINDLE TILT ANGLE

5.2.1 Position Error Analysis:

The results are further used for a regression analysis. This is particularly important in the context that the prediction equations based on distance will enable us to predict the position errors regardless of the component shape and size. The data for all three Axis are hence used for development of displacement based equations for position errors. The resulting regression for Y axis is presented here as Fig 5.5.

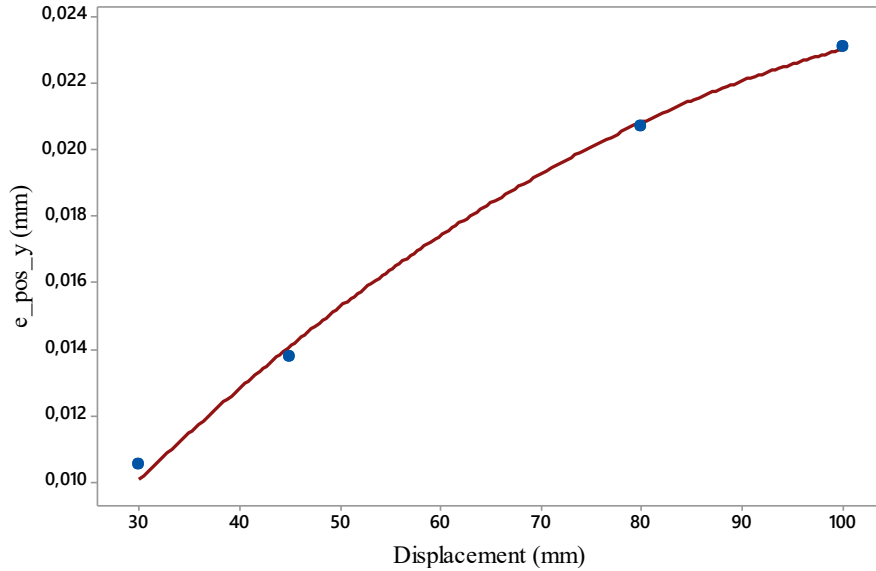


FIGURE 5.5 STEP WISE MECHANICAL POSITION ERROR IN Y-AXIS

The regression equations for the three Axis are presented here as equation 5.1 to 5.3. In case of Z-Axis a linear regression model is used with a correction factor of -0.001933. The actual position error in Z axis is expected to be zero at zero position. However, there is one micrometer difference for prediction at zero position and by introducing the factor the overall prediction accuracy is improved for all predictions other than that at zero.

$$e_{pos_x} = 0,000249252 \times dx - 9,57162e - 007 \times dx^2 \quad Eq. 5.1$$

$$e_{pos_y} = 0,000381399 \times dy - 1,51152e - 006 \times dy^2 \quad Eq. 5.2$$

$$e_{pos_z} = -0,001933 + 0,000020 \times dz \quad Eq. 5.3$$

Here ' dx ' ' dy ' and ' dz ' represents the distance moved in the respective axis.

It is important to notice here that a prediction model for only positional errors have been developed. As the orientation errors are generally constant with negligible variations hence an average orientation error will be used for further calculations.

The next step in the process is the analysis of data from workpiece 1, workpiece 6 and workpiece 7 for determination of effect of temperature changes on the position and orientation errors in the machine. The following section hence deals with the thermal error results and analysis.

5.3 Thermal Error Measurement Results and Analysis:

The most important factor associated with the thermal errors is the change in spindle lengths that can cause errors in Z direction. As per presented methodology the results from workpiece 1 are used for thermal error analysis while the results for position errors are incorporated in the calculations to provide the true magnitude of change in error along Z axis.

5.3.1 Change in Spindle length:

Fig 5.6 presents the change in spindle length due to changes in temperature state.

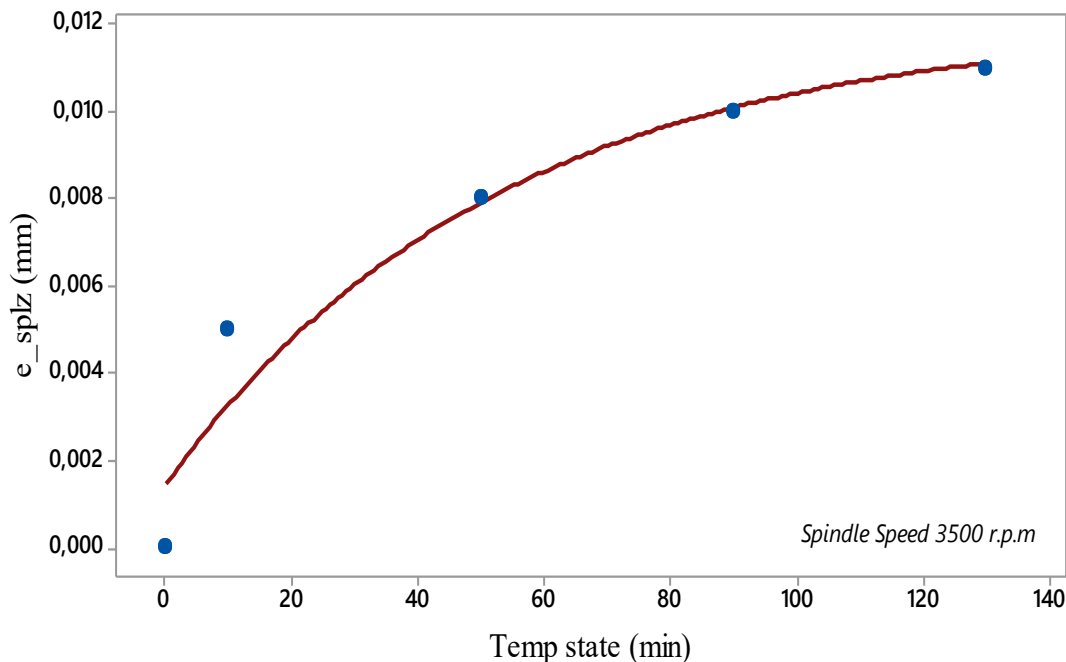


FIGURE 5.6 TEMPERATURE STATE WISE CHANGE IN SPINDLE LENGTH

From the figure, it can be observed that the spindle expands up to approximately 8 micrometers in the first 50 minutes. The rate of expansion slows down after 60 minutes and over the next 70 minutes the spindle only expands by a value of approximately 3 micrometers. It may be observed here that the regression model adopted for the prediction is based on a free Y-intercept which in turn provides the value for thermal error at supposed zero stage. Meanwhile, a backward prediction analysis is performed for each model and the selection of model is done based on the least error magnitude. The same is presented in the later part of this chapter as Section 5.7. Figure 5.7 however provides a comparison of different models considered for the final regression equations.

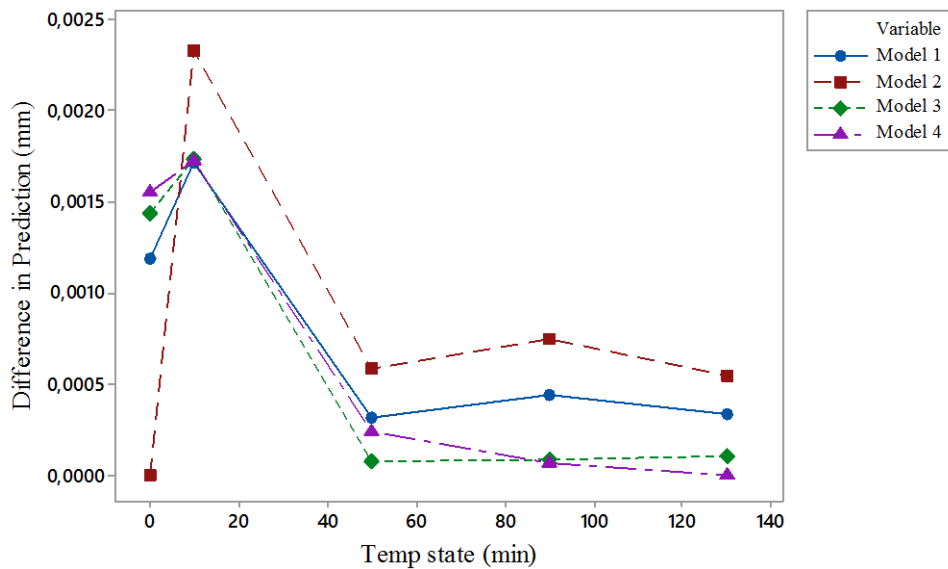


FIGURE 5.7 TEMPERATURE STATE WISE DIFFERENCE IN BACKWARD PREDICTION

The final prediction model is hence given by equation 5.4:

$$e_{splz} = 0,012 - 0,0104453 \times \exp(-0,01862 \times Temp\ state') \quad Eq. 5.4$$

Further on the error in overall dimension in X and Y axis due to change in temperature state is presented in the following sub-section.

5.3.2 Error in Position due to change in Temperature state:

The data is further utilized along with the identified position errors to obtain the position errors due to thermal deformations in both X and Y axis. The results along with fitted regression model are presented here as figure 5.8 and Fig 5.9

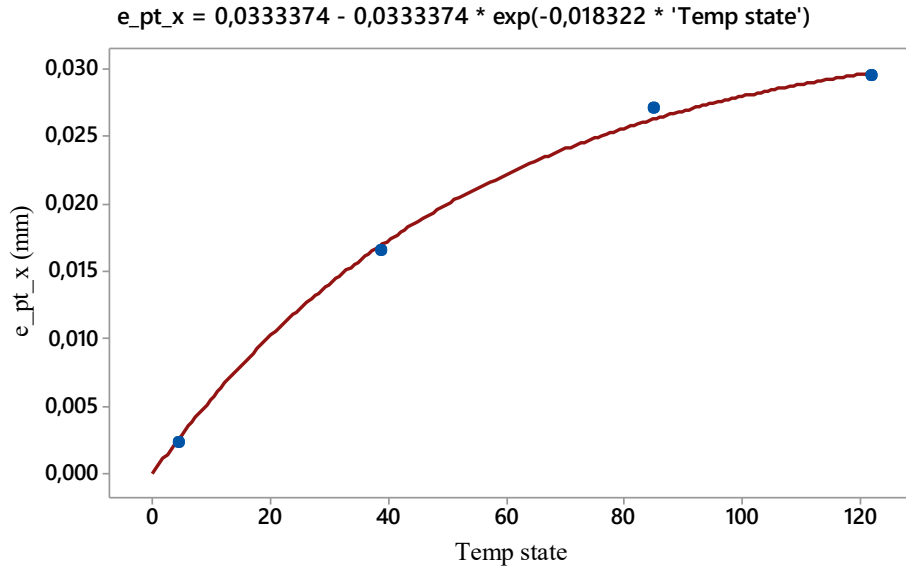


FIGURE 5.8 TEMPERATURE STATE WISE CHANGE IN POSITION ERROR IN X-AXIS

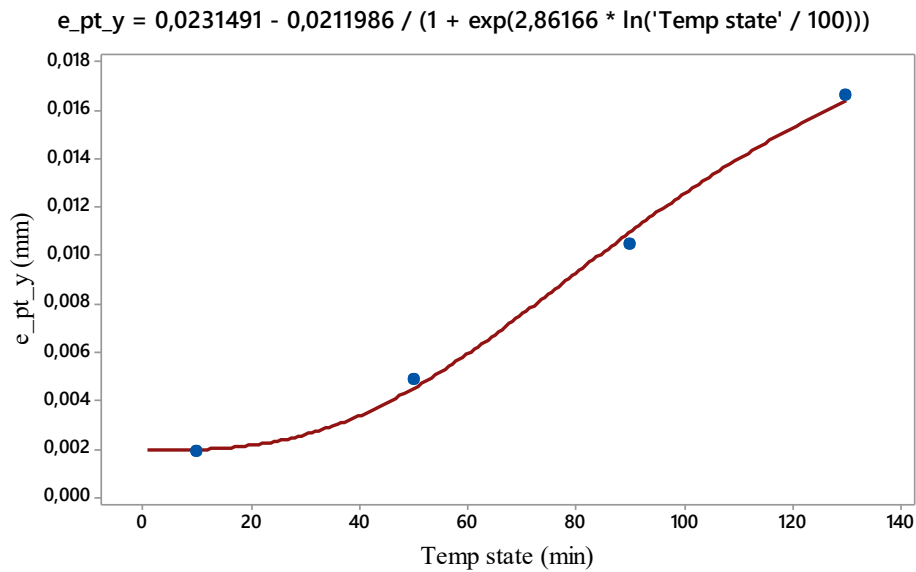


FIGURE 5.9 TEMPERATURE STATE WISE CHANGE IN POSITION ERROR IN X-AXIS

In X-Axis, the position error increase swiftly up to 40 minutes from the start time, however the increase is slowed down towards a constant value as the time of operation increases. In case of Y-Axis however the increase is slow in the start followed by a period of steeper increase which is then followed by a decrease in the magnitude of change towards the last temperature stage. As the spindle and table tilt contribute towards such errors hence it is important to observe these errors in conjunction with spindle and table tilt. It is also important to mention here that the current study deals with only change in error magnitude from temperature zero state onwards hence an initial

regression is performed to identify Y-intercept and incorporate the same in final regression model. One such example is presented here for position error due to temperature change in Y-Axis in Fig 5.10.

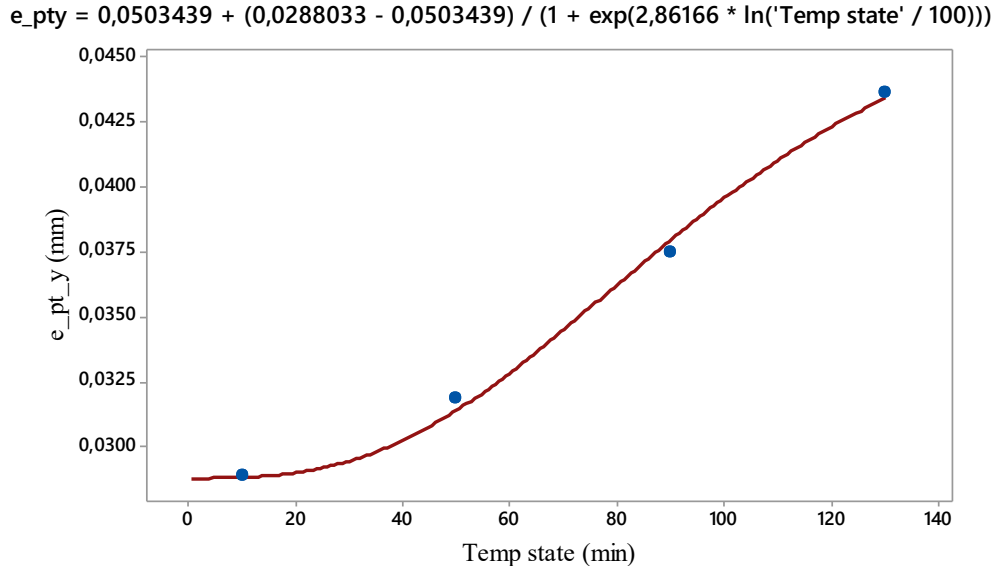


FIGURE 5.10 TEMPERATURE STATE WISE CHANGE IN POSITION ERROR (Y-INTERCEPT)

The final regression equations are presented here as equation 5.5 and equation 5.6.

$$e_{pt_y} = 0,0231491 - 0,0211986 / (1 + \exp(2,86166 \times \ln('Temp\ state' / 100))) \quad Eq. 5.5$$

$$e_{pt_x} = 0,0333374 - 0,0333374 \times \exp(-0,0188882 \times 'Temp\ state') \quad Eq. 5.6$$

5.3.3 Spindle deflection along X axis

The spindle deflection along X axis due to increase in temperature exhibits a different from normal behavior. It may be observed that the spindle is going through an expansion phase where due to the expansion the resulting deflection observed along X-Axis is at first towards the positive X-direction while the same further moves towards negative X direction. The spindle deflection in the opposite direction may have contributed to the decrease in change of position error. The Spindle tilt in Y axis however provides an almost identical behavior as observed for position errors. Figure 5.11 and 5.12 presents the spindle tilts in both axis.

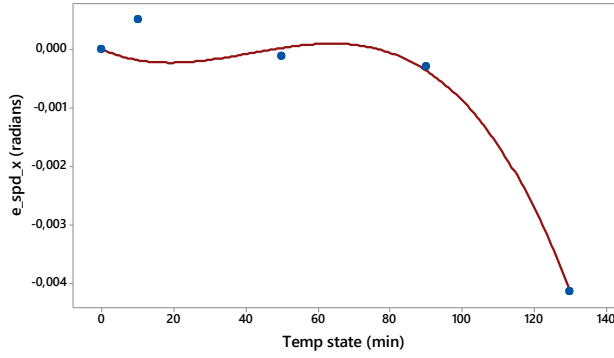


FIGURE 5.11 SPINDLE DEFLECTION X-AXIS

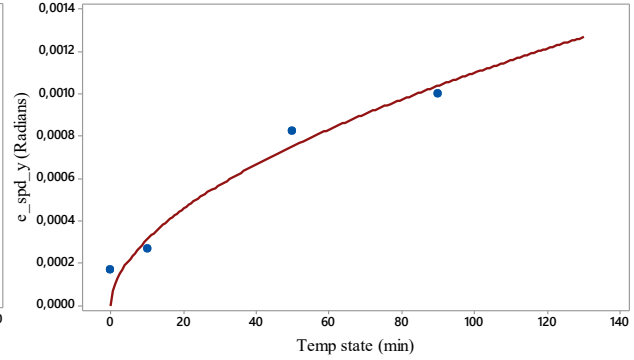


FIGURE 5.12 SPINDLE DEFLECTION Y-AXIS

The final regression equations are presented here as eq. 5.7 and eq. 5.8

$$e_{spd_y} = 8,97328e - 005 \times 'Temp\ state' \times 0,544087 \quad Eq. 5.7$$

$$e_{spd_x} = -2.6e - 005 \times 'Temp\ state' + 8,93558e - 007 \times 'Temp\ state'^2 - 7,20972e - 009 \times 'Temp\ state'^3 \quad Eq. 5.8$$

5.3.4 Change in table tilt due to Temperature change:

The table tilt under thermal deformations is provided by the Figure 5.13 and Figure 5.14. In case of X-Axis for a best fit regression model once point is taken as an outlier. The error appears to be a decreasing function. However, the nature of results indicates a Gompertz growth model that first increase and then remains constant after a certain value of temperature. The table tilt observed along Y-Axis is much smaller than that observed in X axis and depicts a continuous growth in value.

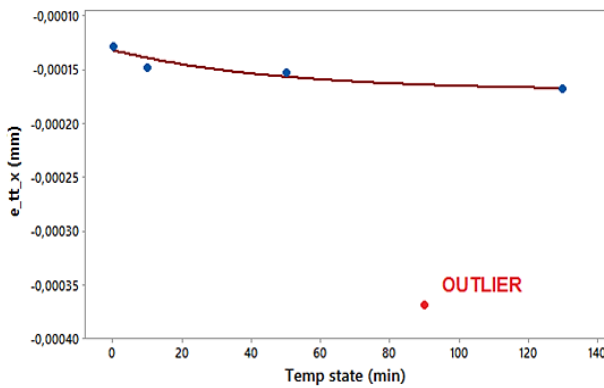


FIGURE 5.13 THERMAL TABLE TILT X-AXIS

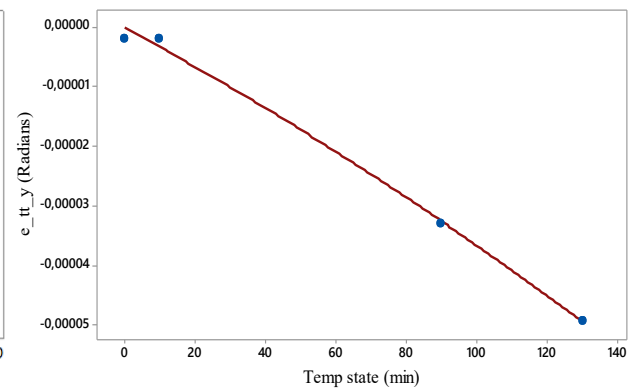


FIGURE 5.14 THERMAL TABLE TILT Y-AXIS

The equations to be used in prediction model are presented here as eq. 5.9 and 5.10.

$$e_{tt_x} = -0,000169619 + 3,78018e - 005 \times \exp(-0,0215319 \times 'Temp\ state')$$
Eq. 5.9

$$e_{tt_y} = -3,18537e - 007 \times 'Temp\ state' - 4,76367e - 010 \times 'Temp\ state' \times 'Temp\ state'$$
Eq. 5.10

Further on the thermal state driving factor for the machine is changed as presented in the methodology and the results for the changed thermal stage and their analysis are presented in the following subsection.

5.3.5 Thermal Stage 2:

With the change in thermal stage the overall magnitude of change in different error components also changes. The behavior for position errors in X and Y axis is however similar in nature however the overall magnitude of position error in Y axis at the final temperature stage is about 9 micrometers as opposed to 14micrometers as observed in first temperature stage. The behavior is presented here as Figure 5.15 and Figure 5.16.

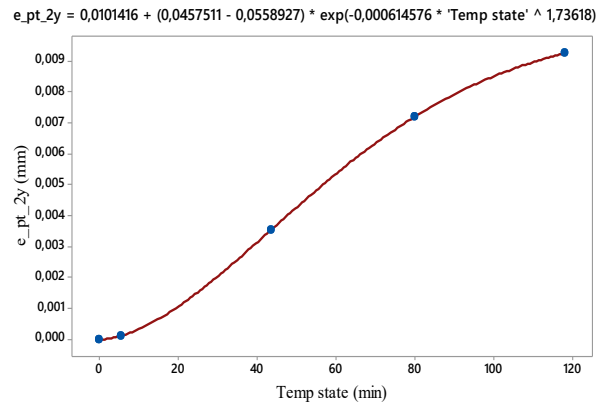
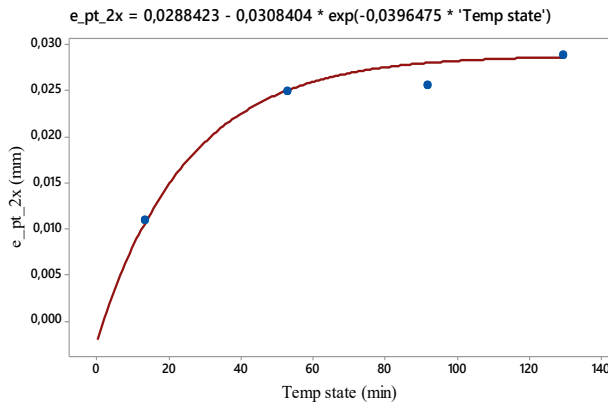


FIGURE 5.15 TEMPERATURE STATE WISE $e_{pt_{2x}}$

FIGURE 5.16 TEMPERATURE STATE WISE $e_{pt_{2y}}$

Similar is the case with Z axis where the obtained data points are fitted into a similar regression model as used in the first workpiece. Meanwhile, the spindle deflection along both X and Y axis is presented here as Figure 5.17 and Figure 5.18.

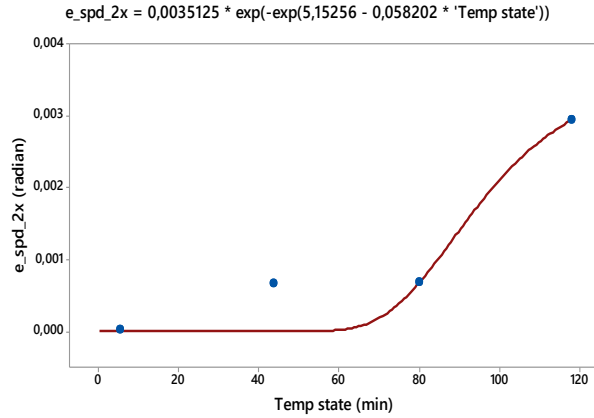


FIGURE 5.17 TEMPERATURE STATE WISE $e_{spd_{2x}}$

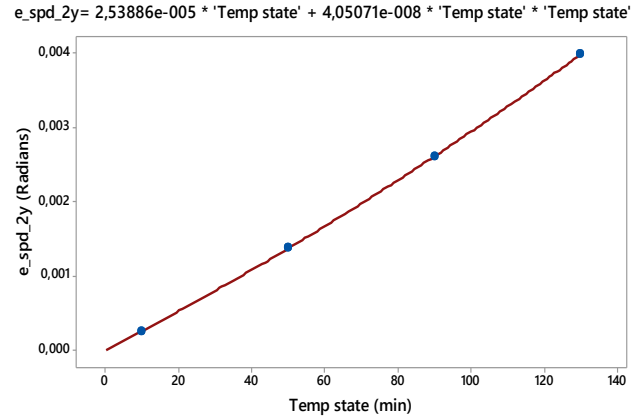


FIGURE 5.18 TEMPERATURE STATE WISE

$e_{spd_{2y}}$
The behavior is similar for Y axis while there is a considerable difference in case of X-Axis. The deflection is opposite to that observed in the first temperature stage while the pattern is similar.

Meanwhile table tilts along both X and Y axis also exhibits a smaller value as compared to thermal stage 1 and are presented here as Figure 5.19 and 5.20 respectively.

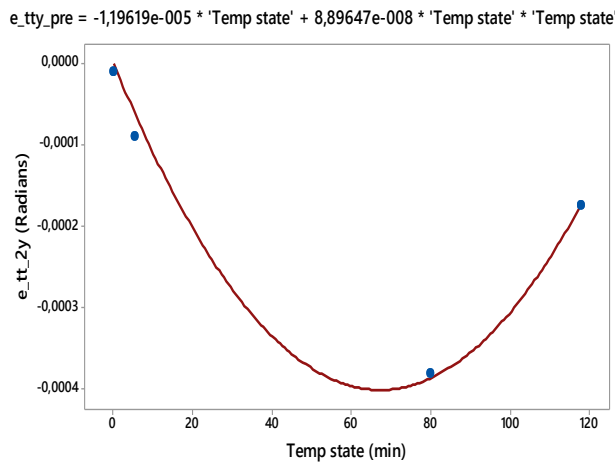


FIGURE 5.19 TEMPERATURE STATE WISE $e_{tt_{2y}}$

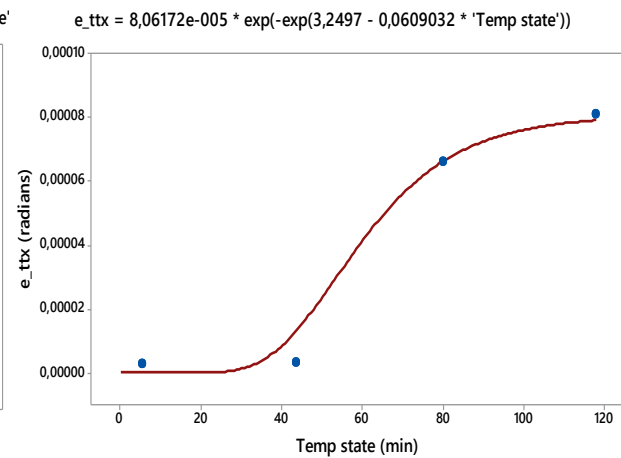


FIGURE 5.20 TEMPERATURE STATE WISE $e_{tt_{2x}}$

Equation 5.11 to 5.13 present the regression model developed for the errors obtained through thermal stage 2.

$$e_{spl_{2z}} = 0,0073584 \times 'Temp\ state' / (28,05 + 'Temp\ state') \quad Eq. 5.11$$

$$\begin{aligned}
e_{pt_{2y}} &= 0,0101416 \\
&\quad + (0,0457511 - 0,0558927) \\
&\quad \times \exp(-0,000614576 \times 'Temp\ state' ^ 1,73618) \\
e_{tt_{2y}} &= -1,19619e - 005 \times 'Temp\ state' + 8,89647e \\
&\quad - 008 \times 'Temp\ state' \times 'Temp\ state' \\
e_{spd_{2y}} &= 2,53886e - 005 \times 'Temp\ state' + 4,05071e \\
&\quad - 008 \times 'Temp\ state' \times 'Temp\ state'
\end{aligned}
\tag{Eq. 5.12}$$

$$\begin{aligned}
e_{pt_{2x}} &= 0,0288423 - 0,0308404 \times \exp(-0,0396475 \\
&\quad * 'Temp\ state') \\
e_{tt_{2x}} &= 8,06172e - 005 \\
&\quad \times \exp(-\exp(3,2497 - 0,0609032 \times 'Temp\ state')) \\
e_{spd_{2x}} &= 0,0035125 \times \exp(-\exp(5,15256 \\
&\quad - 0,058202 \times 'Temp\ state'))
\end{aligned}
\tag{Eq. 5.13}$$

5.3.6 Thermal Stage 3:

The thermal stage is than changed once again through a spindle speed of 5500rpm on workpiece 7 and the measurements are taken for all dimensions as done in previous cases. Figure 5.21 presents the observed thermal position errors in X and Y axis and the change in spindle length along Z-axis.

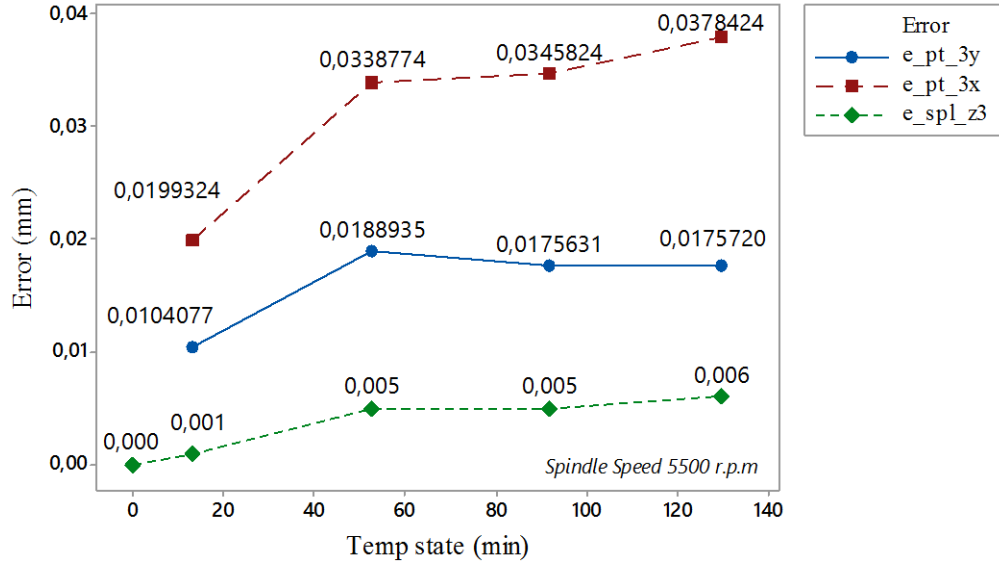


FIGURE 5.21 TEMPERATURE STATE WISE POSITION ERROR (STAGE 3)

The observed values in X and Y axis are larger than the values observed in case of Stage 1 and Stage 2. However, the value observed for the increase in spindle length is smaller than that observed in thermal stage 1. The measured and calculated values for position errors, spindle deflection and table tilt in both X and Y axis and the change in spindle length are further utilized for regression analysis of thermal deformation based errors in stage 3 and the resulting equations are presented here from equation 5.14 to equation 5.16.

$$e_{spl_{z3}} = 0,009125 - 0,009125 \times \exp / (-0,00989956 \times 'Temp\ state') \quad Eq. 5.14$$

$$e_{pt_{3y}} = 0,0196461 \times 'Temp\ state' / (7,90441 + 'Temp\ state')$$

$$e_{tt_{3y}} = -0,00014988 \times 'Temp\ state' / (2,24239 + 'Temp\ state') \quad Eq. 5.15$$

$$e_{spd_{3y}} = 1,84222e - 005 \times 'Temp\ state' - 1,90222e - 007 \times 'Temp\ state' \times 'Temp\ state'$$

$$\begin{aligned}
e_{pt_{3x}} &= 0,0375039 - 0,0375039 * \exp(-0.0523651 \\
&\quad * 'Temp state') \\
e_{spd_{3x}} &= 0,140459 \\
&\quad - 0,141274 \times \exp(-0,000151322 \times 'Temp state') \\
e_{tt_{3x}} &= -8,23447e - 007 \times 'Temp state' \\
&\quad + ('Temp state' ^ 5,80806e - 009)
\end{aligned}
\tag{Eq. 5.16}$$

Once the regression models have been developed for the individual thermal stages a comprehensive error prediction model is developed. The resulting model is presented in the following section.

5.4 Thermal Error Prediction Model:

The models developed for various errors in the three stages are further used for comparison of errors and development of a comprehensive model having the ability to predict the thermal errors at thermal stages other than those measured in the current experimentation.

As indicated in the methodology bisection method is used for the finding the errors between the various thermal stages. While a proportion method is used for identification of errors at thermal stages below stage 2 or above stage 3.

5.4.1 Thermal Prediction Equation for e_{pt_y} :

The prediction model for error in position at a specific thermal state within a particular thermal stage is presented here as a set of equations from equation 5.17 to equation 5.20.

For prediction between spindle speed 3500-5500 rpm:

$$\begin{aligned}
e_{pt_{ypred}} = & ((Spindle\ speed - 3500)/2000) \times (0,0231491 \\
& - 0,0211986 / (1 \\
& + \exp(2,86166 \times \ln('Temp\ state' / 100)))) + ((5500 \\
& - Spindle\ speed) / 2000) \times (0,0196461 \times 'Temp\ state' \\
& / (7,90441 + 'Temp\ state'))
\end{aligned}
\tag{Eq. 5.17}$$

For prediction between spindle speed 1000-3500 rpm:

$$\begin{aligned}
e_{pt_{ypred}} = & ((Spindle\ speed - 1000)/2500) \times (0,0101416 \\
& + (0,0457511 \\
& - 0,0558927) \times \exp(-0,000614576 \\
& \times 'Temp\ state' ^ 1,73618)) + ((3500 \\
& - Spindle\ speed) / 2500) \times (0,0231491 \\
& - 0,0211986 / (1 \\
& + \exp(2,86166 \times \ln('Temp\ state' / 100))))
\end{aligned}
\tag{Eq. 5.18}$$

For Prediction Below spindle speed 1000 rpm:

$$\begin{aligned}
e_{pt_{ypred}} = & (Spindle\ speed / 1000) \times (0,0101416 + (0,0457511 \\
& - 0,0558927) \times \exp(-0,000614576 \\
& \times 'Temp\ state' ^ 1,73618))
\end{aligned}
\tag{Eq. 5.19}$$

For Prediction Above spindle speed 5500 rpm:

$$\begin{aligned}
e_{pt_{ypred}} = & (Spindle\ speed / 5500) \times (0,0196461 \times 'Temp\ state' \\
& / (7,90441 + 'Temp\ state'))
\end{aligned}
\tag{Eq. 5.20}$$

The equations are further used for prediction of thermal error in Y-Axis at various thermal stages. The predicted values are presented here as Fig 5.22.

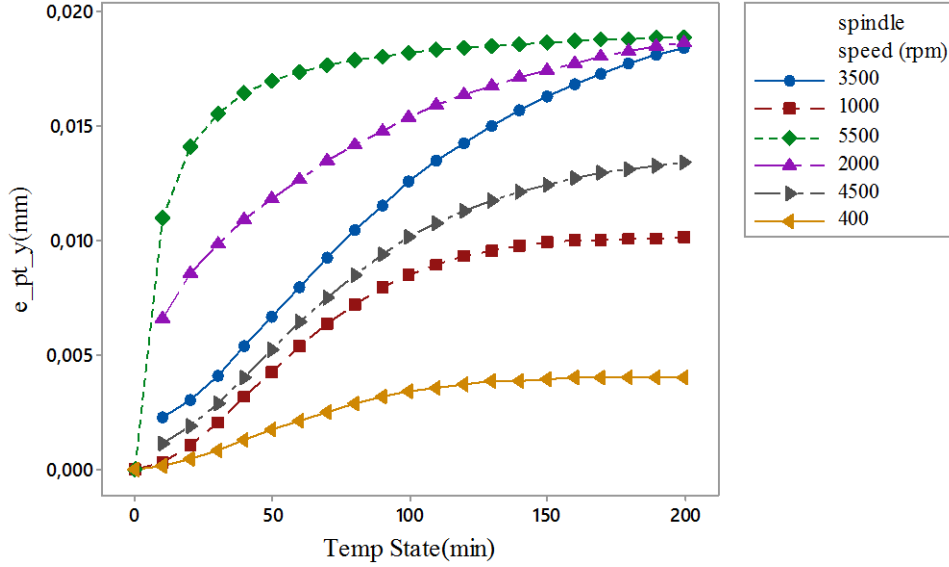


FIGURE 5.22 TEMPERATURE STATE AND STAGE WISE POSITION ERROR IN Y-AXIS

Here the value for spindle speed 400, 2000 and 4500 are predicted based on the model presented earlier. Hence it can be considered that the model is Feasible for prediction of a range of position error changes due to changes in thermal states with appreciation of various spindle speeds. This therefore enhances the capability of the model towards utilization for a comprehensive error profiling and usage in optimization of machining parameters with the objective of minimizing errors.

It is to be noticed here that the errors for spindle speeds of 5500,3500 and 1000 will be predicted with their respective equations.

5.4.2 Prediction Model for e_{pt_x}

The prediction equations for the position error under thermal influence are given here as equation 5.21 to 5.24.

For prediction between Spindle speed 3500-5500 r.p.m:

$$\begin{aligned}
 e_{pt_{xpred}} = & ((Spindle\ speed - 3500)/2000) \times (0,0333374 \\
 & - 0,0333374 \times \exp(-0,0188882 \times 'Temp\ State')) \\
 & + ((5500 - Spindle\ speed) / 2000) \times (0,0375039 \\
 & - 0,0375039 \times \exp(-0,0523651 \times 'Temp\ state'))
 \end{aligned}
 \tag{Eq. 5.21}$$

For prediction between Spindle speed 1000-3500 r.p.m:

$$e_{pt_{xpred}} = ((Spindle\ speed - 1000)/2500) \times (0,0333374 - 0,0333374 \times \exp(-0,0188882 \times 'Temp\ state')) + ((3500 - Spindle\ speed)/2500) \times (0,0308404 - 0,0308404 \times \exp(-0,0396475 \times 'Temp\ state')) \quad Eq. 5.22$$

For Prediction Below Spindle speed 1000 r.p.m:

$$e_{pt_{xpred}} = (Spindle\ speed/1000) \times (0,0333374 - 0,0333374 \times \exp(-0,0188882 \times 'Temp\ state')) \quad Eq. 5.23$$

For prediction above Spindle speed 5500 r.p.m:

$$e_{pt_{xpred}} = ((Spindle\ speed /5500) \times (0,0375039 - 0,0375039 \times \exp(-0,0523651 \times 'Temp\ state')) \quad Eq. 5.24$$

Figure 5.23 presents the forward prediction for the different thermal stages.

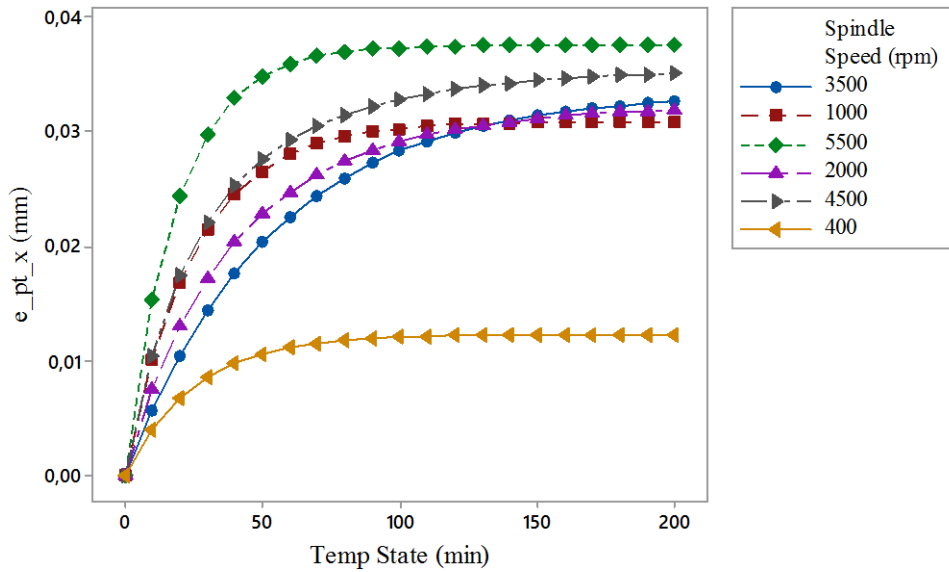


FIGURE 5.23 TEMPERATURE STATE AND STAGE WISE POSITION ERROR IN X-AXIS

5.4.3 Prediction Model for e_{spl_z} :

Equations 5.25 to equation 5.28 exhibits the developed prediction model.

For prediction between Spindle speed 3500-5500 r.p.m:

$$e_{splz_{pred}} = ((Spindle\ speed - 3500)/2000) \times (0,0104453 - 0,0104453 \times \exp(-0,01862 \times Temp\ state')) + (5500 - Spindle\ speed)/2000 \times (0,009125 - 0,009125 \times \exp(-0,00989956 \times 'Temp\ state')) \quad Eq. 5.25$$

For prediction between Spindle speed 1000-3500 r.p.m.

$$e_{splz_{pred}} = ((Spindle\ speed - 1000)/2500) \times (0,0073584 \times 'Temp\ state' / (28,05 + 'Temp\ state')) + ((3500 - Spindle\ speed)/2500) \times (0,0104453 - 0,0104453 \times \exp(-0,01862 \times Temp\ state')) \quad Eq. 5.26$$

For Prediction Below Spindle speed 1000 r.p.m.

$$e_{splz_{pred}} = (Spindle\ speed/1000) \times (0,0073584 \times 'Temp\ state' / (28,05 + 'Temp\ state')) \quad Eq. 5.27$$

For Prediction Below Spindle Above 5500 r.p.m.

$$e_{splz_{pred}} = (Spindle\ speed/5500) \times (0,009125 - 0,009125 \times \exp(-0,00989956 \times 'Temp\ state')) \quad Eq. 5.28$$

Meanwhile Figure 5.24 is obtained through forward prediction through the equations given above.

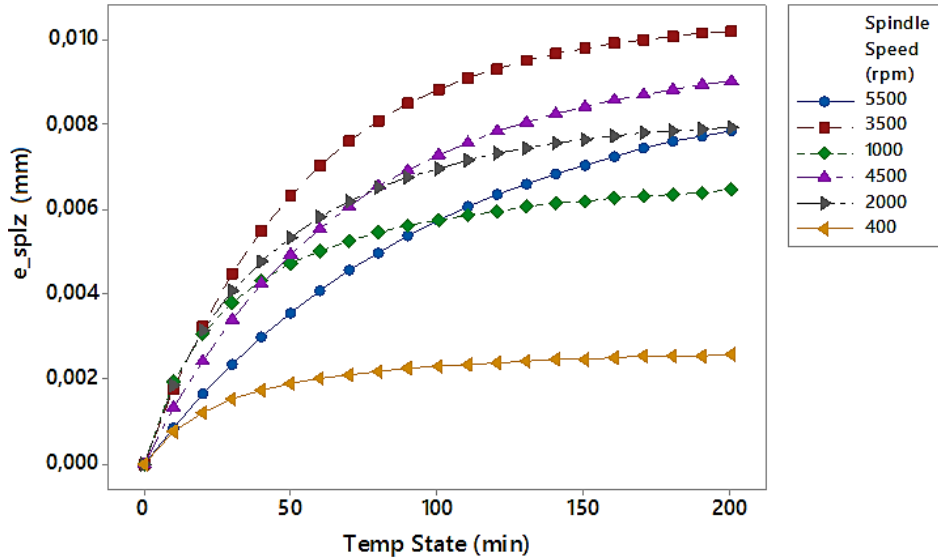


FIGURE 5.24 TEMPERATURE STATE AND STAGE WISE ERROR IN Z-AXIS

It can be observed from the figure that the change in spindle length is smaller in case of spindle speed of 5500 rpm. This seems to contradict the normal behavior as an increase in spindle speed increases the heat generation and hence the change is expected to be larger. However, it is important to notice here that on increasing the spindle speed an increase in the deflection angle is also observed which might contribute towards the apparent shorter increase observed for a spindle speed of 5500 r.p.m against expectation.

5.4.4 Prediction Model for Spindle Deflection and table tilt

The resulting equations for prediction of spindle deflection along Y-Axis across different thermal states and stages are listed below from equation 5.29 to equation 5.32.

For prediction between Spindle speed 3500-5500 rpm:

$$\begin{aligned}
 e_{spd,ypred} = & ((Spindle\ speed - 3500)/2000) \times (8,97328e \\
 & - 005 \times 'Temp\ state'^{0,544087}) + ((5500 \\
 & - Spindle\ speed)/2000) \times (1,84222e \\
 & - 005 \times 'Temp\ state' - 1,90222e \\
 & - 007 \times 'Temp\ state' \times 'Temp\ state')
 \end{aligned}
 \tag{Eq. 5.29}$$

For prediction between Spindle speed 1000-3500 rpm:

$$\begin{aligned}
 e_{spd,ypred} = & ((Spindle\ speed - 1000)/2500) \times (2,53886e \\
 & - 005 \times 'Temp\ state' + 4,05071e \\
 & - 008 \times 'Temp\ state' \times 'Temp\ state') + ((3500 \\
 & - Spindle\ speed)/2500) \times (8,97328e \\
 & - 005 \times 'Temp\ state'^{0,544087})
 \end{aligned}
 \tag{Eq. 5.30}$$

For Prediction Below Spindle speed 1000 rpm:

$$\begin{aligned}
 e_{spd,ypred} = & (Spindle\ speed/1000) \times (2,53886e - 005 \times 'Temp\ state' \\
 & + 4,05071e - 008 \times 'Temp\ state' \times 'Temp\ state')
 \end{aligned}
 \tag{Eq. 5.31}$$

For Prediction Above Spindle speed 5500 rpm:

$$e_{spdy_{pred}} = (Spindle\ speed/5500) \times (1,84222e - 005 \times 'Temp\ state' - 1,90222e - 007 \times 'Temp\ state' \times 'Temp\ state')$$
Eq. 5.32

Similarly, the prediction equations for X-Axis are presented here from equation 5.33 through to equation 5.36.

For prediction between Spindle speed 3500-5500 rpm:

$$e_{spdx_{pred}} = ((Spindle\ speed - 3500)/2000) \times (-2.6e - 005 \times 'Temp\ state' + 8,93558e - 007 \times 'Temp\ state'^2 - 7,20972e - 009 \times 'Temp\ state'^3) + ((5500 - Spindle\ speed)/2000) \times (0,140459 - 0,141274 \times \exp(-0,000151322 \times 'Temp\ state'))$$
Eq. 5.33

For prediction between Spindle speed 1000-3500 rpm:

$$e_{spdx_{pred}} = ((Spindle\ speed - 1000)/2500) \times (0,0035125 \times \exp(-\exp(5,15256 - 0,058202 \times 'Temp\ state')))) + ((3500 - Spindle\ speed)/2500) \times (-2.6e - 005 \times 'Temp\ state' + 8,93558e - 007 \times 'Temp\ state'^2 - 7,20972e - 009 \times 'Temp\ state'^3)$$
Eq. 5.34

For Prediction Below Spindle speed 1000 rpm:

$$e_{spdx_{pred}} = ((Spindle\ speed/1000) \times (0,0035125 \times \exp(-\exp(5,15256 - 0,058202 \times 'Temp\ state'))))$$
Eq. 5.35

For Prediction Above Spindle speed 5500 rpm:

$$e_{spdx_{pred}} = ((Spindle\ speed/1000) \times (0,140459 - 0,141274 \times \exp(-0,000151322 \times 'Temp\ state')))$$
Eq. 5.36

5.4.5 Prediction Model for Table tilt:

The resulting prediction equations for table tilt along Y- Axis are presented here from equation 5.37 to equation 5.40.

For prediction between Spindle speed 3500-5500 rpm:

$$e_{tty_{pred}} = ((Spindle\ speed - 3500)/2000) \times (3,18537e - 007 \times 'Temp\ state' - 4,76367e - 010 \times 'Temp\ state' \times 'Temp\ state') + ((5500 - Spindle\ speed)/2000) \times (-0,00014988 \times 'Temp\ state' / (2,24239 + 'Temp\ state')) \quad Eq. 5.37$$

For prediction between Spindle speed 3500-1000 rpm:

$$e_{tty_{pred}} = ((Spindle\ speed - 1000)/2500) \times (3,18537e - 007 \times 'Temp\ state' - 4,76367e - 010 \times 'Temp\ state' \times 'Temp\ state') + ((3500 - Spindle\ speed)/2500) \times (-1,19619e - 005 \times 'Temp\ state' + 8,89647e - 008 \times 'Temp\ state' \times 'Temp\ state') \quad Eq. 5.38$$

For Prediction Below Spindle speed 1000 rpm:

$$e_{tty_{pred}} = (Spindle\ speed/1000) \times (-1,19619e - 005 \times 'Temp\ state' + 8,89647e - 008 \times 'Temp\ state' \times 'Temp\ state') \quad Eq. 5.39$$

For Prediction above Spindle speed 5500 rpm:

$$e_{tty_{pred}} = (Spindle\ speed/5500) \times (-0,00014988 \times 'Temp\ state' / (2,24239 + 'Temp\ state')) \quad Eq. 5.40$$

Similarly, the prediction equations for X-Axis are presented here from equation 5.41 through to equation 5.44.

For prediction between Spindle speed 3500-5500 rpm:

$$\begin{aligned}
e_{tt_{xpred}} = & ((Spindle\ speed - 3500)/2000) \times (-0,000169619 \\
& + 3,78018e - 005 \times \exp(-0,0215319 \times 'Temp\ state')) \\
& + ((5500 - Spindle\ speed)/2000) \times (-8,23447e \\
& - 007 \times 'Temp\ state') \\
& + ('Temp\ state' ^ 5,80806e - 009)
\end{aligned} \tag{Eq. 5.41}$$

For prediction between Spindle speed 3500-1000 rpm:

$$\begin{aligned}
e_{tt_{xpred}} = & ((Spindle\ speed - 1000)/2500) \times (8,06172e - 005 \\
& \times \exp(-\exp(3,2497 - 0,0609032 \times 'Temp\ state')) + ((3500 \\
& - Spindle\ speed)/2500) \times (-0,000169619 + 3,78018e \\
& - 005 \times \exp(-0,0215319 \times 'Temp\ state'))
\end{aligned} \tag{Eq. 5.42}$$

For Prediction Below Spindle speed 1000 rpm:

$$\begin{aligned}
e_{tt_{xpred}} = & (Spindle\ speed/1000) \times (8,06172e - 005 \\
& \times \exp(-\exp(3,2497 - 0,0609032 \times 'Temp\ state'))
\end{aligned} \tag{Eq. 5.43}$$

For Prediction above Spindle speed 5500 rpm:

$$\begin{aligned}
e_{tt_{ypred}} = & (Spindle\ speed/5500) \times (-8,23447e - 007 \times 'Temp\ state' \\
& + ('Temp\ state' ^ 5,80806e - 009))
\end{aligned} \tag{Eq. 5.44}$$

Once the thermal errors prediction across various temperatures stages and states is completed the next stage is the calculation and reporting of process errors.

5.5 Process Error Results and Analysis:

For calculation of process errors based on feed the measurement results of workpiece 8 are utilized and once the thermal and position errors are removed from the overall dimensional errors the remaining errors are attributed to the errors due to changes in process parameters which in this case is cutting feed. It is important to observe at this point that the transition feed between cut on two walls is taken as 100mm/min which is low and hence the control errors are taken as zero for

this feed. Fig 5.25 and Fig 5.26 depicts the process errors and the result of regression analysis for process errors in Y-axis and X-axis respectively.

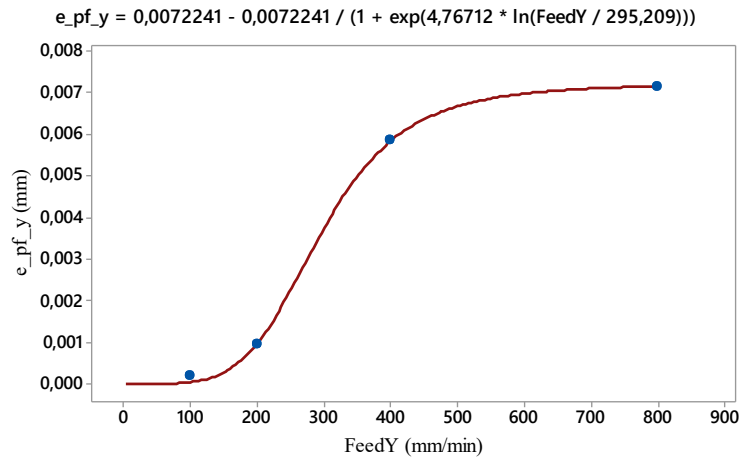


FIGURE 5.25 FEED WISE CHANGE IN POSITION ERROR IN Y-AXIS

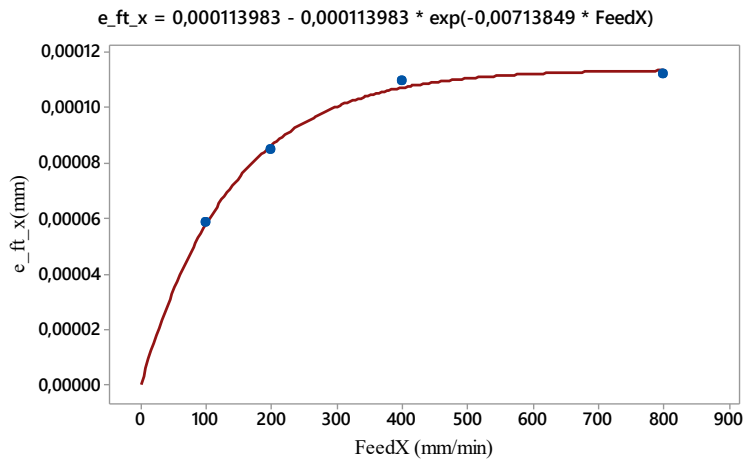


FIGURE 5.26 FEED WISE CHANGE IN TABLE TILT ALONG Y-AXIS

It is important to observe here that the process errors are reported here as a cumulative effect of process errors on both walls in case of both X and Y-axis. However, the actual process error for forward prediction will be half the value reported of the overall process error. An important observation is the result that the increase in feed is causing the overall reported dimensions of the workpiece to increase. This observation can be related to the fact that an increase in cutting force increases the overall tool and workpiece deflection and hence may cause an increase in the reported dimensions of the workpiece. The feed wise change in error along Z axis is further reported in figure 5.27. While the spindle deflection is reported here as figure 5.28.

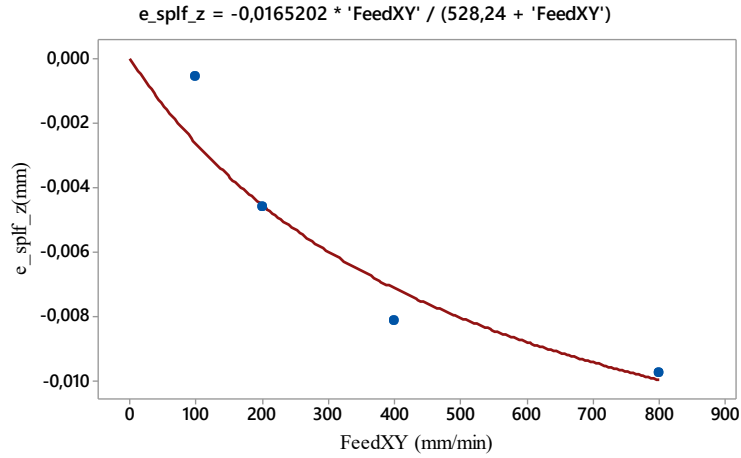


FIGURE 5.27 FEED WISE CHANGES IN PROCESS ERROR ALONG Z-AXIS

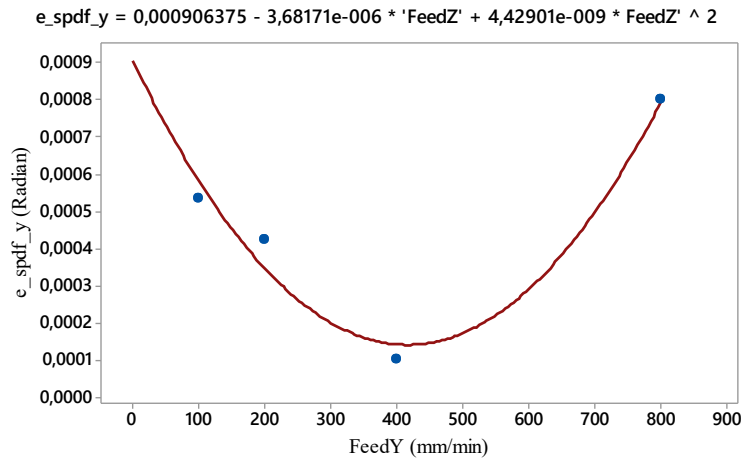


FIGURE 5.28 FEED WISE CHANGE IN SPINDLE DEFLECTION ALONG Y-AXIS

Further on the table tilt is reported here as Figure 5.29

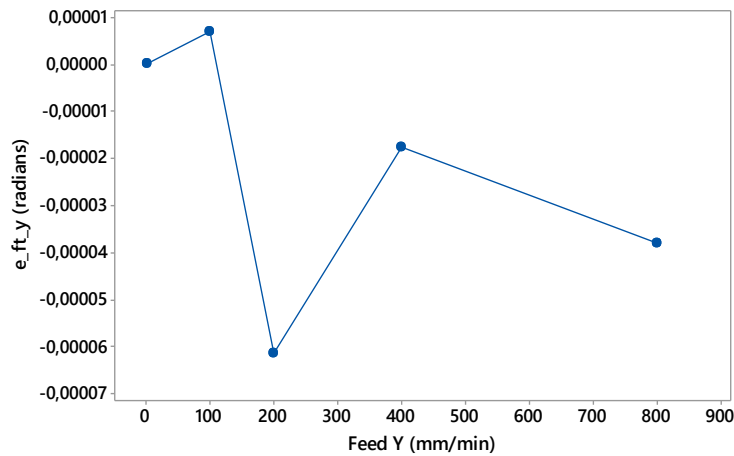


FIGURE 5.29 FEED WISE CHANGE IN TABLE TILT ALONG Y-AXIS

The graph above shows the changes in table tilt angle under different feeds. It can be observed that the effect of change in Feed on table tilt is almost negligible owing to its very small magnitude. The pattern however, is similar to the one observed as a result of change in thermal state. It is also important to observe that the above graph only shows the increase associated with changes in feed only and the effect of other errors are already incorporated in the results. The regression equation for the same is given below as equation 5.45.

$$e_{ft_y} = -2,87348e - 006 - 1,26299e - 007 \times 'FeedY' + 1,0724e - 010 \times 'FeedY' ^ 2 \quad Eq. 5.45$$

For the feed case, the values below a feed of 100 could not be taken into the model accurately and hence due their relatively small magnitude the variation below a feed of 100mm/min can be taken as zero or can be simply calculated as a fraction of error at feed of 100mm/min. For the current research however, due to their small magnitude and the scarcity of use of a table feed below 100mm/min, the variations in spindle tilt have been taken as zero for feeds below 100mm/min.

Calculations have also been carried out for X-Axis and the regression equations are developed for the overall process errors based on feed. The equations are given here as Equation 5.46 to 5.48

$$e_{splf_z} = -0,0165202 * 'FeedXY' / (528,24 + 'FeedXY') \quad Eq. 5.46$$

$$e_{pf_y} = 0,0072241 - 0,0072241 / (1 + exp(4,76712 \times ln('FeedY' / 295,209))) \quad Eq. 5.47$$

$$e_{spdf_y} = 0,000906375 - 3,68171e - 006 \times 'FeedZ' + 4,42901e - 009 \times 'FeedZ' ^ 2$$

$$e_{pf_x} = 0,0257241 - 0,0257241 / (1 + exp(4,09199 \times ln(FeedY / 660,765)))$$

$$e_{ft_x} = 0,000113983 - 0,000113983 \times exp(-0,00713849 \times FeedX) \quad Eq. 5.48$$

$$e_{spdf_x} = 0,0065 - 0,0065 / (1 + exp(6,37987 * ln(FeedY / 660,765)))$$

It is pertinent to mention that at the current stage the process errors dependent on feed and hence any change in other machining parameters may not produce an effect on the predicted process errors. Therefore, for generalizing the process error it is necessary to link the process errors with the cutting force so that the overall errors can be predicted based on the any tool diameter and cutting force. As presented in the methodology the following section deals presents the results and analysis for such conversion.

5.5.1 Conversion to Force Based Process Error:

A MATLAB program calculating process errors based on force model is used for generation of process errors at various feeds and a fixed spindle speed of 3500 r.p.m and the resulting feed wise errors are reported here as Figure 5.30.

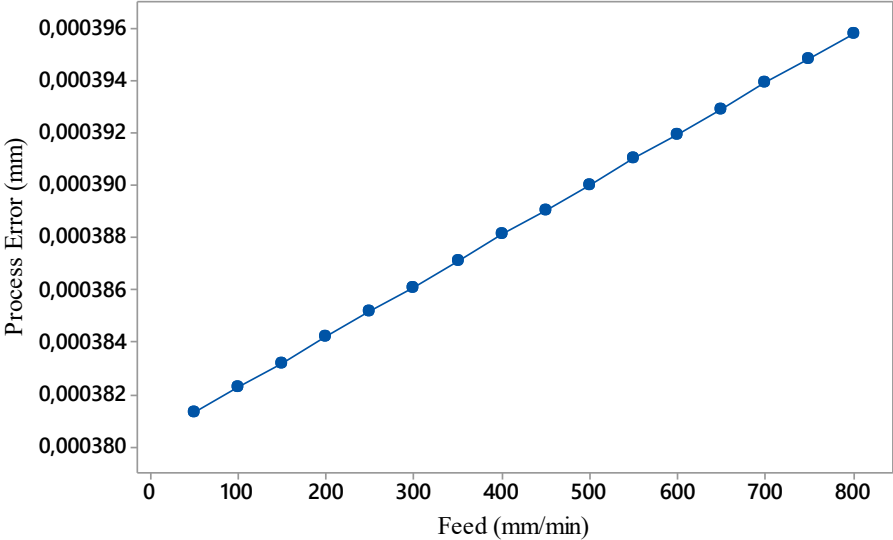


FIGURE 5.30 FEED WISE PROGRAM GENERATED PROCESS ERRORS

The program generated errors are different in magnitude however the trend they exhibit is actual and hence once they are linked with the errors generated by the process itself the overall model can be used for prediction of errors based on the program generated errors. This is similar to calibrating the program based on the available data. Figure 5.31 presents the linkage between program generated and process generated errors in X-Axis.

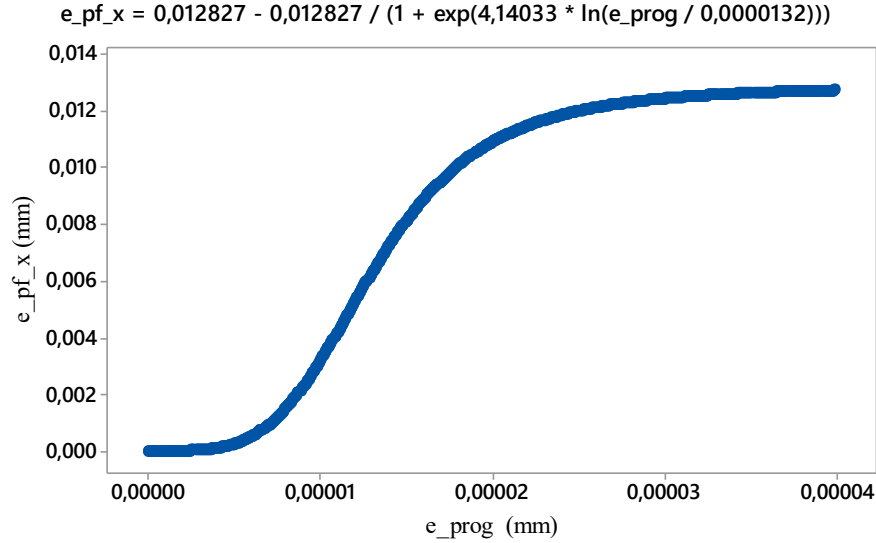


FIGURE 5.31 PROGRAM GENERATED WISE CHANGE IN ACTUAL PROCESS ERRORS

Similar methodology is adopted for Y and Z axis. The equations providing relationship between software generated and actual process errors are given here from equation 5.49 to 5.51:

$$e_{pf_y} = 0,00361205 - 0,00361205 / (1 + \exp(4,76712 \times \ln(e_{prog} / 5,88564e - 006))) \quad Eq. 5.49$$

$$e_{pf_x} = 0,012827 - 0,012827 / (1 + \exp(4,14033 \times \ln(e_{prog} / 0,0000132))) \quad Eq. 5.50$$

$$e_{spfl_z} = -0,0165202 \times e_{prog} / (1,05316e - 005 + e_{prog}) \quad Eq. 5.51$$

The next stage is the separate identification of control errors due to distance against a specific feed and the control error due to force. The following section presents the results and analysis of such identification.

5.6 Control errors Results and analysis:

A comparison between the dimensions of workpiece 2 and workpiece 8 after taking out the effect of thermal, positional and process errors for the corresponding workpiece machining conditions,

yields us the control errors. due to change in feed at each step while the difference across the steps provides the change in control errors based on change in distance.

5.6.1 Distance and Feed Based Control Errors:

Figure 5.32 presents the result of analysis for control errors in X-axis when the feed rate is changed from 2400mm/min to 100mm/min across 100mm. The data is further used for generation of regression equations given here as equation 5.52 and equation 5.53.

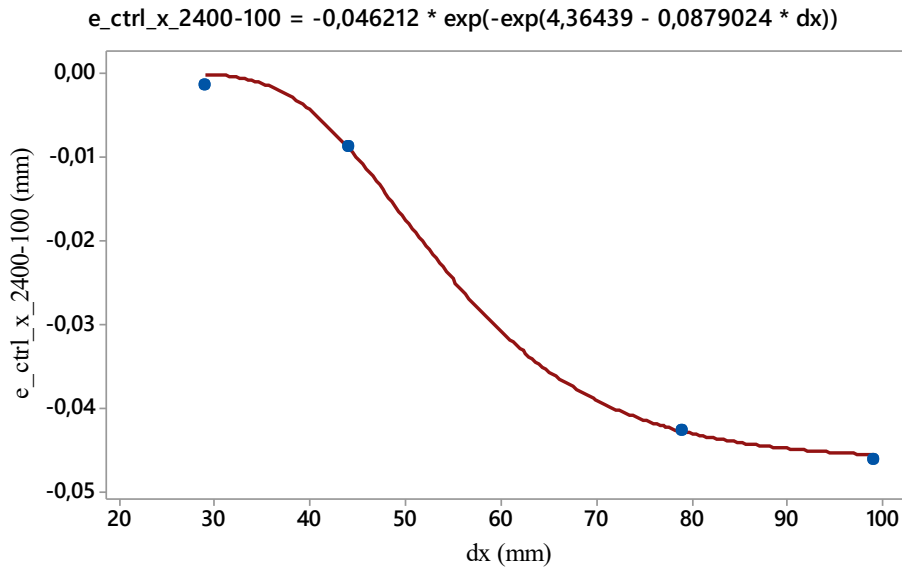


FIGURE 5.32 DISTANCE WISE CONTROL ERROR DUE TO FEED CHANGE

$$e_{ctrl_y(2400-100)} = -0,000845512 \times dy + 6,40112e - 006 \times dy \times dy + 0,0167701 \quad Eq. 5.52$$

$$e_{ctrl_x(2400-100)} = -0,036 + 0,036 / (1 + \exp(7,60716 \times \ln(dx / 77,1779))) \quad Eq. 5.53$$

It is important to observe here that due to absence of relation between control errors and the table and spindle tilt the same have not been predicted. The data for Z axis also has not been found significant primarily due to the limitation of inseparable spindle deflection and process errors from the control errors.

The Feed can be incorporated in equation 5.52 and 5.53 to obtain prediction equations with appreciation of both feed and position. The new equations are therefore given as equation 5.54 and equation 5.55.

$$e_{ctrl_y} = (Feed - 100/2400 - 100) \times -0,000845512 \times dy \quad Eq. 5.54$$

$$+ 6,40112e - 006 \times dy \times dy + 0,0167701$$

$$e_{ctrl_y} = (Feed - 100/2400 - 100) \times -0,036 + 0,036 / (1 \quad Eq. 5.55$$

$$+ exp(7,60716 \times ln(dx / 77,1779)))$$

5.6.2 Conversion to Force based Control Errors:

Once the prediction model for control errors based on prediction is obtained the next step is to obtain the prediction model for control errors based on force. The same is obtained through a comparison between dimensions of workpiece 2 and workpiece 5 while also taking out the effects of position and feed based control errors, thermal errors, process errors and mechanical position errors. The dimension results for 2nd, 5th and 8th workpieces are presented here as Table 5.6.

TABLE 5.6 REPORTED X AND Y DIMENSIONS FOR W2, W5 AND W8

Step	X-W2	X-W8	X-W5	Y-W2	Y-W8	Y-W5
1	29,0486	30,0447	29,0237	29,04575	29,0562	29,0112
2	44,0510	45,0492	44,0355	44,052	44,0626	44,0348
3	79,0570	80,0629	79,0526	79,0625	79,0805	79,0388
4	99,0603	99,0832	99,0646	99,079	99,0898	99,0570

Table 5.7 presents the various errors calculated for workpiece 2 and workpiece 5 using the regression models developed in all other errors.

TABLE 5.7 ERRORS CALCULATED USING PREDICTION MODEL FOR W2 AND W5

$\frac{dx}{dy}$	$e_{pf_{xw2}}$	$e_{pf_{xw5}}$	$e_{pf_{yw2}}$	$e_{pf_{yw5}}$	$e_{pt_{xw2}}$	$e_{pt_{xw5}}$	$e_{pt_{yw2}}$	$e_{pt_{yw5}}$	e_{pos_x}	e_{pos_y}
29	0,00019 1988	1,13377 E-05	0,00097 635	4,12225 E-05	0,00123 5877	0,00242 5937	0,00195 0791	0,00195 2618	0,00642 3335	0,00978 9383
44	0,00292 3753	0,00019 1988	0,00584 9463	0,00097 635	0,01644 7688	0,01767 6739	0,00303 1592	0,00338 6255	0,00911 4022	0,01385 5253
79	0,01765 2045	0,00292 3753	0,00716 2287	0,00584 9463	0,02509 7789	0,02494 0679	0,00824 6326	0,00807 5374	0,01371 726	0,02069 7125
99	0,02505 2323	0,01765 2045	0,00722 1811	0,00716 2287	0,02946 674	0,02874 9516	0,01451 3989	0,01328 8542	0,01529 4803	0,02294 4093

The final errors in control due to process based is calculated as per model given in previous chapter and regression analysis is performed on both X and Y axis values. The regression result for X-Axis is presented here as equation 5.56.

$$e_{cpr_x} = 0,007907 - 3,85058e - 005 \times 'FeedX' + 3,64143e - 008 \times 'FeedX' \times 'FeedX' \quad Eq. 5.56$$

The Process parameter based control errors for Y-axis could not be fitted into a regression model as their variation is random in nature while the variation is also much smaller than that observed in case of X-Axis. An average value of 0.0012 micrometer is taken as compensation factor for Y-Axis for forward prediction model. The variation against feed is presented here as Fig 5.33.

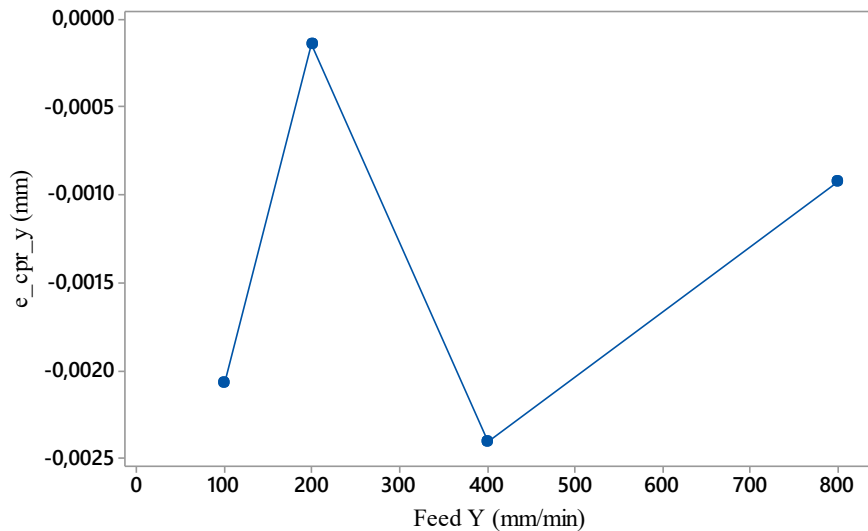


FIGURE 5.33 FEED BASED CONTROL ERROR ALONG Y-AXIS

The regression model is further used for comparison with the errors generated for a range of feeds through the MATLAB code introduced earlier. The final regression model is given as equation 5.57.

$$e_{cpr_x} = 0,007907 - 1931,35 \times eprog + 9,16102e + 007 \times eprog \times eprog \quad Eq. 5.57$$

Meanwhile figure 5.34 represents the software based process error wise control errors:

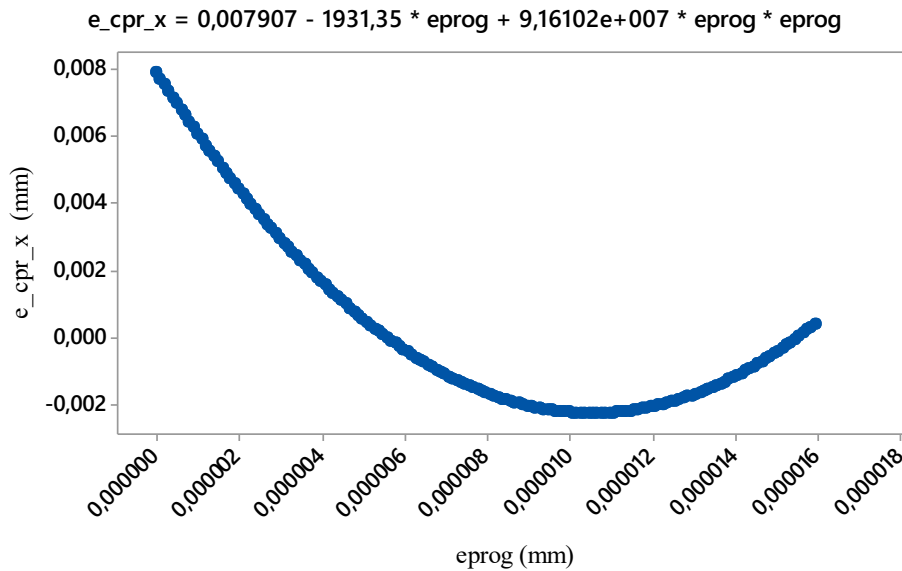


FIGURE 5.34 SOFTWARE GENERATED PROCESS ERROR WISE CHANGE IN CONTROL ERRORS

The reporting of control errors based on position and force concludes the error measurement and analysis along with the development of forward prediction model. However before concluding the chapter brief results of backward prediction analysis for model selection are reported in the next section.

5.7 Prediction Model Variation analysis:

As described earlier, each prediction model is selected based on a comparison between at least four different models and the parameters within the model are also adjusted to reach a prediction model where the value for backward prediction error is minimum. Table 5.8 presents the results for one such analysis carried out for ' e_{spl_z} '.

TABLE 5.8 BACKWARD PREDICTION ERROR ANALYSIS

Temp state	e_{splz}	model 1	model 2	model 3	model 4	diff 1	diff 2	diff 3	diff 4
0	0	0,001191	0	0,00144	0,001555	0,001191	0	0,00144	0,001555
10	0,005	0,003284	0,00267	0,003267	0,003275	0,001716	0,00233	0,001733	0,001725
50	0,008	0,008316	0,00859	0,007916	0,007753	0,000316	0,00059	8,4E-05	0,000247
90	0,01	0,010443	0,010754	0,01009	0,009933	0,000443	0,000754	9,01E-05	6,71E-05
130	0,011	0,011342	0,011545	0,011107	0,010994	0,000342	0,000545	0,000107	6,17E-06

A graphical plot for the data is provided here as Figure 5.35.

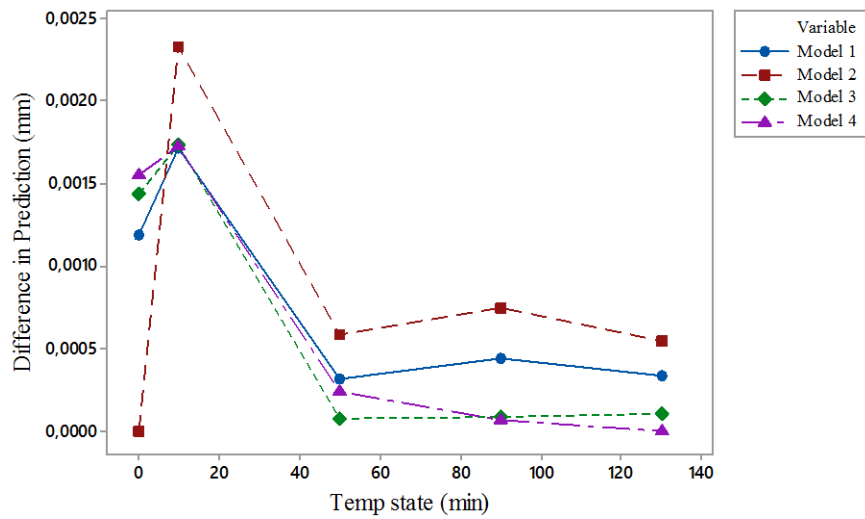


FIGURE 5.35 TEMPERATURE STATE WISE BACKWARD PREDICTION DIFFERENCE e_{splz}

Meanwhile figure 5.36 presents a case for ' e_{ptx} ' backward prediction model comparison.

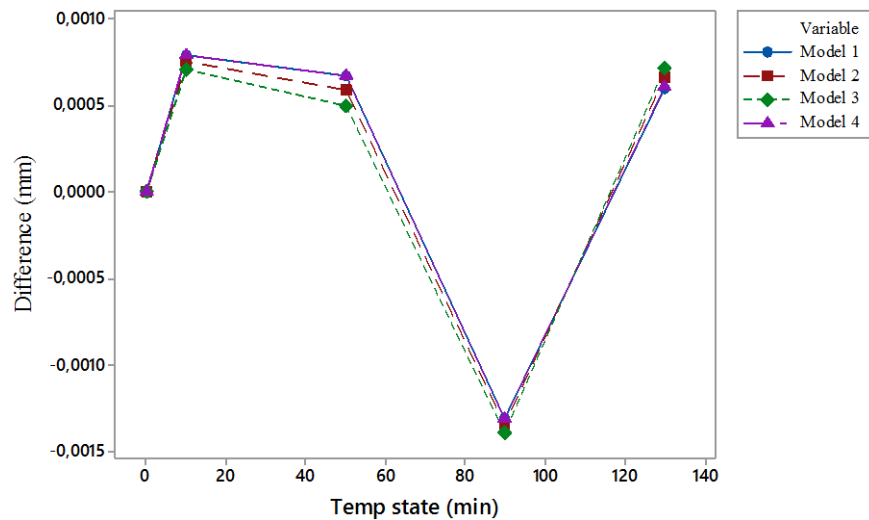


FIGURE 5.36 TEMPERATURE STATE WISE BACKWARD PREDICTION DIFFERENCE (e_{ptx})

For more than 80% of all cases the backward prediction error was within 5% while apart from a few anomalies the overall backward prediction error remained within 10% of the actual value.

5.8 Conclusion

The results depict the capacity of the current model in terms of not only measurement of all relevant error parameters but also shows the capability of the proposed model for development of behavior prediction models. These models can then be used for prediction of errors under different machining conditions. It is also pertinent to mention here that the results contain two different aspects in terms of determined errors. The shorter version of results without the MATLAB model is useful for a production scenario while the comprehensive error model can be used for both production and job shop scenarios. As the obtained equations are based on machine behavior hence the equations can be used for study of machine behavior under different cutting conditions. Similarly, the use of equations can also be made towards development of optimization models for feed and Spindle speeds with the objective of minimizing errors while maximizing Material Removal Rate.

At this stage, it is further deemed necessary to challenge the model through comparison of model generated errors with the actual errors obtained on the surface of the workpiece. The next chapter therefore deals with implementation of the model on various scenarios for determining the accuracy of prediction of the model.

Chapter 6. Implementation

The methodology presented in the current research is radically different from the existing methodologies. Apart from this being a contribution of the current research this also indicates the need for challenging the model for analyzing the effectiveness of the methodology. The current chapter therefore deals with the implementation of the resulting model developed in the previous chapter.

Two different scenarios have been considered for implementation, and the overall results have been evaluated against the error predictions obtained through the developed model. One of the scenarios considered for the accuracy evaluation of predicted errors is the application of generated compensation on the workpiece while the same workpiece is machined at different feeds and speeds. This is followed by CMM measurements to identify the effectiveness of the generated compensation. The second scenario involves the application of different feeds and spindle speeds on two different, more complex shapes. The errors generated on the surfaces are identified through use of CMM and the magnitudes are compared with the error magnitudes predicted through the defining equations.

6.1 Case 1: MRR Maximization:

For the first scenario, a simple compensation program has been generated for a set of feeds and speeds presented in table 4.1 as workpiece 3. The compensation program is developed using simple wall and floor offsets. The same are presented here as Table 6.1.

TABLE 6.1 STEP WISE COMPENSATIONS USED:

Step	X-Axis	Y-Axis	Z-Axis
1	0,018864025	0,016471358	0,005047021
2	0,028918242	0,025052479	0,008047021
3	0,036108621	0,032637448	0,010047021
4	0,041506224	0,039341905	0,080047021

Once the experiment is carried out the measurement results shows a decrease in overall error magnitudes. The decrease in error magnitude is presented here as Fig 6.1.

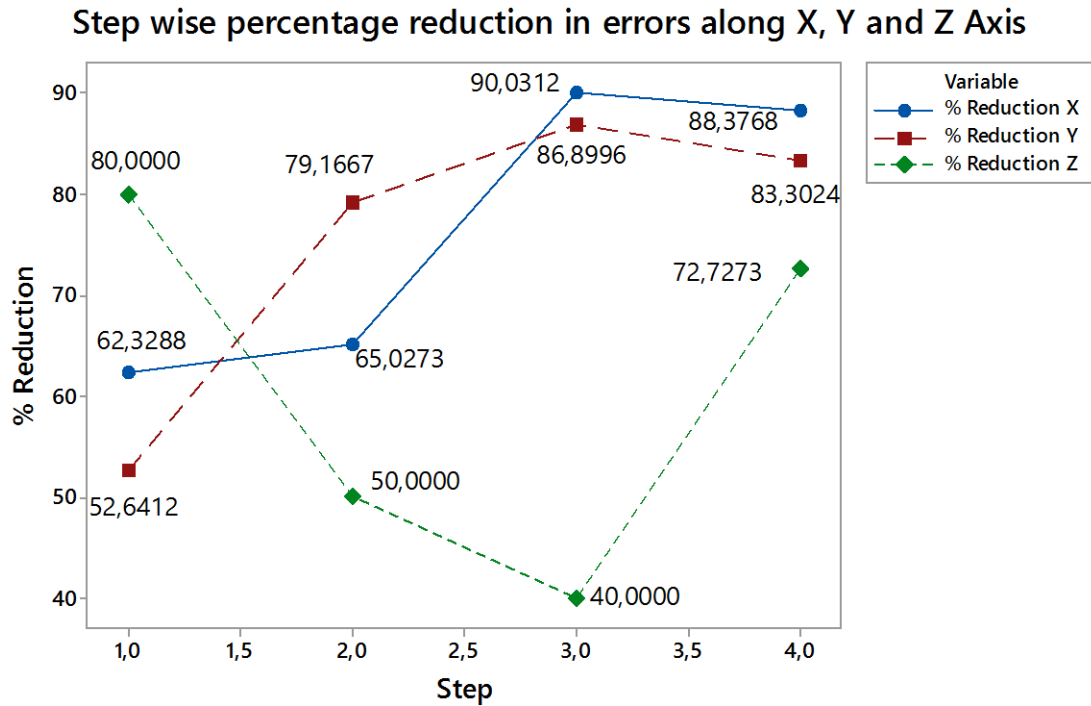


FIGURE 6.1 STEPWISE PERCENTAGE REDUCTION IN ERRORS ALONG X, Y AND Z AXIS

The error reduction in X and Y axis is above 79% in most of cases except for the first case where the error reduction for x and y axis is approximately 62.3% and 52.6% respectively. The main reason for a low percentage error reduction in the first two cases for X and Y axis is the small magnitude of process, control and thermal errors on the first stage. The difference is compounded by the fact that at the first stage the errors due spindle deflection and table tilts form a considerable part of total error magnitude and as a simple compensation based on only axis coordinates is used hence there is a considerable gap between the compensation generated and actual error magnitude for stage 1. For the Z- axis the average percentage reduction is approximately 60%. This is again due to the fact that the overall spindle deflection plays an important role in the total error magnitude reported for Z axis. Therefore, a program with no appreciation for deflections can only produce a compensation along Z axis only therefore causing a difference in the reported magnitude. Therefore, the author proposes the use of adaptive compensation technique for actual error compensation. Such a technique is not in scope of the current research and therefore has not been adopted.

The percentage errors meanwhile may not provide the actual picture in a correct manner. Therefore, a comparison against the original total error magnitude is required. The same is presented here as Figure 6.2

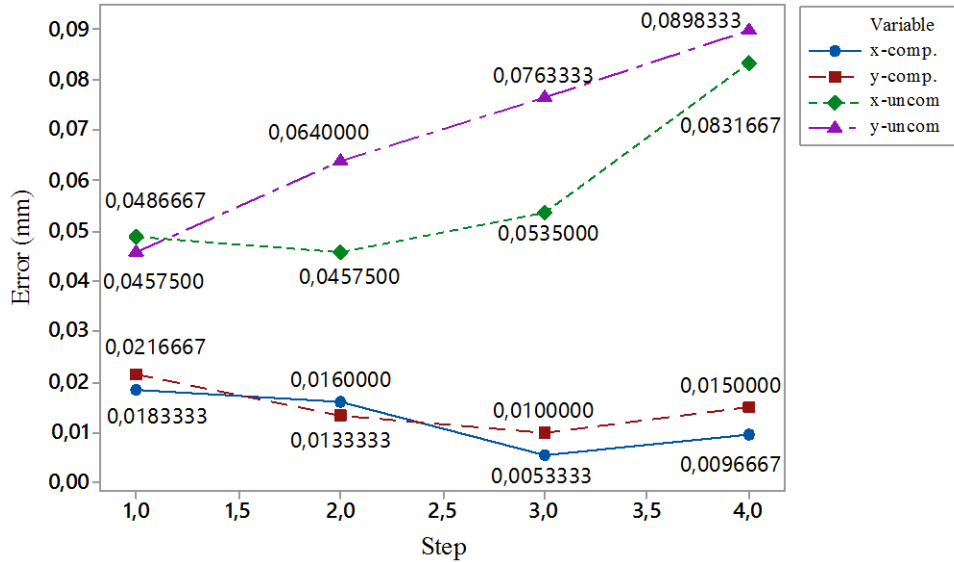


FIGURE 6.2 COMPENSATED VS UNCOMPENSATED ERROR MAGNITUDE IN X AND Y AXIS.

From figure 6.2 the most important observation is the reduction in variation of error magnitudes at different combinations of feeds and spindle speeds. The reduction in variation indicates that apart from a small uncompensated magnitude the overall variations in position, thermal process and control errors have been largely compensated. This is important for practical purposes in parts which are generally larger in magnitude and thus these variations play an important role in generation of different magnitude of errors at different dimensions of the workpiece. It is also pertinent to mention here that a small magnitude of thermal errors is neglected in this comparison process as time stamps for W3 and other compared parts were slightly different.

It is therefore important to notice that a maximization of MRR can be obtained through the proposed prediction. However, the surface finish of the final workpiece may also need to be considered in a trade-off for such maximization. The overall results therefore indicate that the developed model can be feasibly used for error prediction and reduction.

6.2 Case 2: Change in Shape:

The model has already been applied in a simple compensation scenario however, there is a need for further demonstration of capability of model when the shape is changed. This is achieved through machining of a cylindrical shape components followed by measurement of the resulting geometry obtained. Table 6.2 presents the measurement data obtained.

TABLE 6.2 MEASURED COORDINATE DATA FOR X AND Y AXIS

X-coordinate	Y-Coordinate	Angle X	Angle Y	Actual X	Actual Y
10,102	1,161	82:44:00	07:16:01	10,088	1,157
15,546	0,905	128:21:25	38:21:25	15,531	0,901
22,291	4,383	135:18:51	45:18:51	22,273	4,377
25,56	9,375	140:36:32	50:36:34	25,540	9,367
24,923	19,656	170:10:36	99:48:55	24,904	19,644
18,255	25,827	126:59:27	143:00:33	18,239	25,813
7,785	25,618	40:24:36	130:24:33	7,772	25,603
0,839	17,72	43:19:17	133:19:17	0,825	17,706
1,35	8,252	20:21:38	110:21:34	1,336	8,244
6,447	2,694	42:53:14	47:06:47	6,429	2,687
13,705	0,769	100:18:17	10:18:17	13,687	0,764
17,28	1,373	90:19:45	00:19:45	17,264	1,368
21,566	3,719	143:18:37	53:18:37	21,547	3,714
25,512	9,192	133:52:01	43:52:01	25,493	9,182
26,278	14,747	172:22:34	82:23:25	26,258	14,736

Random points are taken and the respective actual positions of X and Y coordinates are located through the observed angular data from the actual workpiece model. The extracted points for both X-Axis and Y-Axis are also presented in table 6.2 as X-Actual and Y-Actual respectively. The overall error in X- Axis and Y-Axis at each point is hence taken as the difference between actual and measured dimensions.

Meanwhile measurement for Z axis and the point wise dimension is directly taken from CMM by measuring 9 different points on top face and using the points to formulate a plane. The plane is then used as a base plane for measurement of point wise Z-height.

The actual and measured dimensions along Z-Axis and predicted and actual errors therein are presented here as Table 6.3 though to Table 6.5.

TABLE 6.3 ACTUAL AND MEASURED Z DIMENSIONS AND ERROR COMPONENTS

X-cord	Y-cord	Z-meas.	Z-Actual	Feed Z	e_{posz}	e_{splz}	e_{tty}	e_{tt_x}	e_{splf_z}
1,884	3,115	-8,999	9	100	-0,00175	7,09E-05	-1,4E-05	-6,6E-05	-0,00263
1,692	4,426	-8,998	9	100	-0,00175	0,00012	-2,1E-05	-6,7E-05	-0,00263
22,856	1,318	-9,002	9	100	-0,00175	0,000173	-2,7E-05	-6,7E-05	-0,00263
25,127	3,645	-9,001	9	100	-0,00175	0,000224	-3,1E-05	-6,7E-05	-0,00263
25,186	5,892	-9,001	9	100	-0,00175	0,000274	-3,5E-05	-6,7E-05	-0,00263
25,165	25,312	-9,003	9	100	-0,00175	0,000324	-3,8E-05	-6,8E-05	-0,00263
22,654	24,855	-9,002	9	100	-0,00175	0,000374	-4,1E-05	-6,8E-05	-0,00263
21,931	25,501	-9,001	9	100	-0,00175	0,000424	-4,4E-05	-6,8E-05	-0,00263
3,703	25,787	-9,002	9	100	-0,00175	0,000473	-4,6E-05	-6,9E-05	-0,00263
2,307	25,218	-8,999	9	100	-0,00175	0,000523	-4,8E-05	-6,9E-05	-0,00263
2,795	24,317	-9,001	9	100	-0,00175	0,000571	-4,9E-05	-6,9E-05	-0,00263
0,975	22,393	-9,000	9	100	-0,00175	0,00062	-5,1E-05	-6,9E-05	-0,00263
0,976	20,924	-9,000	9	100	-0,00175	0,000668	-5,2E-05	-7E-05	-0,00263
0,626	19,636	-9,000	9	100	-0,00175	0,000716	-5,3E-05	-7E-05	-0,00263

TABLE 6.4 MODEL BASED ERROR COMPONENTS

Point	e_{posz}	e_{splz}	e_{tty}	e_{tt_x}	e_{spd_x}	e_{spd_y}
1	-0,001753	7,09248E-05	-1,3743E-05	-6,63161E-05	-0,000408544	6,1541E-05
2	-0,001753	0,000120239	-2,07342E-05	-6,65992E-05	-0,000409144	8,21389E-05
3	-0,001753	0,000173471	-2,67417E-05	-6,69046E-05	-0,000409675	0,000100431
4	-0,001753	0,000223607	-3,13453E-05	-6,7192E-05	-0,000410062	0,000115486
5	-0,001753	0,000274149	-3,52168E-05	-6,74815E-05	-0,000410341	0,000129229
6	-0,001753	0,000324399	-3,84782E-05	-6,77691E-05	-0,000410506	0,000141843
7	-0,001753	0,00037436	-4,12652E-05	-6,80549E-05	-0,00041056	0,00015358
8	-0,001753	0,000424034	-4,36758E-05	-6,83387E-05	-0,000410502	0,000164609
9	-0,001753	0,000473422	-4,57831E-05	-6,86207E-05	-0,000410335	0,00017505
10	-0,001753	0,000522526	-4,76421E-05	-6,89008E-05	-0,000410058	0,000184994
11	-0,001753	0,000571348	-4,92954E-05	-6,91791E-05	-0,000409674	0,000194508
12	-0,001753	0,00061989	-5,07764E-05	-6,94555E-05	-0,000409183	0,000203648
13	-0,001753	0,000668152	-5,21117E-05	-6,97301E-05	-0,000408585	0,000212456
14	-0,001753	0,000716138	-5,33224E-05	-7,00029E-05	-0,000407883	0,000220968

TABLE 6.5 MODEL BASED ERROR COMPONENTS

Point	e_{splf_z}	e_{ztty}	e_{zttx}	e_{zspd_x}	e_{zspdy}
1	-0,0026296	-0,000663161	-0,00013743	0,003676901	0,000553869
2	-0,0026296	-0,000665992	-0,000207342	0,0036823	0,00073925
3	-0,0026296	-0,000669046	-0,000267417	0,003687072	0,000903878
4	-0,0026296	-0,00067192	-0,000313453	0,003690555	0,001039373
5	-0,0026296	-0,000674815	-0,000352168	0,003693065	0,001163062
6	-0,0026296	-0,000677691	-0,000384782	0,003694557	0,001276589
7	-0,0026296	-0,000680549	-0,000412652	0,003695039	0,001382219
8	-0,0026296	-0,000683387	-0,000436758	0,003694522	0,001481477
9	-0,0026296	-0,000686207	-0,000457831	0,003693014	0,00157545
10	-0,0026296	-0,000689008	-0,000476421	0,003690525	0,001664944
11	-0,0026296	-0,000691791	-0,000492954	0,003687065	0,001750575
12	-0,0026296	-0,000694555	-0,000507764	0,003682643	0,001832832
13	-0,0026296	-0,000697301	-0,000521117	0,003677268	0,001912105
14	-0,0026296	-0,000700029	-0,000533224	0,003670951	0,001988715

Figure 6.3 further presents the errors observed along Z axis as compared to the software predicted errors.

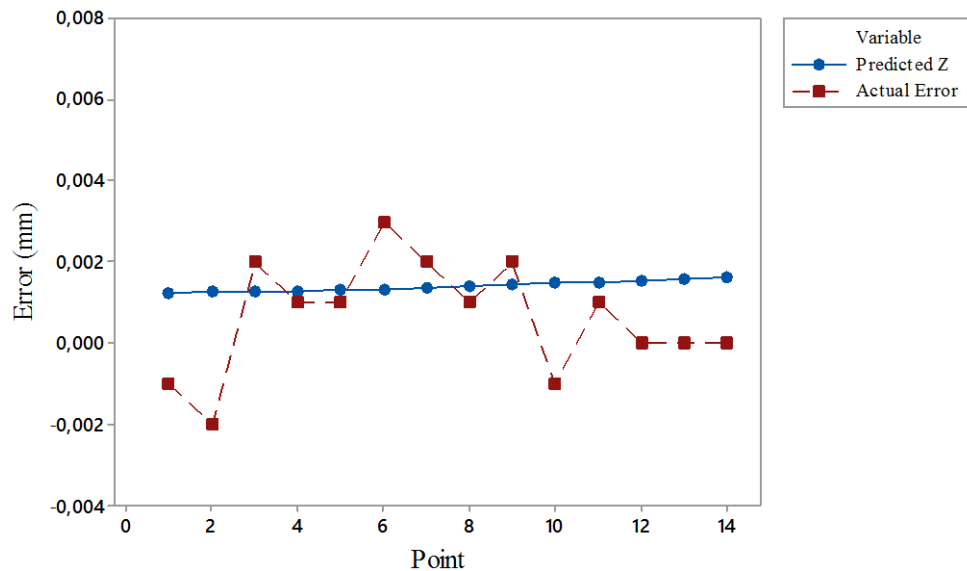


FIGURE 6.3 POINT WISE OBSERVED AND PREDICTED ERRORS ALONG Z-AXIS

It is important to observe that the predicted table tilt spindle tilt due to various machining parameters are also considered for the calculation of Z-Axis predicted error magnitude. The

prediction accuracy in most cases is above 70% with two outliers. It is also important to mention that one point in Z measurement has been casted as outlier and hence not taken into consideration for the calculation or comparison process. Meanwhile it is also important to observe the prediction accuracy in X and Y axis. Table 6.6 and Table 6.7 presents the calculated errors in X and Y axis.

TABLE 6.6 CALCULATED ERRORS IN X AND Y AXIS- PART 1

Point	Feed	SpindleSpeed	e_{pt_x}	e_{pt_y}	e_{pf_x}	e_{pf_y}
1	200	4500	0,000129393	0,001098012	9,5994E-05	0,000488175
2	200	4500	0,000322412	0,001276625	9,5994E-05	0,000488175
3	200	4500	0,000577789	0,001504983	9,5994E-05	0,000488175
4	200	4500	0,000788888	0,001687246	9,5994E-05	0,000488175
5	200	4500	0,001008878	0,001871247	9,5994E-05	0,000488175
6	200	4500	0,001227177	0,002048137	9,5994E-05	0,000488175
7	200	4500	0,001443801	0,002218329	9,5994E-05	0,000488175
8	200	4500	0,001658763	0,002382207	9,5994E-05	0,000488175
9	200	4500	0,001872078	0,002540128	9,5994E-05	0,000488175
10	200	4500	0,002083759	0,002692422	9,5994E-05	0,000488175
11	200	4500	0,002293821	0,002839395	9,5994E-05	0,000488175
12	200	4500	0,002502276	0,002981332	9,5994E-05	0,000488175
13	200	4500	0,00270914	0,003118499	9,5994E-05	0,000488175
14	200	4500	0,002914425	0,003251142	9,5994E-05	0,000488175
15	200	4500	0,003118144	0,003379493	9,5994E-05	0,000488175

TABLE 6.7 CALCULATED ERRORS IN X AND Y AXIS- PART 2

Point	e_{pos_x}	e_{pos_y}	e_{ctrl_x}	e_{ctrl_y}	e_{cpr_x}	e_{cpr_y}
1	0,002420265	0,000440767	0,006999993	-3,40518E-05	0,001662412	-4,1528E-05
2	0,003643546	0,000343928	0,006999817	-2,80264E-05	0,001662412	-4,1528E-05
3	0,005080473	0,001642634	0,00699716	-3,81553E-05	0,001662412	-4,1528E-05
4	0,005745554	0,003442767	0,006991959	0,00021796	0,001662412	-4,1528E-05
5	0,005617561	0,00691279	0,006993364	0,001750544	0,001662412	-4,1528E-05
6	0,004231126	0,008842157	0,006999379	0,003320328	0,001662412	-4,1528E-05
7	0,001882417	0,008778696	0,006999999	0,003259186	0,001662412	-4,1528E-05
8	0,000208449	0,006283775	0,007	0,00135853	0,001662412	-4,1528E-05
9	0,000334746	0,003044377	0,007	0,000132532	0,001662412	-4,1528E-05
10	0,001567144	0,001016519	0,007	-5,25782E-05	0,001662412	-4,1528E-05
11	0,003236218	0,000292402	0,006999993	-2,44841E-05	0,001662412	-4,1528E-05
12	0,004021268	0,000520811	0,006999591	-3,84065E-05	0,001662412	-4,1528E-05
13	0,0049302	0,001397517	0,006997792	-4,8182E-05	0,001662412	-4,1528E-05
14	0,005735937	0,003378107	0,006992074	0,000202938	0,001662412	-4,1528E-05
15	0,005888892	0,005295775	0,006990074	0,000849957	0,001662412	-4,1528E-05

The values have been further plotted in Figure 6.4 for X-Axis.

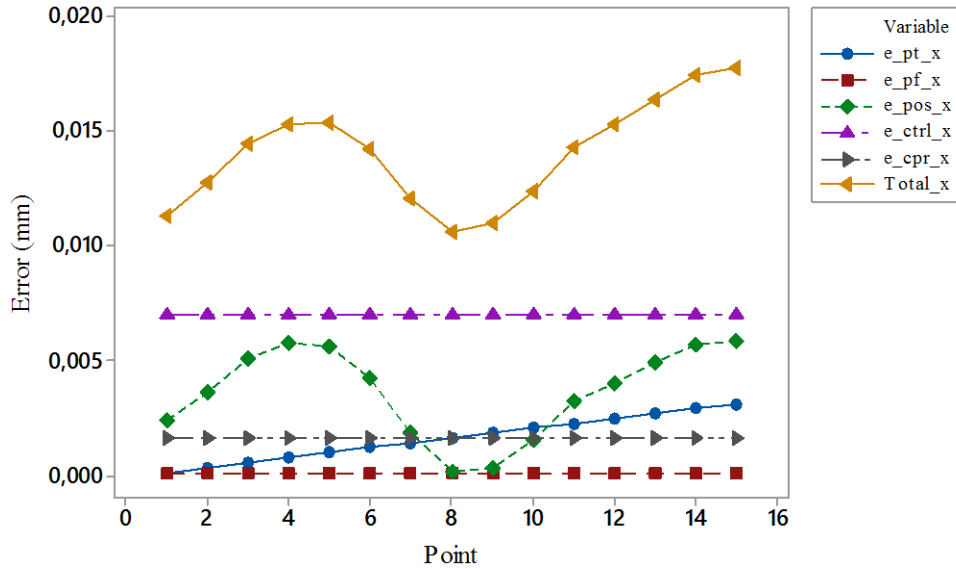


FIGURE 6.4 POINT WISE TOTAL AND VARIOUS ERROR COMPONENTS ALONG X-AXIS

It can be observed that the position error forms the major component of the errors predicted for the workpiece surface. This is mainly since the time interval for the actual cutting is short while the process errors are small due to high spindle speed and small feed. It is also important to observed that the error due to control in X axis is not changing much in this case as the difference between minimum and maximum observed value is 26 mm only. Similarly Figure 6.5 presents the error component data for Y-axis.

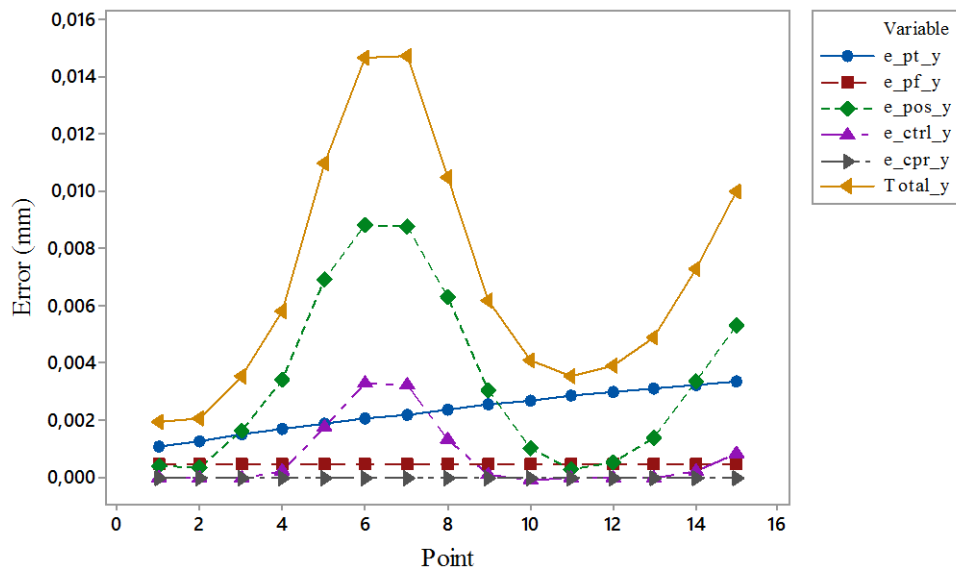


FIGURE 6.5 POINT WISE TOTAL AND VARIOUS ERROR COMPONENTS ALONG Y-AXIS

It can be observed that the predicted value for Y- Axis is smaller than that observed in X-axis. Here the axis response to cutting force seems to be more rigid than X-Axis as the overall change in control errors due to cutting force denoted as 'e_cpr_y' is much smaller than that observed for X-Axis in figure 6.4.

A comparison of the actual and predicted errors is presented in Figure 6.6.

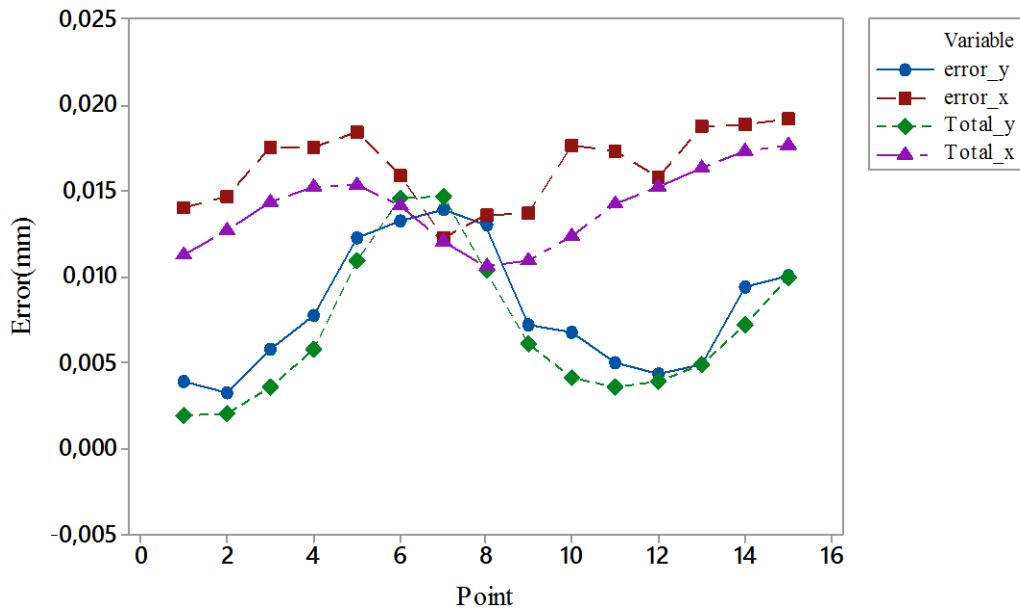


FIGURE 6.6 POINT WISE ERROR IN X AND Y AXIS

Here 'error_y' and 'error_x' represents the observed error on the machined surface for Y and X axis respectively while the symbols 'Total_y' and 'Total_x' represents the total magnitude of predicted errors. It can be observed from the figure that a close match is observed between the measured and predicted errors in both Axis. While an over compensation in case of Y axis is also apparent. However, the magnitude of overcompensation is within single digit at micrometer level. The accuracy of prediction in case of Y axis is more than that observed in case of X Axis where a maximum deviation from predicted errors is observed up to 4 μ m.

6.3 Conclusion:

The methodology presented in the current research can be implemented on various shapes and sizes of workpiece while machining under various conditions. Maximization of MRR through use of methodology is an important aspect of the current methodology and can be carried out with the

predicted model. The model also possesses the capability of prediction of errors for different shapes.

Meanwhile several issues need to be considered for the implementation. One of the key issues is regarding the absence of a compensation methodology as most compensation methodologies are mainly focused towards a specific model, meanwhile the general compensation models often lack the appreciation for changing time and parameter based errors. The location mapping methodologies for actual position of workpiece also needs to be comprehensively modified for inclusion of thermal, process and control errors.

Several general observations regarding the machine based on the error prediction model have also been made.

1. The response of control towards changing forces in case of X-Axis is less rigid than that observed in Y-Axis. This may be due to the size of table and the consequent larger mass of the X axis table.
2. The spindle tilt under thermal influence is observed to be larger in case of X-Axis. This may also be due to the Z-Axis assembly.
3. The position error variation in X-Axis is larger than the variation in case of Y-Axis.
4. The spindle tilt is observed towards both X and Y axis for a minimum of approx. 50 minutes after which a relatively stable value is achieved. Meanwhile the spindle length and deflections also exhibit changes during the stable period also. This may be attributed to the variation in spindle temperature due to cooling of the spindle.

It is important to reiterate that the model has the capability to measure and predict the errors in a machine tool under different machining parameters. The next chapter presents a summary of the model and the conclusion of the research along with identification of various applications and the recommendations for future work.

Chapter 7. Summary and Conclusion

7.1 Summary

This thesis presents a new methodology for error measurement with appreciation of positional, thermal, control and process errors. As per knowledge of the author a few methodologies utilize the workpiece measurement methodology for error analysis mainly dealing with position errors however, no methodology is found in the current research dealing extensively with multiple type of errors in a single model.

At first a comprehensive model is presented that details the experimental requirements, workpiece geometry and various machining parameters for identification of different errors while also providing an insight into the methodology for error separation and reporting. The model enables the separate reporting of displacement based position errors, time based thermal errors, force and displacement based control errors and force based process errors. A further regression based analysis technique that utilizes the available data for development of defining equation for each error against their respective parameters is also presented in the current model.

The model is then utilized for experimentation followed by on-machine probing and measurements on CMM. The data available after measurements and collected during experiments in form of machining times is then utilized to generate regression equations for each type of errors. The selection of regression equations is done through comparison of various models based on least backward prediction error. It is important to notice here that the main idea of the current model is about defining machining parameters for making some error constant in magnitude while changing the others. Various errors are then linked to their respective process parameters. A MATLAB program has also been developed for linking force based process errors to the errors generated through the program based on machining and tool data. A detailed discussion on the methodology have been presented in chapter 3.

As a result of measurement and analysis a prediction model comprising of a large number of equations with appreciation for 35 different error parameters has been proposed. The model has then been used for providing compensation for a workpiece machined with different feeds and spindle speeds at four different thermal states. The model is also used for prediction of errors on a different shape of workpiece. The overall results have been found as being promising with respect to prediction and compensation.

7.2 Conclusion:

This thesis provides a comprehensive methodology for error measurement, analysis and error prediction. The methodology presented in the current research requires a set of experimentation and extensive analysis. A large number of points have been reported as a result of experimentation. These points enable the measurement of various error components while the repetitions of points and the calculation of each dimension at least at six different positions provides statistical significance to the obtained dimensions.

Actual errors are extracted from the surface of machined workpiece and the errors have been linked to their respective control parameters therefore the model possesses the ability for prediction of actual machining performance of a machine tool. The error in backward prediction models however poses potential risk of variation within predicted errors. The error in backward prediction model is less than 5% in majority of cases, meanwhile the final errors are obtained through sum of individual errors hence the errors are not stacked onto each other. This reduces the severity of risk for a large variation in prediction.

The position errors are reported based on displacement, this provides a generic solution to error determination regardless of the shape. However, one limitation may be the differences in position errors at various positions of the table. The model has the ability to be applied to various table positions. However, the current research focuses on reporting of position errors at the center of the worktable which is mostly utilized for machining of components.

The thermal error analysis is a completely new approach that not only provides the magnitude of thermal errors at various temperature states based on machining time instance but also provide the appreciation for changes in thermal error with changes in spindle speed. One of the important

aspects of the current methodology is that the in-process spindle behavior under thermal influence is extensively reported. This is an important aspect for various design studies and corresponding applications.

The process errors are reported based on measurements and further linked to process forces. This is also a completely new approach where a program is 'calibrated' against known process parameters and resulting errors. The final presented equations relate the expected process errors to the program generated errors. Hence the process errors can be predicted for different tool diameters, depth of cuts, feeds and spindle speeds. Similar is the case for control errors based on process forces where the control errors are represented as a function of program generated errors and hence the same can be predicted for any value of cutting forces generated due to different machining parameters. Similar to thermal model the methodology has the capability for providing the in-process behavior of spindle and table, in terms of deflection and tilt respectively, in both X and Y axis.

Further onwards the proposed methodology provides the control errors as a function of distance and feed. It is important to notice here that some process errors due to small feed of 100mm/min may have been reported as part of control errors and vice-versa. However, their magnitude is small and close to negligible when evaluated using the obtained defining equations for process and control errors.

Overall the presented methodology and the overall results obtained therein are generic in terms of shape and size of workpiece, machining parameters and cutting tool geometry. Yet they apply for the particular machine that has been used for experimentation. The presented methodology is also generic for machine tools as the application of methodology on any 3 Axis machining centers will result in the generation of defining for the particular machine on which the methodology is being applied. The model also can be used in parts for users interested in extracting only a certain type of errors. However, the magnitude and defining equations for thermal errors is necessary for. This combined with the ease of application of the model hence improves the scope of model for application in various industrial scenarios.

7.2.1 Applications:

The model can be used primarily for error prediction and subsequent generation of compensation for components to be manufacturing in machine shops. The overall cost for implementation of this methodology is low as it utilizes the resources commonly available in most machine shops. Industrial applications for the presented methodology includes the pre-machining assessment of errors on a workpiece and optimization of machining parameters based on minimum or in some cases acceptable error magnitudes. A prediction model generated through the presented methodology would also enable the user for deciding between compensating or making a part within acceptable tolerance levels.

The model can also be used for maximization of Material Removal Rate (MRR) within a certain given tolerance. While an optimization of orientation of the workpiece in a production scenario can also be carried out. It has been observed that the error magnitudes in each axis and their changes with changing machining parameters are different. Hence error minimization can also be performed through optimum orientation settings of the workpiece.

Meanwhile as the developed model provides a complete picture of machine's behavior under different cutting conditions and thermal states, the results can provide valuable information regarding the in-process behavior of machine tool for machine tool designers. In such cases the main contributors of errors can also be identified.

7.2.2 Original Contribution:

The current research measures and provides prediction models for Mechanical Based position, Time and spindle speed based thermal errors, Displacement and Feed based control errors, force based control errors and cutting force based process errors. This comprehensive combination, as per authors knowledge, has not been detailed in any other research.

The workpiece measurement based Technique is applied for Thermal error measurement in a 3 Axis machine for the first time. The current research has also contributed to the existing literature through provision of a generic solution that takes into consideration both the time instance of machining and the spindle speed.

As per the knowledge of author the measurement methodology and prediction model for displacement and feed based control errors are also presented for the first time. The calibration of cutting force model based errors against control based errors is also a new addition in the current literature.

Meanwhile the proposed use of prediction model in conjunction with the cutting force models for correlating the actual process errors with software generated errors is also an important contribution of the current Thesis towards existing literature.

7.2.3 Future Work:

Several future research areas have been identified for the current work:

1. The research will be further expanded into development of error measurement and prediction methodology for five axis machining centers.
2. One of the areas where work needs to be done in connection with the current research is the development of adaptive compensation technique for the error values obtained through the current methodology.
3. The changes in control errors can also be expanded to include the control errors due to interaction between various axial motions simultaneously.
4. Work also needs to be done towards development of optimization models for machining parameters based on the developed model.
5. The research also can be expanded to include the position error identification through use of laser Tracking Interferometer and linkage of the results with current model.
6. A software development for comprehensive error prediction is the final goal of the ongoing research.

References

- [1] Schwenke, H., et al. "Geometric error measurement and compensation of machines—an update." *CIRP Annals-Manufacturing Technology* 57.2 (2008): 660-675.
- [2] Mekid, Samir, and Tunde Ogedengbe. "A review of machine tool accuracy enhancement through error compensation in serial and parallel kinematic machines." *International Journal of Precision Technology* 1.3-4 (2010): 251-286.
- [3] Ramesh, R., M. A. Mannan, and A. N. Poo. "Error compensation in machine tools—a review: part I: geometric, cutting-force induced and fixture-dependent errors." *International Journal of Machine Tools and Manufacture* 40.9 (2000): 1235-1256.
- [4] Okafor, A. C., and Yalcin M. Ertekin. "Derivation of machine tool error models and error compensation procedure for three axes vertical machining center using rigid body kinematics." *International Journal of Machine Tools and Manufacture* 40.8 (2000): 1199-1213.
- [5] Zhu, Shaowei, et al. "Integrated geometric error modeling, identification and compensation of CNC machine tools." *International journal of machine tools and manufacture* 52.1 (2012): 24-29.
- [6] Wang, JinDong, and JunJie Guo. "Research on volumetric error compensation for NC machine tool based on laser tracker measurement." *Science China Technological Sciences* 55.11 (2012): 3000-3009.
- [7] Seng Khim, Chin Keong. "Modeling the volumetric errors in calibration of five-axis cnc machine." (2010).
- [8] Srivastava, A. K., S. C. Veldhuis, and M. A. Elbestawit. "Modelling geometric and thermal errors in a five-axis CNC machine tool." *International Journal of Machine Tools and Manufacture* 35.9 (1995): 1321-1337.
- [9] Tian, Wenjie, et al. "Error modeling and sensitivity analysis of a five-axis machine tool." *Mathematical Problems in Engineering* 2014 (2014).
- [10] Hao, Wu, et al. "Thermal error optimization modeling and real-time compensation on a CNC turning center." *Journal of materials processing technology* 207.1 (2008): 172-179.
- [11] Yang, S., J. Yuan, and Jun Ni. "The improvement of thermal error modeling and compensation on machine tools by CMAC neural network." *International Journal of Machine Tools and Manufacture* 36.4 (1996): 527-537.

- [12] Kim, S. K., and D. W. Cho. "Real-time estimation of temperature distribution in a ball-screw system." *International Journal of Machine Tools and Manufacture* 37.4 (1997): 451-464.
- [13] Fines, John M., and Arvin Agah. "Machine tool positioning error compensation using artificial neural networks." *Engineering Applications of Artificial Intelligence* 21.7 (2008): 1013-1026.
- [14] Aguado, Sergio, et al. "Identification strategy of error parameter in volumetric error compensation of machine tool based on laser tracker measurements." *International Journal of Machine Tools and Manufacture* 53.1 (2012): 160-169.
- [15] Bryan, J. B., D. L. Carter, and S. L. Thompson. "Angle interferometer cross-axis errors." *CIRP Annals-Manufacturing Technology* 43.1 (1994): 453-456.
- [16] Lin, P. D., and K. F. Ehmann. "Direct volumetric error evaluation for multi-axis machines." *International Journal of Machine Tools and Manufacture* 33.5 (1993): 675-693.
- [17] Wang, JinDong, and JunJie Guo. "Research on volumetric error compensation for NC machine tool based on laser tracker measurement." *Science China Technological Sciences* 55.11 (2012): 3000-3009.
- [18] Lee, Eung-Suk, Suk-Hwan Suh, and Jin-Wook Shon. "A comprehensive method for calibration of volumetric positioning accuracy of CNC-machines." *The International Journal of Advanced Manufacturing Technology* 14.1 (1998): 43-49.
- [19] Donmez, M. Alkan, et al. "A general methodology for machine tool accuracy enhancement by error compensation." *Precision Engineering* 8.4 (1986): 187-196.
- [20] Gu, Jie, Sheri K. Kurgin, and Paula J. Deeds. "Electronic system and method for compensating the dimensional accuracy of a 4-axis CNC machining system using global and local offsets." U.S. Patent No. 8,712,577. 29 Apr. 2014.
- [21] Mares, Martin, et al. "Robustness and portability of machine tool thermal error compensation model based on control of participating thermal sources." *Journal of machine engineering* 13.1 (2013): 24-36.
- [22] Lo, Chin-Hao, Jingxia Yuan, and Jun Ni. "An application of real-time error compensation on a turning center." *International Journal of Machine Tools and Manufacture* 35.12 (1995): 1669-1682.
- [23] Fan, K. C., J. F. Lin, and S. S. Lu. "Measurement and compensation of thermal error on a machining center." *Proceedings of the Twenty-Ninth International Matador Conference*. Macmillan Education UK, 1992.
- [24] Chen, Jenq Shyong, Tzu Wei Kou, and Shen Hwa Chiou. "Geometric error calibration of multi-axis machines using an auto-alignment laser interferometer." *Precision Engineering* 23.4 (1999): 243-252.

- [25] Ibaraki, Soichi, Chiaki Oyama, and Hisashi Otsubo. "Construction of an error map of rotary axes on a five-axis machining center by static R-test." *International Journal of Machine Tools and Manufacture* 51.3 (2011): 190-200.
- [26] Bringmann, B., and W. Knapp. "Model-based 'chase-the-ball' calibration of a 5-axes machining center." *CIRP Annals-Manufacturing Technology* 55.1 (2006): 531-534.
- [27] Ota, Kentaro, Koji Teramoto, and Ryota Hayashi. "0112 Study of rapid on-machine shape measurement for accuracy assured machining." *Proceedings of International Conference on Leading Edge Manufacturing in 21st century: LEM21 2015.8*. The Japan Society of Mechanical Engineers, 2015.
- [28] Muelaner, J. E., et al. "Rapid machine tool verification." *Procedia CIRP* 25 (2014): 431-438.
- [29] Jung, Ji-Hun, Jin-Phil Choi, and Sang-Jo Lee. "Machining accuracy enhancement by compensating for volumetric errors of a machine tool and on-machine measurement." *Journal of Materials Processing Technology* 174.1 (2006): 56-66.
- [30] Ibaraki, Soichi, Takeyuki Iritani, and Tetsuya Matsushita. "Calibration of location errors of rotary axes on five-axis machine tools by on-the-machine measurement using a touch-trigger probe." *International Journal of Machine Tools and Manufacture* 58 (2012): 44-53.
- [31] Mou, J., M. A. Donmez, and S. Cetinkunt. "An adaptive error correction method using feature-based analysis techniques for machine performance improvement, Part 1: Theory derivation." *Journal of engineering for industry* 117.4 (1995): 584-590.
- [32] Morimoto, Yoshitaka, Shinji Tada, and Yusuke Muroichi. "B1 Study on Accuracy Compensation of Machining Center Based on Measurement Results of Machined Workpiece: Evaluation of Accuracy of 5-axis Controlled Machining Center (Advanced machine tool)." *Proceedings of International Conference on Leading Edge Manufacturing in 21st century: LEM21 2009.5*. The Japan Society of Mechanical Engineers, 2009.
- [33] Sousa, A. R., and C. A. Schneider. "AN ALTERNATIVE TECHNIQUE TO THE GEOMETRIC TEST OF MACHINING CENTERS."
- [34] Ibaraki, Soichi, et al. "Machining tests to identify kinematic errors on five-axis machine tools." *Precision Engineering* 34.3 (2010): 387-398.
- [35] Ibaraki, Soichi, and Yusuke Ota. "A machining test to calibrate rotary axis error motions of five-axis machine tools and its application to thermal deformation test." *International Journal of Machine Tools and Manufacture* 86 (2014): 81-88.
- [36] Ibaraki, Soichi, and Yusuke Ota. "A machining test to evaluate geometric errors of five-axis machine tools with its application to thermal deformation test." *Procedia CIRP* 14 (2014): 323-328.
- [37] Zhu, S. W., et al. "Workpiece locating error prediction and compensation in fixtures." *The International Journal of Advanced Manufacturing Technology*(2013): 1-10.

- [38] Krulewich, Debra A. "Temperature integration model and measurement point selection for thermally induced machine tool errors." *Mechatronics* 8.4 (1998): 395-412.
- [39] ISO-230-3:2007, "Test code for machine tools- Part 3: Determination of thermal effects." *Geneva, Switzerland, 2007*
- [40] Raksiri, Chana, and Manukid Parnichkun. "Geometric and force errors compensation in a 3-axis CNC milling machine." *International Journal of Machine Tools and Manufacture* 44.12 (2004): 1283-1291.
- [41] DeVor, R. E., and I. A. Shareef. "The prediction of surface accuracy in end milling." *Trans, of ASME Aug* 104.3 (1982): 272-278.
- [42] Krulewich, Debra A. "Temperature integration model and measurement point selection for thermally induced machine tool errors." *Mechatronics* 8.4 (1998): 395-412.
- [43] Budak, Erhan. "Analytical models for high performance milling. Part I: Cutting forces, structural deformations and tolerance integrity." *International Journal of Machine Tools and Manufacture* 46.12 (2006): 1478-1488.